



Supplementary Materials for

Evidence for neutrino emission from the nearby active galaxy NGC 1068

IceCube Collaboration

Corresponding authors: analysis@icecube.wisc.edu; F. Halzen, francis.halzen@icecube.wisc.edu

Science **378**, 538 (2022)
DOI: 10.1126/science.abg3395

The PDF file includes:

Materials and Methods
Supplementary Text
Figs. S1 to S30
Tables S1 to S4
IceCube Collaboration Author List
References

Supplementary Materials for:
Evidence for neutrino emission from the nearby active galaxy NGC 1068

IceCube Collaboration*:

R. Abbasi¹⁷, M. Ackermann⁶¹, J. Adams¹⁸, J. A. Aguilar¹², M. Ahlers²², M. Ahrens⁵¹, J.M. Alameddine²³, C. Alispach²⁸, A. A. Alves Jr.³¹, N. M. Amin⁴³, K. Andeen⁴¹, T. Anderson⁵⁸, G. Anton²⁶, C. Argüelles¹⁴, Y. Ashida³⁹, S. Axani¹⁵, X. Bai⁴⁷, A. Balagopal V.³⁹, A. Barbano²⁸, S. W. Barwick³⁰, B. Bastian⁶¹, V. Basu³⁹, S. Baur¹², R. Bay⁸, J. J. Beatty^{20, 21}, K.-H. Becker⁶⁰, J. Becker Tjus¹¹, C. Bellenghi²⁷, S. BenZvi⁴⁹, D. Berley¹⁹, E. Bernardini^{61, 62}, D. Z. Besson³⁴, G. Binder^{8, 9}, D. Bindig⁶⁰, E. Blaufuss¹⁹, S. Blot⁶¹, M. Boddenberg¹, F. Bontempo³¹, J. Borowka¹, S. Böser⁴⁰, O. Botner⁵⁹, J. Böttcher¹, E. Bourbeau²², F. Bradascio⁶¹, J. Braun³⁹, B. Brinson⁶, S. Bron²⁸, J. Brostean-Kaiser⁶¹, S. Browne³², A. Burgman⁵⁹, R. T. Burley², R. S. Busse⁴², M. A. Campana⁴⁶, E. G. Carnie-Bronca², C. Chen⁶, Z. Chen⁵², D. Chirkin³⁹, K. Choi⁵³, B. A. Clark²⁴, K. Clark³³, L. Classen⁴², A. Coleman⁴³, G. H. Collin¹⁵, J. M. Conrad¹⁵, P. Coppin¹³, P. Correa¹³, D. F. Cowen^{57, 58}, R. Cross⁴⁹, C. Dappen¹, P. Dave⁶, C. De Clercq¹³, J. J. DeLaunay⁵⁶, D. Delgado López¹⁴, H. Dembinski⁴³, K. Deoskar⁵¹, A. Desai³⁹, P. Desiati³⁹, K. D. de Vries¹³, G. de Wasseige³⁶, M. de With¹⁰, T. DeYoung²⁴, A. Diaz¹⁵, J. C. Díaz-Vélez³⁹, M. Dittmer⁴², H. Dujmovic³¹, M. Dunkman⁵⁸, M. A. DuVernois³⁹, E. Dvorak⁴⁷, T. Ehrhardt⁴⁰, P. Eller²⁷, R. Engel^{31, 32}, H. Erpenbeck¹, J. Evans¹⁹, P. A. Evenson⁴³, K. L. Fan¹⁹, A. R. Fazely⁷, A. Fedynitch⁵⁵, N. Feigl¹⁰, S. Fiedlschuster²⁶, A. T. Fienberg⁵⁸, K. Filimonov⁸, C. Finley⁵¹, L. Fischer⁶¹, D. Fox⁵⁷, A. Franckowiak^{11, 61}, E. Friedman¹⁹, A. Fritz⁴⁰, P. Fürst¹, T. K. Gaisser⁴³, J. Gallagher³⁸, E. Ganster¹, A. Garcia¹⁴, S. Garrappa⁶¹, L. Gerhardt⁹, A. Ghadimi⁵⁶, C. Glaser⁵⁹, T. Glauch²⁷, T. Glüsenkamp²⁶, A. Goldschmidt⁹, J. G. Gonzalez⁴³, S. Goswami⁵⁶, D. Grant²⁴, T. Grégoire⁵⁸, S. Griswold⁴⁹, C. Günther¹, P. Gutjahr²³, C. Haack²⁷, A. Hallgren⁵⁹, R. Halliday²⁴, L. Halve¹, F. Halzen³⁹, M. Ha Minh²⁷, K. Hanson³⁹, J. Hardin³⁹, A. A. Harnisch²⁴, A. Haungs³¹,

D. Hebecker¹⁰, K. Helbing⁶⁰, F. Henningsen²⁷, E. C. Hettinger²⁴, S. Hickford⁶⁰, J. Hignight²⁵, C. Hill¹⁶, G. C. Hill², K. D. Hoffman¹⁹, R. Hoffmann⁶⁰, B. Hokanson-Fasig³⁹, K. Hoshina^{39, 63}, F. Huang⁵⁸, M. Huber²⁷, T. Huber³¹, K. Hultqvist⁵¹, M. Hünnefeld²³, R. Hussain³⁹, K. Hymon²³, S. In⁵³, N. Iovine¹², A. Ishihara¹⁶, M. Jansson⁵¹, G. S. Japaridze⁵, M. Jeong⁵³, M. Jin¹⁴, B. J. P. Jones⁴, D. Kang³¹, W. Kang⁵³, X. Kang⁴⁶, A. Kappes⁴², D. Kappesser⁴⁰, L. Kardum²³, T. Karg⁶¹, M. Karl²⁷, A. Karle³⁹, U. Katz²⁶, M. Kauer³⁹, M. Kellermann¹, J. L. Kelley³⁹, A. Kheirandish⁵⁸, K. Kin¹⁶, T. Kintscher⁶¹, J. Kiryluk⁵², S. R. Klein^{8, 9}, R. Koirala⁴³, H. Kolanoski¹⁰, T. Kontrimas²⁷, L. Köpke⁴⁰, C. Kopper²⁴, S. Kopper⁵⁶, D. J. Koskinen²², P. Koundal³¹, M. Kovacevich⁴⁶, M. Kowalski^{10, 61}, T. Kozynets²², E. Kun¹¹, N. Kurahashi⁴⁶, N. Lad⁶¹, C. Lagunas Gualda⁶¹, J. L. Lanfranchi⁵⁸, M. J. Larson¹⁹, F. Lauber⁶⁰, J. P. Lazar^{14, 39}, J. W. Lee⁵³, K. Leonard³⁹, A. Leszczyńska³², Y. Li⁵⁸, M. Lincetto¹¹, Q. R. Liu³⁹, M. Liubarska²⁵, E. Lohfink⁴⁰, C. J. Lozano Mariscal⁴², L. Lu³⁹, F. Lucarelli²⁸, A. Ludwig^{24, 35}, W. Luszczak³⁹, Y. Lyu^{8, 9}, W. Y. Ma⁶¹, J. Madsen³⁹, K. B. M. Mahn²⁴, Y. Makino³⁹, S. Mancina³⁹, I. C. Mariş¹², I. Martinez-Soler¹⁴, R. Maruyama⁴⁴, K. Mase¹⁶, T. McElroy²⁵, F. McNally³⁷, J. V. Mead²², K. Meagher³⁹, S. Mechbal⁶¹, A. Medina²¹, M. Meier¹⁶, S. Meighen-Berger²⁷, J. Micallef²⁴, D. Mockler¹², T. Montaruli²⁸, R. W. Moore²⁵, R. Morse³⁹, M. Moulai¹⁵, R. Naab⁶¹, R. Nagai¹⁶, R. Nahnauer⁶¹, U. Naumann⁶⁰, J. Necker⁶¹, L. V. Nguy~en²⁴, H. Niederhausen²⁴, M. U. Nisa²⁴, S. C. Nowicki²⁴, D. Nygren^{9, 4}, A. Obertacke Pollmann⁶⁰, M. Oehler³¹, B. Oeyen²⁹, A. Olivas¹⁹, E. O'Sullivan⁵⁹, H. Pandya⁴³, D. V. Pankova⁵⁸, N. Park³³, G. K. Parker⁴, E. N. Paudel⁴³, L. Paul⁴¹, C. Pérez de los Heros⁵⁹, L. Peters¹, J. Peterson³⁹, S. Philippen¹, S. Pieper⁶⁰, M. Pittermann³², A. Pizzuto³⁹, M. Plum⁴¹, Y. Popovych⁴⁰, A. Porcelli²⁹, M. Prado Rodriguez³⁹, P. B. Price⁸, B. Pries²⁴, G. T. Przybylski⁹, C. Raab¹², J. Rack-Helleis⁴⁰, A. Raissi¹⁸, M. Rameez²², K. Rawlins³, I. C. Rea²⁷, A. Rehman⁴³, P. Reichherzer¹¹, R. Reimann¹, G. Renzi¹², E. Resconi²⁷, S. Reusch⁶¹, W. Rhode²³, M. Richman⁴⁶, B. Riedel³⁹, E. J. Roberts², S. Robertson^{8, 9}, G. Roellinghoff⁵³, M. Rongen⁴⁰, C. Rott^{50, 53}, T. Ruhe²³, D. Ryckbosch²⁹, D. Rysewyk Cantu²⁴, I.

Safa^{14, 39}, J. Saffer³², S. E. Sanchez Herrera²⁴, A. Sandrock²³, J. Sandroos⁴⁰, M. Santander⁵⁶, S. Sarkar⁴⁵, S. Sarkar²⁵, K. Satalecka⁶¹, M. Schaufel¹, H. Schieler³¹, S. Schindler²⁶, T. Schmidt¹⁹, A. Schneider³⁹, J. Schneider²⁶, F. G. Schröder^{31, 43}, L. Schumacher²⁷, G. Schwefer¹, S. Sclafani⁴⁶, D. Seckel⁴³, S. Seunarine⁴⁸, A. Sharma⁵⁹, S. Shefali³², M. Silva³⁹, B. Skrzypek¹⁴, B. Smithers⁴, R. Snihur³⁹, J. Soedingrekso²³, D. Soldin⁴³, C. Spannfellner²⁷, G. M. Spiczak⁴⁸, C. Spiering⁶¹, J. Stachurska⁶¹, M. Stamatikos²¹, T. Stanev⁴³, R. Stein⁶¹, J. Stettner¹, A. Steuer⁴⁰, T. Stezelberger⁹, R. Stokstad⁹, T. Stürwald⁶⁰, T. Stuttard²², G. W. Sullivan¹⁹, I. Taboada⁶, S. Ter-Antonyan⁷, S. Tilav⁴³, F. Tischbein¹, K. Tollefson²⁴, C. Tönnis⁵⁴, S. Toscano¹², D. Tosi³⁹, A. Trettin⁶¹, M. Tselengidou²⁶, C. F. Tung⁶, A. Turcati²⁷, R. Turcotte³¹, C. F. Turley⁵⁸, J. P. Twagirayezu²⁴, B. Ty³⁹, M. A. Unland Elorrieta⁴², N. Valtonen-Mattila⁵⁹, J. Vandebroucke³⁹, N. van Eijndhoven¹³, D. Vannerom¹⁵, J. van Santen⁶¹, S. Verpoest²⁹, C. Walck⁵¹, T. B. Watson⁴, C. Weaver²⁴, P. Weigel¹⁵, A. Weindl³¹, M. J. Weiss⁵⁸, J. Weldert⁴⁰, C. Wendt³⁹, J. Werthebach²³, M. Weyrauch³¹, N. Whitehorn^{24, 35}, C. H. Wiebusch¹, D. R. Williams⁵⁶, M. Wolf²⁷, K. Woschnagg⁸, G. Wrede²⁶, J. Wulff¹¹, X. W. Xu⁷, J. P. Yanez²⁵, S. Yoshida¹⁶, S. Yu²⁴, T. Yuan³⁹, Z. Zhang⁵², P. Zhelnin¹⁴

¹ III. Physikalisches Institut, Rheinisch-Westfälische Technische Hochschule Aachen University, D-52056 Aachen, Germany

² Department of Physics, University of Adelaide, Adelaide, 5005, Australia

³ Department of Physics and Astronomy, University of Alaska Anchorage, 3211 Providence Dr., Anchorage, AK 99508, USA

⁴ Department of Physics, University of Texas at Arlington, 502 Yates St., Science Hall Rm 108, Box 19059, Arlington, TX 76019, USA

⁵ The Center for Theoretical Studies of Physical Systems, Clark-Atlanta University, Atlanta, GA 30314, USA

⁶ School of Physics and Center for Relativistic Astrophysics, Georgia Institute of Technology,

Atlanta, GA 30332, USA

⁷ Department of Physics, Southern University, Baton Rouge, LA 70813, USA

⁸ Department of Physics, University of California, Berkeley, CA 94720, USA

⁹ Lawrence Berkeley National Laboratory, Berkeley, CA 94720, USA

¹⁰ Institut für Physik, Humboldt-Universität zu Berlin, D-12489 Berlin, Germany

¹¹ Fakultät für Physik & Astronomie, Ruhr-Universität Bochum, D-44780 Bochum, Germany

¹² Science Faculty CP230, Université Libre de Bruxelles, B-1050 Brussels, Belgium

¹³ Physics Department, Vrije Universiteit Brussel, B-1050 Brussels, Belgium

¹⁴ Department of Physics and Laboratory for Particle Physics and Cosmology, Harvard University, Cambridge, MA 02138, USA

¹⁵ Department of Physics, Massachusetts Institute of Technology, Cambridge, MA 02139, USA

¹⁶ Department of Physics and Institute for Global Prominent Research, Chiba University, Chiba 263-8522, Japan

¹⁷ Department of Physics, Loyola University Chicago, Chicago, IL 60660, USA

¹⁸ Department of Physics and Astronomy, University of Canterbury, Private Bag 4800, Christchurch, New Zealand

¹⁹ Department of Physics, University of Maryland, College Park, MD 20742, USA

²⁰ Department of Astronomy, Ohio State University, Columbus, OH 43210, USA

²¹ Department of Physics, Ohio State University, Columbus, OH 43210, USA

²² Niels Bohr Institute, University of Copenhagen, DK-2100 Copenhagen, Denmark

²³ Department of Physics, Technical University Dortmund, D-44221 Dortmund, Germany

²⁴ Department of Physics and Astronomy, Michigan State University, East Lansing, MI 48824, USA

²⁵ Department of Physics, University of Alberta, Edmonton, Alberta, Canada T6G 2E1

²⁶ Erlangen Centre for Astroparticle Physics, Friedrich-Alexander-Universität Erlangen-Nürnberg,

D-91058 Erlangen, Germany

²⁷ Physik-department, Technische Universität München, D-85748 Garching, Germany

²⁸ Département de physique nucléaire et corpusculaire, Université de Genève, CH-1211 Genève, Switzerland

²⁹ Department of Physics and Astronomy, University of Gent, B-9000 Gent, Belgium

³⁰ Department of Physics and Astronomy, University of California, Irvine, CA 92697, USA

³¹ Karlsruhe Institute of Technology, Institute for Astroparticle Physics, D-76021 Karlsruhe, Germany

³² Karlsruhe Institute of Technology, Institute of Experimental Particle Physics, D-76021 Karlsruhe, Germany

³³ Department of Physics, Engineering Physics, and Astronomy, Queen's University, Kingston, ON K7L 3N6, Canada

³⁴ Department of Physics and Astronomy, University of Kansas, Lawrence, KS 66045, USA

³⁵ Department of Physics and Astronomy, University of California, Los Angeles, CA 90095, USA

³⁶ Centre for Cosmology, Particle Physics and Phenomenology, Université catholique de Louvain, Louvain-la-Neuve, Belgium

³⁷ Department of Physics, Mercer University, Macon, GA 31207-0001, USA

³⁸ Department of Astronomy, University of Wisconsin–Madison, Madison, WI 53706, USA

³⁹ Department of Physics and Wisconsin IceCube Particle Astrophysics Center, University of Wisconsin–Madison, Madison, WI 53706, USA

⁴⁰ Institute of Physics, University of Mainz, Staudinger Weg 7, D-55099 Mainz, Germany

⁴¹ Department of Physics, Marquette University, Milwaukee, WI, 53201, USA

⁴² Institut für Kernphysik, Westfälische Wilhelms-Universität Münster, D-48149 Münster, Germany

⁴³ Department of Physics and Astronomy, University of Delaware, Newark, DE 19716, USA

⁴⁴ Department of Physics, Yale University, New Haven, CT 06520, USA

⁴⁵ Department of Physics, University of Oxford, Parks Road, Oxford OX1 3PU, UK

⁴⁶ Department of Physics, Drexel University, 3141 Chestnut Street, Philadelphia, PA 19104, USA

⁴⁷ Physics Department, South Dakota School of Mines and Technology, Rapid City, SD 57701, USA

⁴⁸ Department of Physics, University of Wisconsin, River Falls, WI 54022, USA

⁴⁹ Department of Physics and Astronomy, University of Rochester, Rochester, NY 14627, USA

⁵⁰ Department of Physics and Astronomy, University of Utah, Salt Lake City, UT 84112, USA

⁵¹ Oskar Klein Centre and Department of Physics, Stockholm University, SE-10691 Stockholm, Sweden

⁵² Department of Physics and Astronomy, Stony Brook University, Stony Brook, NY 11794-3800, USA

⁵³ Department of Physics, Sungkyunkwan University, Suwon 16419, Korea

⁵⁴ Institute of Basic Science, Sungkyunkwan University, Suwon 16419, Korea

⁵⁵ Institute of Physics, Academia Sinica, Taipei, 11529, Taiwan

⁵⁶ Department of Physics and Astronomy, University of Alabama, Tuscaloosa, AL 35487, USA

⁵⁷ Department of Astronomy and Astrophysics, Pennsylvania State University, University Park, PA 16802, USA

⁵⁸ Department of Physics, Pennsylvania State University, University Park, PA 16802, USA

⁵⁹ Department of Physics and Astronomy, Uppsala University, Box 516, S-75120 Uppsala, Sweden

⁶⁰ Department of Physics, University of Wuppertal, D-42119 Wuppertal, Germany

⁶¹ Deutsches Elektronen-Synchrotron, D-15738 Zeuthen, Germany

⁶² Dipartimento di Fisica e Astronomia "Galileo Galilei", Università di Padova, I-35131 Padova,
Italy

⁶³ Earthquake Research Institute, University of Tokyo, Bunkyo, Tokyo 113-0032, Japan

*E-mail: francis.halzen@icecube.wisc.edu, analysis@icecube.wisc.edu

Materials and Methods

Data Analysis Methods

Maximum Likelihood Implementation

To search for neutrino point sources, we use a maximum likelihood technique and related likelihood ratio hypothesis testing. The signal hypothesis consists of point-like neutrino emission from a source at a given location and with a given energy spectrum in addition to the atmospheric and diffuse neutrino backgrounds. The background hypothesis is purely atmospheric and diffuse astrophysical neutrino emission (62). As observables, we consider the reconstructed direction $\hat{\mathbf{d}} = (\hat{\alpha}, \hat{\delta})$ of the muon track with reconstructed right ascension $\hat{\alpha}$ and declination $\hat{\delta}$, its estimated uncertainty $\hat{\sigma}$, and reconstructed energy \hat{E}_μ . The likelihood \mathcal{L} relates to the joint probability density functions (pdfs) f that describe these observables for each event i in the data sample of size N :

$$\mathcal{L}(\boldsymbol{\theta} | \mathbf{x}, N) = f(\mathbf{x}, N | \boldsymbol{\theta}) = \prod_{i=1}^N f(\mathbf{x}_i | \boldsymbol{\theta}) \quad (\text{S1})$$

$$\mathbf{x}_i = (\hat{\mathbf{d}}_i, \hat{\sigma}_i, \hat{E}_{\mu,i}). \quad (\text{S2})$$

The parameters $\boldsymbol{\theta} = (\mu_{\text{ns}}, \gamma)$ are the mean number of signal events μ_{ns} and the spectral index γ . These characterize the neutrino emission spectrum of the source, assumed to be an unbroken power-law: $\Phi_{\nu_\mu + \bar{\nu}_\mu}(E_\nu) = \Phi_0 \cdot (E_\nu/E_0)^{-\gamma}$ where E_ν is the neutrino energy, and Φ_0 is the flux normalization at a fixed neutrino energy E_0 . Using the energy- and direction-dependent effective area of the detector and assuming a spectral index γ , the number of signal events μ_{ns} can be directly converted to Φ_0 via the event rate equation

$$\mu_{\text{ns}} = \int_0^\infty dE_\nu A_{\text{eff}}(E_\nu, d_{\text{src}}) \times \Phi_{\nu_\mu + \bar{\nu}_\mu}(E_\nu) \quad (\text{S3})$$

where d_{src} is the direction of the source, and $A_{\text{eff}}(E_{\nu}, d_{\text{src}})$ is the effective area calculated at energy E_{ν} and direction d_{src} .

We decompose the likelihood function into signal and background components by introducing the signal and background pdfs, f_S and f_B (63)

$$\mathcal{L}(\mu_{\text{ns}}, \gamma | \mathbf{x}, N) = \prod_{i=1}^N \left\{ \frac{\mu_{\text{ns}}}{N} \cdot f_S(\mathbf{x}_i | \gamma) + \left(1 - \frac{\mu_{\text{ns}}}{N}\right) \cdot f_B(\mathbf{x}_i) \right\}. \quad (\text{S4})$$

The pdf for atmospheric neutrinos is taken from previous studies (64–67). For the power-law associated with the diffuse astrophysical neutrino flux $\Phi_{\nu_{\mu}+\bar{\nu}_{\mu}}(E_{\nu}) = \Phi_{\text{astro}} \cdot (E_{\nu}/100 \text{ TeV})^{-\gamma_{\text{astro}}}$ we adopt the best-fitting parameter values from a study of the same data sample of neutrino events: $\Phi_{\text{astro}} = 1.44 \times 10^{-18} \text{ GeV}^{-1} \text{ cm}^{-2} \text{ s}^{-1} \text{ sr}^{-1}$ and $\gamma_{\text{astro}} = 2.28$ (62). Small remaining discrepancies between data and Monte Carlo simulations, observed at low energies in some declination regions, are removed empirically by matching the Monte Carlo distributions to the experimental data, that are strongly dominated by background. A comparison between the experimental data and the Monte Carlo simulations is shown in Fig. S1. The time-averaged background pdf is uniform in the observed right ascension $\hat{\alpha}$ due to Earth rotation and neglects small seasonal variations of the atmospheric neutrino flux (68). Hence,

$$f_B(\mathbf{x}_i) = f_B(\hat{E}_{\mu,i}, \hat{\mathbf{d}}_i, \hat{\sigma}_i) = \frac{1}{2\pi} f_B(\hat{E}_{\mu,i}, \sin \hat{\delta}_i, \hat{\sigma}_i) \quad (\text{S5})$$

where $\hat{\delta}_i$ is the event declination. The time-integrated signal pdf is:

$$f_S(\hat{E}_{\mu,i}, \hat{\mathbf{d}}_i, \hat{\sigma}_i | \sin \delta_{\text{src}}, \gamma) = \frac{1}{2\pi \sin \hat{\psi}_i} f_S(\hat{E}_{\mu,i}, \hat{\psi}_i, \hat{\sigma}_i | \sin \delta_{\text{src}}, \gamma), \quad (\text{S6})$$

where the relevant spatial observable is the angular distance $\hat{\psi}$ between the reconstructed direction and the assumed source position, and δ_{src} is the assumed source declination. Using the law of conditional probabilities, the signal pdf becomes a product of a spatial term, an energy term and an angular error conditional pdf

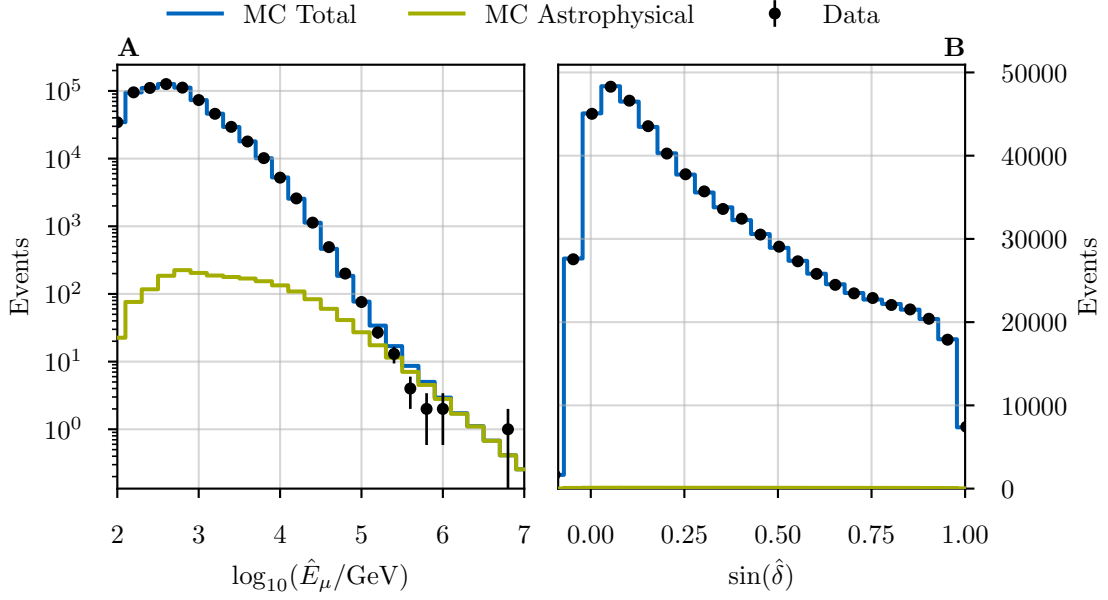


Figure S1: Comparison between experimental data (black) and Monte Carlo (MC) simulations (blue) for the two observables - reconstructed energy (A**) and sine of the declination (**B**). The error bars visualize 68% confidence intervals for the poisson mean in each bin. Superimposed, the contribution of the diffuse astrophysical flux is shown as a green line (62). In (**B**) this contribution is close to zero.**

$$f_S \left(\hat{E}_{\mu,i}, \hat{\mathbf{d}}_i, \hat{\sigma}_i \mid \sin \delta_{\text{src}}, \gamma \right) = \frac{1}{2\pi \sin \hat{\psi}_i} f_S \left(\hat{\psi}_i \mid \hat{E}_{\mu,i}, \hat{\sigma}_i, \sin \delta_{\text{src}}, \gamma \right) \cdot f_S \left(\hat{E}_{\mu,i}, \hat{\sigma}_i \mid \sin \delta_{\text{src}}, \gamma \right) \quad (\text{S7})$$

$$= \frac{1}{2\pi \sin \hat{\psi}_i} f_S \left(\hat{\psi}_i \mid \hat{E}_{\mu,i}, \hat{\sigma}_i, \sin \delta_{\text{src}}, \gamma \right) \cdot f_S \left(\hat{E}_{\mu,i} \mid \sin \delta_{\text{src}}, \gamma \right) \cdot f_S \left(\hat{\sigma}_i \mid \hat{E}_{\mu,i}, \sin \delta_{\text{src}}, \gamma \right). \quad (\text{S8})$$

All pdfs in this equation depend on the spectral index γ , a free parameter in the source hypothesis, but the dependence is strongest for the energy term. Similarly, the background term reads

$$f_B(\hat{E}_{\mu,i}, \hat{\mathbf{d}}_i, \hat{\sigma}_i) = \frac{1}{2\pi} f_B(\hat{E}_{\mu,i}, \sin \hat{\delta}_i) \cdot f_B(\hat{\sigma}_i \mid \hat{E}_{\mu,i}, \sin \hat{\delta}_i). \quad (\text{S9})$$

The signal angular error conditional pdf $f_S(\hat{\sigma} \mid \hat{E}_\mu, \sin \delta_{\text{src}}, \gamma)$ depends only weakly on the spec-

tral index γ . We approximate it as a constant that is equal to the corresponding factor in the background term $f_B(\hat{\sigma} | \hat{E}_\mu, \sin \hat{\delta})$. Likelihood-based inference procedures do not depend on constant factors in the likelihood function. We can therefore ignore both terms, trading a reduction in numerical complexity for a minor impact on the statistical rigor. The final signal and background pdfs are then

$$f_S(\hat{E}_{\mu,i}, \hat{\mathbf{d}}_i, \hat{\sigma}_i | \sin \delta_{\text{src}}, \gamma) \approx \frac{1}{2\pi \sin \hat{\psi}_i} f_S(\hat{\psi}_i | \hat{E}_{\mu,i}, \hat{\sigma}_i, \gamma) \cdot f_S(\hat{E}_{\mu,i} | \sin \delta_{\text{src}}, \gamma) \quad (\text{S10})$$

$$f_B(\hat{E}_{\mu,i}, \hat{\mathbf{d}}_i, \hat{\sigma}_i) \approx \frac{1}{2\pi} f_B(\hat{E}_{\mu,i}, \sin \hat{\delta}_i). \quad (\text{S11})$$

In Eq. (S10), the spatial term is treated as conditionally independent of the declination, since it is absorbed by the angular error estimated using Boosted Decision Trees (BDT) $\hat{\sigma}_{BDT}$ (see below and Fig. S4). Finally, the test statistic (TS) to compare the signal hypothesis ($\mu_{\text{ns}} > 0$) and background hypothesis ($\mu_{\text{ns}} = 0$) at a given source location \mathbf{d}_{src} is defined as

$$TS(\mathbf{d}_{\text{src}}) \equiv -2 \times \log(A) = -2 \times \log \left(\frac{\mathcal{L}(\mu_{\text{ns}} = 0 | \mathbf{x})}{\sup_{\mu_{\text{ns}}, \gamma} \mathcal{L}(\mu_{\text{ns}}, \gamma, \mathbf{d}_{\text{src}} | \mathbf{x})} \right) \quad (\text{S12})$$

where the signal likelihood is maximized over the two free parameters $\mu_{\text{ns}} \geq 0$ and $\gamma \in [1, 4.5]$. The maximum is obtained numerically by minimizing the negative test-statistic function using the gradient-based L-BFGS-B algorithm through the SCIPY software package (69).

The Signal and Background Likelihood: Kernel Density Estimation

In previous searches (63), the spatial term in Eq. S10 was approximated by a spectral index independent bivariate Gaussian, with standard deviation given by the estimated angular error of each event, i.e. $\sigma_i = \hat{\sigma}_i$. Instead, we construct the pdfs in Eq. S9 and Eq. S10 non-parametrically via kernel density estimation (KDE) from Monte Carlo simulations using the software package MEERKAT (70). Each conditional pdf is obtained from the ratio of two KDEs, one which

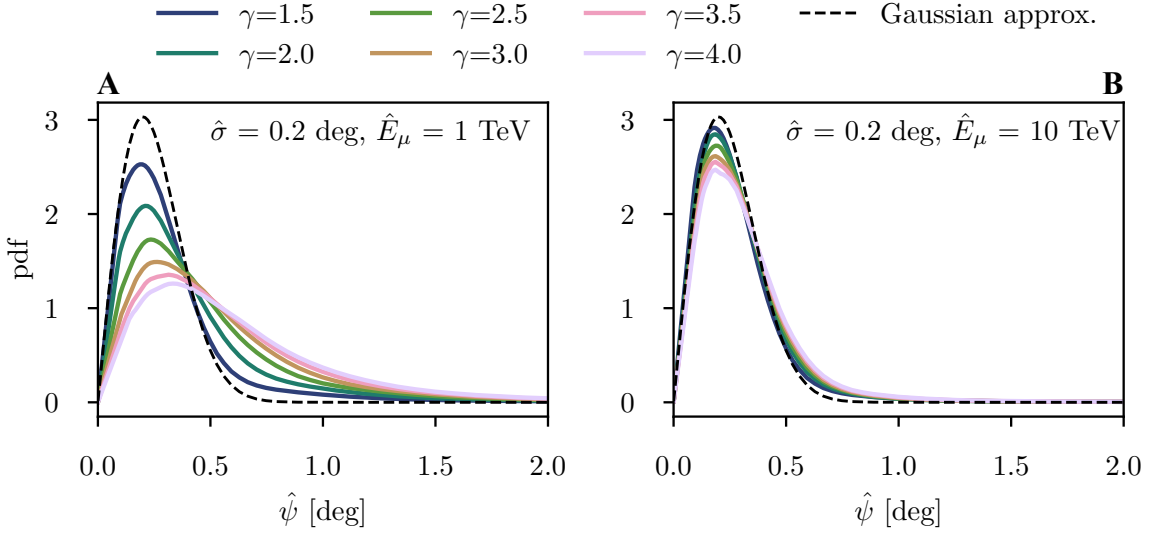


Figure S2: Spatial term as function of spectral index γ (examples). The distribution of the angular distance $\hat{\psi}$ for an angular uncertainty $\hat{\sigma} = 0.2^\circ$ for different spectral indices and at muon energy 1 TeV (**A**) and 10 TeV (**B**). The spectral index dependence as well as the non-Gaussian tails are visible. The Gaussian assumption is shown as a dashed line.

represents the joint pdf and one that represents the marginal pdf, i.e.

$$f(A|B) = \frac{f(A, B)}{f(B)} \quad (\text{S13})$$

Generating these KDEs is straightforward for pdfs that describe one or two observables. The spatial term, however, depends on three observables, which poses a numerical challenge given that the sample of simulated events is limited. Therefore, for the spatial term we use a relative KDE method (70). It constructs the KDEs by modeling numerically the deviations of the spatial dimension in the joint pdf from a semi-analytic guess $\tilde{f}(.)$ of the form

$$\tilde{f}(\hat{E}_\mu, \hat{\psi}, \hat{\sigma} | \gamma) = f_S(\hat{E}_\mu, \hat{\sigma} | \gamma) \times \frac{\hat{\psi}}{\sigma_{\text{tot}}^2(\hat{E}_\mu, \gamma)} e^{-\hat{\psi}^2/(2\sigma_{\text{tot}}^2(\hat{E}_\mu, \gamma))}, \quad (\text{S14})$$

where $f_S(\hat{E}_\mu, \hat{\sigma} | \gamma)$ is generated as any of the other 2-dimensional KDEs. Here, σ_{tot} combines the estimated reconstruction uncertainty and the kinematic angle, the angular separation between the original neutrino direction and the secondary muon trajectory, which is obtained

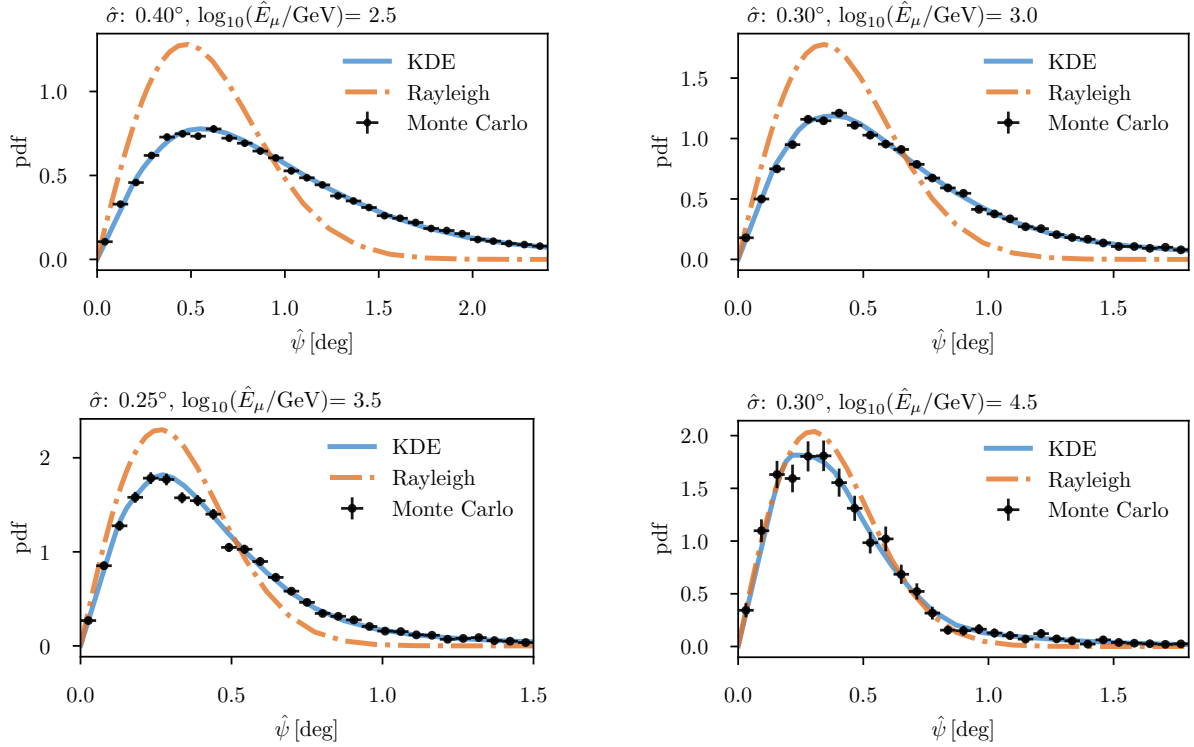


Figure S3: **Spatial terms for $\gamma = 3.2$.** The KDE-based parametrization (blue) is compared to the Rayleigh approximation (orange) from previous works (23) and the Monte Carlo expectation (black). The conditional observables – energy and angular uncertainty – are given on top.

from simulations

$$\sigma_{\text{tot}}(\hat{E}_\mu, \gamma) = \sqrt{\hat{\sigma}^2 + \sigma_{\text{kin}}^2(\hat{E}_\mu, \gamma)}. \quad (\text{S15})$$

KDEs require tuning of smoothing parameters h , usually referred to as bandwidth (70). We used a 5-fold cross-validation technique to determine the optimal values. The signal KDEs are generated on a grid of spectral indices between $\gamma = 0.5$ and $\gamma = 4.5$ by re-weighting of the Monte Carlo dataset. The step size $\Delta\gamma = 0.05$ was chosen to be sufficiently small to smoothly interpolate during the minimization of the likelihood. At high reconstructed energies, $\hat{E}_\mu \gtrsim 10$ TeV, the KDEs match the projection on the angular distance of the bivariate Gaussian, known to generate a Rayleigh distribution, and used in previous works (23). However, in contrast to the bivariate Gaussian, the KDEs account for the spectral-index dependent, non-Gaussian tails, that

the spatial term exhibits at low energies, $\hat{E}_\mu \lesssim 10$ TeV, as shown in Fig. S2. In this region, the quality of the directional reconstruction degrades rapidly, and the kinematic angle between the neutrino and muon trajectories becomes non-negligible. Fig. S3 shows that, for such events, the KDEs provide a better match to the Monte Carlo simulations, especially for $\gamma \gtrsim 3.0$ spectra.

Angular Uncertainty Estimation Using Boosted Decision Trees

The most relevant observable in the search for neutrino sources is the reconstructed direction $\hat{d}_i = (\hat{\alpha}_i, \hat{\delta}_i)$ of the muon track. We determined those directions using the `SplineReco` algorithm (27, 28), which optimizes a likelihood function constructed from the arrival times of the first photon measured by each optical sensor, and photon arrival time pdfs extracted from Monte Carlo simulations of minimum-ionizing muons as function of their trajectory through the detector. It includes modifications that, as a function of energy, mitigate the effect of not having included the muon stochastic energy losses in the simulations. The median angular resolution as function of muon energy are shown in Fig. S17A. An initial guess of the associated angular uncertainties $\hat{\sigma}_{p,i}$ for individual events is derived by approximating the `SplineReco` likelihood function around its 2D optimum using a paraboloid (71). By construction, it does not account for the kinematic angle between the direction of the primary neutrino and the secondary muon track, relevant at low energies $E_\nu \lesssim 10$ TeV, and it is limited at high energies by the `SplineReco` treatment of stochastic energy losses and other model miss-specifications (28). Therefore, depending on the muon energy, a Gaussian spatial term that is based directly on $\hat{\sigma}_{p,i}$ underestimates the scattering of track events around a point source by up to a factor of ~ 2 , as determined from simulations. In a previous search (23), the average mismatch was corrected with an energy-dependent correction function $c(E)$ via $\hat{\sigma}'_{p,i}(E) = c(E) \cdot \hat{\sigma}_{p,i}$ assuming a spectral index of $\gamma = 2$. Because we do not use the Gaussian assumption but construct the general form of the spatial term in (S7) numerically from simulations, the absolute scale of the directional

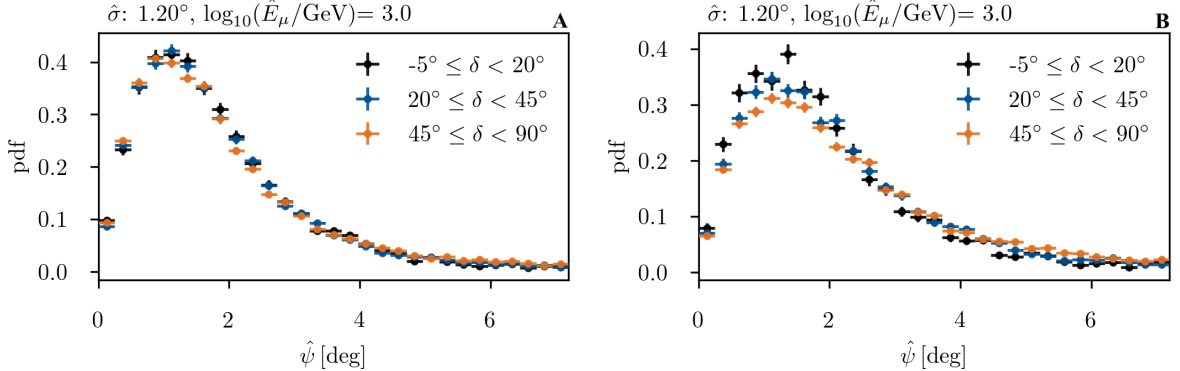


Figure S4: Influence of declination on spatial term. The spatial term is shown for 1 TeV events in different declination bands using the BDT (**A**) and Paraboloid angular uncertainty estimators (**B**). The BDT-based spatial term does not depend on the declination.

uncertainty estimate is irrelevant and such correction is not necessary. Since the limitations of $\hat{\sigma}_{p,i}$ can vary depending on additional event characteristics beyond the energy observable, we use a multi-variate method, Gradient Boosted Decision Trees (BDTs) (72), to parametrize the median of the angular separation between reconstructed muon direction and simulated muon direction as a function of 17 event observables. In addition to energy and paraboloid $\hat{\sigma}'_{p,i}$, these include an estimate of the position of the largest energy deposition in the detector, a measure of the stochasticity of the event energy loss pattern, the track declination, and angular separations between different track reconstruction methods. The BDT simply serves as a method to reduce dimensions. In rare cases, when the original paraboloid fit does not converge, the BDT treats $\hat{\sigma}'_{p,i}$ as missing input and hence does not fail. This accounts for the variety of possible track signatures in the detector. For example, at low energies below a few TeV, it provides the conditional independence of the spatial term in Eq. (S7) from the track declination as assumed in the likelihood function Eq. (S10). This is shown in Fig. S4. The simulated distributions of the angular separation between reconstructed and true track directions (at $\hat{E}_\mu \approx 1$ TeV) for the same BDT angular uncertainty (Fig. S4A) appear identical regardless of the track declination,

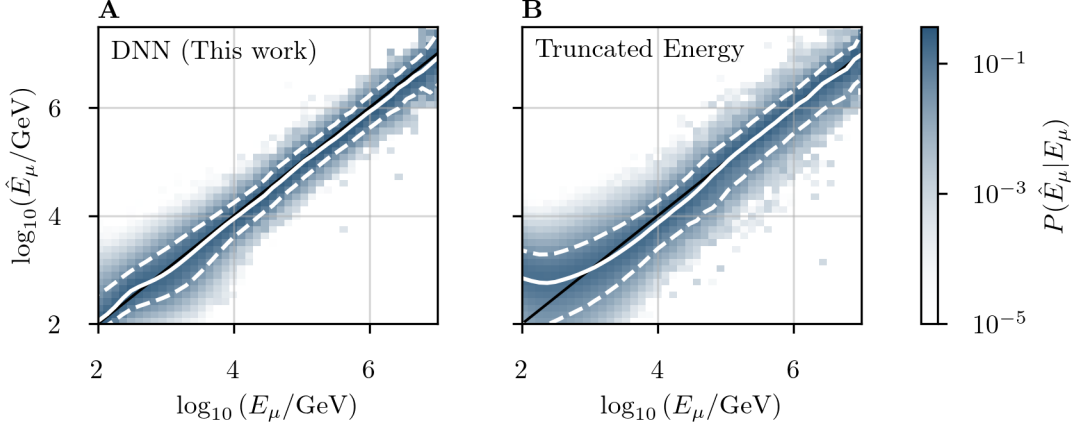


Figure S5: Performance of the deep neural network energy reconstruction. Comparison between the DNN prediction of the muon energy on entry (**A**) and a likelihood-based algorithms as used in previous analyses (**B**). The solid white line shows the median prediction and the dashed lines the 90% central quantile. The expectation for an unbiased estimator is shown as black solid line.

while the one using the paraboloid $\hat{\sigma}_{p,i}$ (Fig. S4B), show small differences depending on the true track declination.

Muon Energy Estimation Using Deep Learning

We use a deep neural network (DNN) to estimate the muon energy associated with track-like events. We reconstruct the energy of the muon when it crosses the boundary of the detector. The method is inspired by image recognition approaches. We transform the hexagonal IceCube grid to a $10 \times 10 \times 60$ pixel grid, including zero-padding, and convert the time series of detected photons at each DOM into a set of 15 features that contain information on the collected charge versus time. Overall, this results in an input tensor of $10 \times 10 \times 60 \times 15$ for each event (73). The network architecture follows the INCEPTION-RESNET (74) with 775,205 free parameters, which are optimized using a training sample of 6 million simulated muon neutrino events (75). Fig. S5A shows the performances of the DNN energy reconstruction and demonstrates that it is unbiased across the entire energy range, including the region below a few TeV, where previously

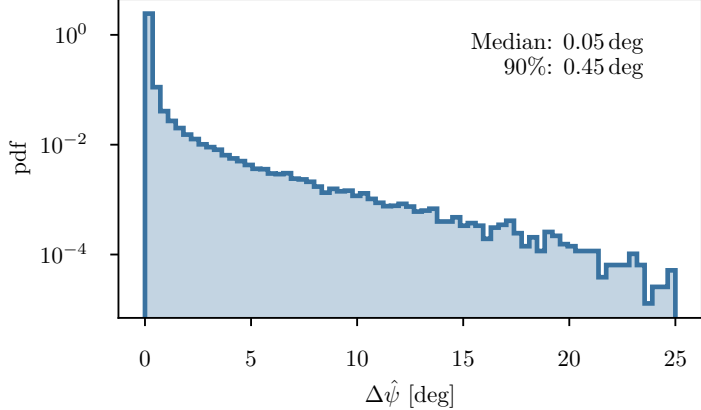


Figure S6: Angular difference between the directions before and after recalibration. The median and 90% quantile are given in the plot.

used reconstruction algorithms (76) produce degenerate energy estimates as ionization energy losses start to dominate (see Fig. S5B). The excess at the position of NGC 1068 is dominated by events with energies between 1.5 TeV and 15 TeV. Compared to the previously used algorithm, the DNN estimator improves the energy resolution in this range between $\sim 5\%$ (at ~ 1.5 TeV) and $\sim 30\%$ (at ~ 10 TeV) in $\log_{10}(\hat{E}_\mu)$.

Data Processing and Event Reconstructions

Each IceCube DOM is equipped with a photomultiplier tube (PMT) which measures a waveform, i.e. the voltage signal due to photo-electrons produced by incoming Cherenkov photons over time. Using templates of the detector response to single photo-electrons, the total waveform can be decomposed into single photon hits or pulses. The IceCube data we use have been reprocessed to include revisions to the calibration of the PMT charge response (18). On average, this change reduces the inferred deposited PMT charge (and thus the deposited energy) by 4.3%. In addition, updates to the waveform unfolding algorithm can result in small changes of the extracted times of PMT pulses. The median impact of the reprocessing on the angular reconstruction is small (0.05°). However, 10% of the events are reconstructed with more than

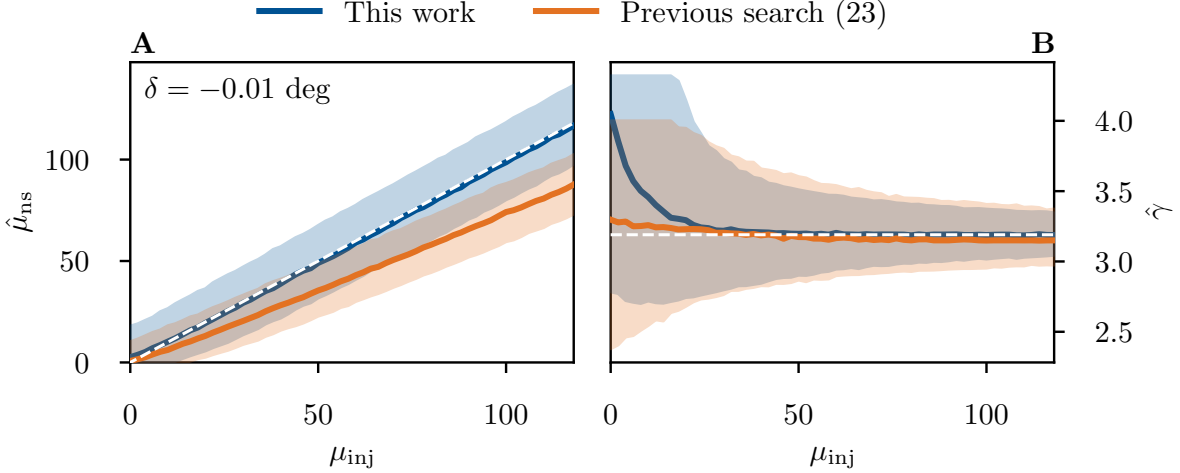


Figure S7: Recovery of the signal parameters at the position of NGC 1068. The recovery of the number of signal events $\hat{\mu}_{ns}$ (**A**) and the spectral index $\hat{\gamma}$ (**B**) are shown as a function of the number of injected signal events μ_{inj} . The plot is based on pseudo experiments assuming a source with best-fitting spectral index of NGC 1068, $\hat{\gamma} = 3.2$. This work is shown by the blue colors, the previous search (23) in orange. The white dashed line represents the unbiased expectation. The solid lines show the median estimated parameters. The shaded bands correspond to central 68% quantiles.

0.45° change in incoming direction, as shown in Fig. S6. The reprocessing applies consistent data selection criteria throughout the entire data-taking period, thus removing previous fragmentations of the sample. As a consequence, we only need a single Monte Carlo dataset with corresponding pdfs for the entire analysis.

Analysis Performance

To quantify how well the analysis identifies and characterizes sources, we evaluate simulations of several hypothetical experiments, hereafter referred to as pseudo experiments. In Fig. S7, we show the estimated number of signal events $\hat{\mu}_{ns}$ and spectral index $\hat{\gamma}$ for pseudo experiments with different source strengths injected at the position of NGC 1068. The spectral index of $\gamma = 3.2$ is chosen to match the best-fitting spectrum of the source. For both parameters, we

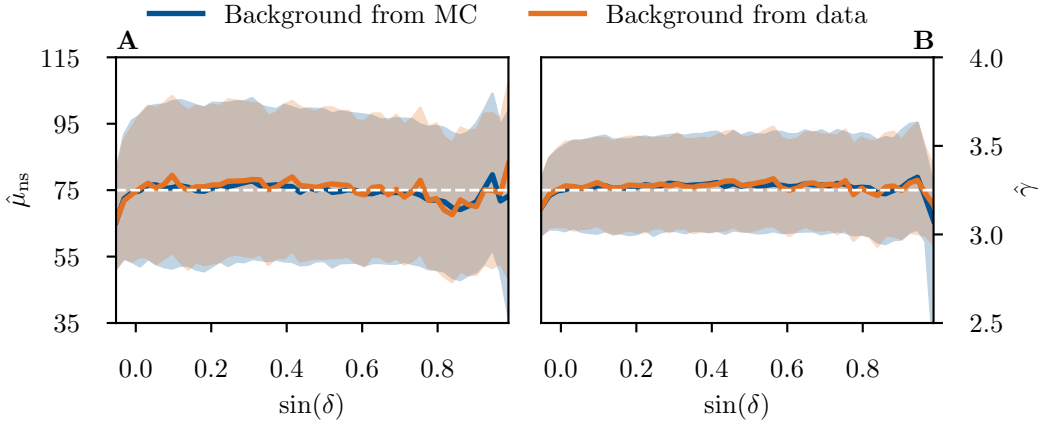


Figure S8: Recovery of the signal parameters across the northern hemisphere. The analysis performs equally in recovering the true model parameters when the background is generated from experimental data by randomizing the right ascension coordinate (orange) and when it is generated from Monte Carlo (MC) simulation instead (blue). Shown is the case of injected signal events $\mu_{inj} = 75$, assuming a source with spectral index $\gamma_{inj} = 3.25$. The meaning of the different lines and shaded areas is the same as in Fig. S7.

find the analysis is unbiased except for very small signal strengths, well below the measured value. We have verified that the analysis method performs equally well and recovers the true model parameters when pseudo experiments use background events that were generated from experimental data by randomizing the right ascension coordinate, a method referred to as data scrambling, instead of Monte Carlo simulations (Fig. S8). This demonstrates that unknown imperfections in the background model do not affect the analysis.

The localization performance is shown in Fig. S9. The median offset between the true coordinates and the best-fitting position from the pseudo experiments with a source placed at the location of NGC 1068 is 0.12° , assuming the best-fitting flux for NGC 1068.

As a measure for the detectability of neutrino sources, we determine the sensitivity and the discovery potential. The former is defined as the flux value at which the 10% quantile of the signal TS distribution is larger than the median of the TS distribution for the background hypothesis. The latter corresponds to the flux necessary to make a 5σ discovery with 50% probability,

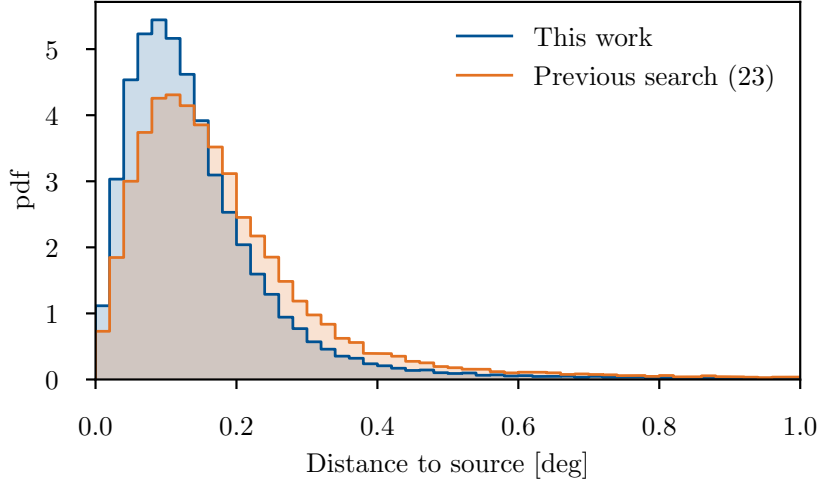


Figure S9: Localizing a source like NGC 1068. The distribution of the angular distance from the location of a simulated neutrino source with best-fitting parameter values of NGC 1068 to the global maximum of the likelihood. The search of the global maximum was performed within a box of area $6 \times 6 \text{ deg}^2$ centered at the position of NGC 1068.

i.e. the flux at which the median of the signal TS distribution is equal to the 5σ quantile of the background distribution. Examples of background TS distributions are shown in Fig. S10. We parametrize the tail of our distributions towards large TS values with a truncated gamma function

$$f(TS) \underset{TS \geq \eta}{=} \Gamma(TS | a, b, \eta) \underset{TS \geq \eta}{=} (\xi/C_0) \cdot \Gamma(TS | a, b) \quad (\text{S16})$$

which matches our pseudo experiments, see Fig. S10. Here, η is the lower threshold for the integration of the distribution, a and b are the shape and scale parameter of the gamma distribution, respectively, ξ is the fraction of pseudo experiments having a value larger than η and $C_0 = \int_{\eta}^{\infty} \Gamma(TS | a, b)$ is a normalization constant. We choose the truncation threshold $\eta = 3$. The parameter ξ is directly estimated from pseudo experiments, and a and b are left as free parameters. Pseudo experiments to determine the TS distributions are generated for each spectral index hypothesis and at 309 declinations equally-spaced in $\sin(\delta)$.

Fig. S11 shows the sensitivity and the discovery potential for injected sources with $\gamma = 2.0$ and

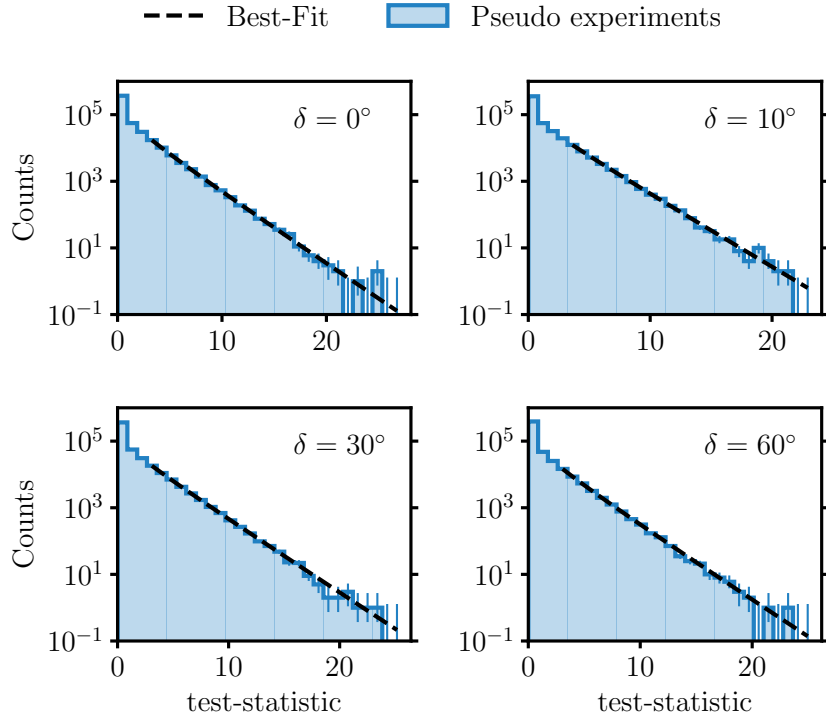


Figure S10: **Test statistic distributions at various declinations** assuming the free spectral index hypothesis.

$\gamma = 3.2$ and the different spectral index hypotheses considered in our analysis. For the free spectral index hypothesis, the discovery potential improves by around 20% - 30% for $\gamma = 2.0$ and 5% for $\gamma = 3.2$ compared to previous searches (23), as shown in Fig. S12.

Search methods for Point Sources of Neutrino Emission

Searching the Northern Hemisphere

We scan the Northern Hemisphere on a grid, testing the signal hypothesis ($\mu_{\text{ns}} > 0$) with spectral index γ treated as free parameter, and then repeat the scan with γ fixed to 2.0 and 2.5. The Northern Sky is binned with a HEALPi \times (77, 78) resolution parameter $\text{Nside} = 256$, resulting in equally-sized pixels with 0.052 deg^2 ($\sim 0.2^\circ \times 0.2^\circ$) each. Using the pixel centers as coordinates of a candidate source, the signal likelihood is maximized and the TS value (eq.

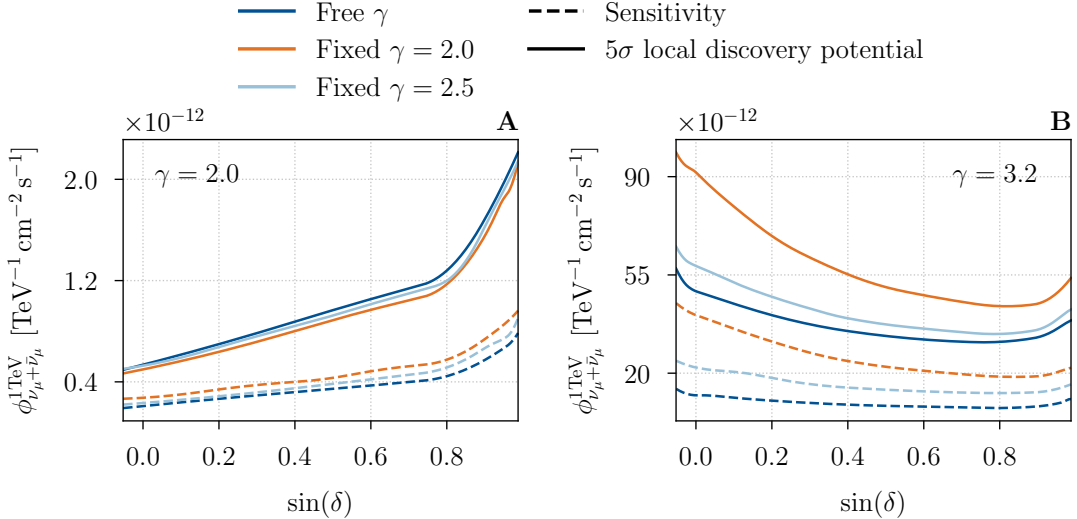


Figure S11: Sensitivity and Discovery Potential for the three signal hypotheses. Local sensitivity (dashed) and 5σ discovery potential (solid) fluxes are shown for the various spectral index hypothesis discussed in the text, indicated by the different colors. The two plots assume neutrino emission with spectral index $\gamma = 2.0$ (**A**) and $\gamma = 3.2$ (**B**). In each case the flux normalization is given at a neutrino energy of 1 TeV.

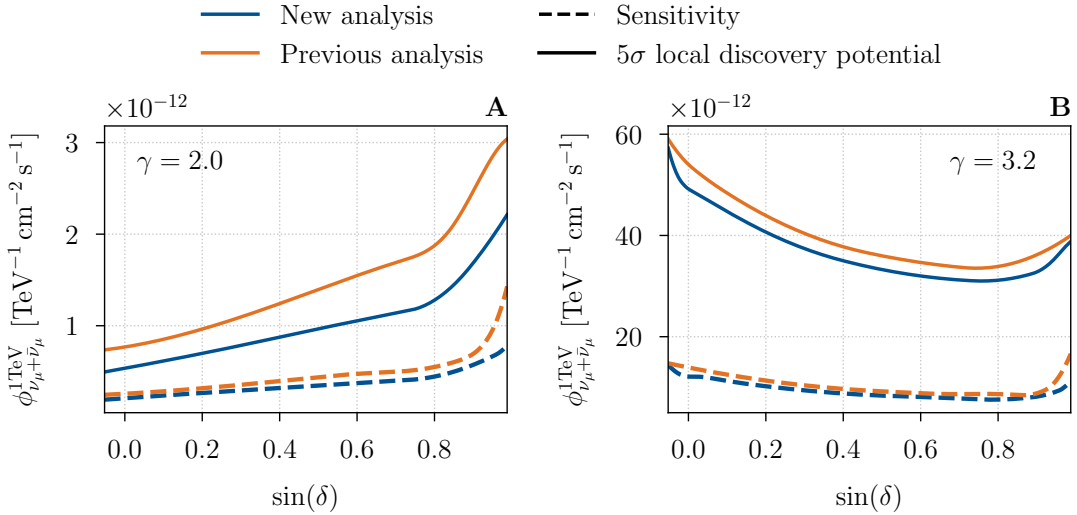


Figure S12: Comparison of Sensitivity and Discovery Potential with a previous search (23). Similar to Fig. S11, but only the free spetracl index hypothesis is tested. Local sensitivity (dashed) and 5σ discovery potential (solid) fluxes are shown for this work (blue) and for a previous search (23) (orange).

S12) calculated for each pixel individually. Using the background TS distributions at the respective declinations (see Fig. S10), the TS values are converted into p-values. For $TS < 5$, the p-value is estimated directly from pseudo experiments, whereas for $TS \geq 5$, the truncated gamma function is used to extrapolate the distribution and obtain the p-value. For the 20 most significant locations, i.e. those with lowest p-values, the scan is repeated on a square grid of total size $1.5^\circ \times 1.5^\circ$ with increased resolution ($N_{\text{side}} = 2048$). The final result is the most significant location, the one with the lowest p-value, identified throughout the three scans of the Northern Sky, including the high-resolution follow-up. This procedure results in a large number of correlated statistical tests being performed. Using pseudo experiments, we studied the probability that background fluctuations produce a most significant location in this search with significance equal or greater than the one observed in experimental data. We estimate the expected distribution of p-values by performing the scans on 3000 background-only pseudo experiments. The probability of the lowest local p-value is assessed and the global p-value extracted (Fig. S13, Fig. S14). This procedure takes into account that we perform three correlated scans with different assumptions about the spectral index γ .

Pre-defined List of Sources

We follow the same procedure as the previous search (23) to select 110 potential neutrino sources. The candidate source list (Tab. S3) differs from the one given in (23) due to the restricted declination range ($-3^\circ < \delta < 81^\circ$), the change in sensitivity as function of declination, and the second release of the fourth Fermi Large Area Telescope catalog (4FGL-DR2) (32). First, we select all galaxies from the 4FGL-DR2 catalog (32) within our declination range, as well as one Galactic source, MGRO J1908+06. This is the only source in the TeV catalog TeVCAT (33) with an estimated neutrino flux reaching the energy-dependent sensitivity of IceCube, assuming the TeV gamma-ray flux is generated by proton-proton interactions. For the

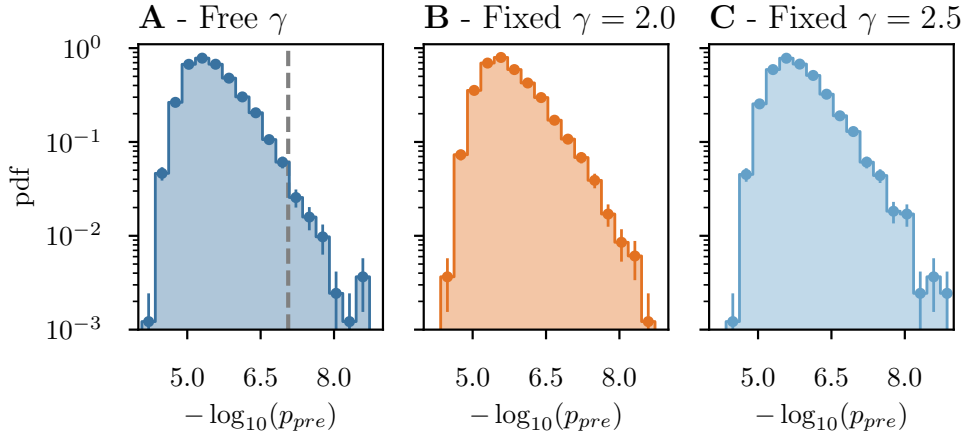


Figure S13: **Background distributions of local p-values in the Northern Sky scan.** Each plot shows the distribution for a different signal hypotheses as indicated in the titles. Overall, 3000 pseudo experiments have been generated assuming only background neutrinos, i.e. atmospheric neutrino and the diffuse astrophysical background. The grey dashed line in (A) indicates the significance of the most significant location identified from the scan of the experimental data under the free spectral index hypothesis.

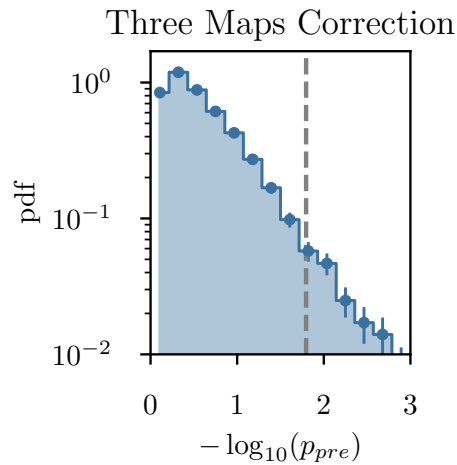


Figure S14: **Background distribution of local p-values from the three scans.** Based on the same 3000 pseudo experiments as Fig. S13. The grey dashed line indicates the experimental p-value.

remaining sources, we select the same fraction ($\sim 5\%$) from the classes of BL Lacertae (BL Lac), Flat Spectrum Radio Quazar (FSRQ) and other types of AGNs by choosing the objects with the highest γ -ray flux after weighting by the IceCube sensitivity. Blazars of uncertain type are chosen if their flux in the 4FGL-DR2 catalog is higher than the faintest selected BL Lac or FSRQ. The final list consists of 59 BL Lac candidates, 34 FSRQ candidates, 2 blazar candidates of uncertain type, 5 AGNs, 9 other galaxies and 1 Galactic source. Overall, 83 out of 110 candidate sources in the updated list were previously searched (23) and 27 were not.

Binomial Test

We perform the binomial test described in (23) and apply it to the three assumptions about the energy spectrum ($\gamma = 2.0$, $\gamma = 2.5$, and γ free). The results of the three tests are shown in Fig. S23. Since the binomial p-value p_{min} of each of the three tests is obtained by scanning the threshold p-value p_k , below which the number of sources k is counted, we effectively test multiple hypotheses and need to correct each binomial p-value accordingly. We estimate the expected distribution of p_{min} for the background case from pseudo experiments, i.e. many repetitions of the experimental procedure. The resulting distributions of p_{min} for each of the spectral index hypotheses are shown in Fig. S15. Finally we need to account for having tested three different signal hypotheses: the corresponding background distribution of p-values is shown in Fig. S16. For further discussion on the results of the binomial test, see the Supplementary Text below.

Systematic Uncertainties

The IceCube detector is equipped with several devices to measure the optical properties of the glacial ice around the detector and to study the detection efficiency of its optical modules *in situ*. They are used to calibrate the detector response to incoming neutrino events. We have performed Monte Carlo simulations to estimate the impact of the corresponding systematic

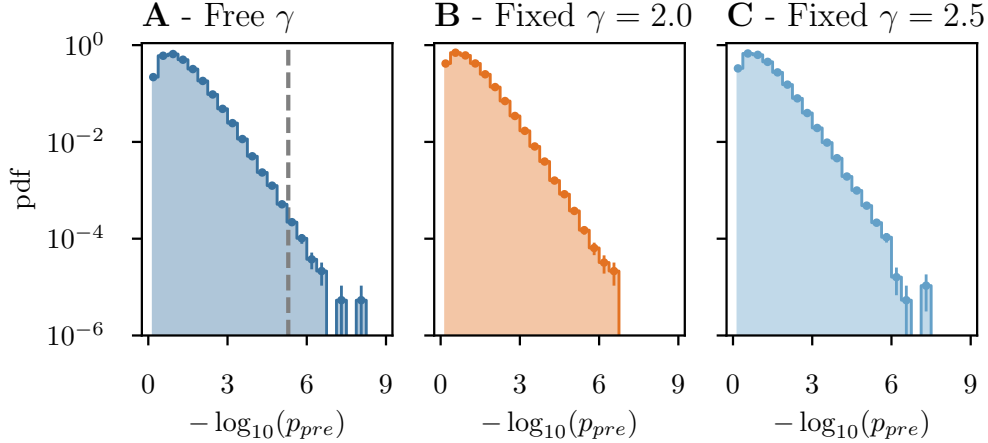


Figure S15: Background distributions of p-values in the binomial test. Based on 500,000 pseudo experiments and for the different signal hypotheses as indicated in the title. The most significant experimental result is shown as the grey dashed line in **A**.

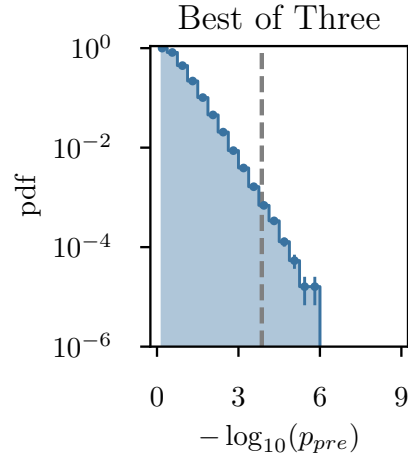


Figure S16: Background distribution of p-values after choosing the (trial-corrected) most significant value from the three binomial scans. The distribution is based on the same 500,000 pseudo experiments as for Fig. S15. The grey dashed line indicates the experimental p-value after the first trial correction.

uncertainties in our analysis: the absorption and scattering length of the ice, the detection efficiency of the DOMs, and the hole ice, produced when the drill holes were refreezing. The effect of the hole ice is modeled via the angular acceptance of the IceCube DOM, and mostly affected

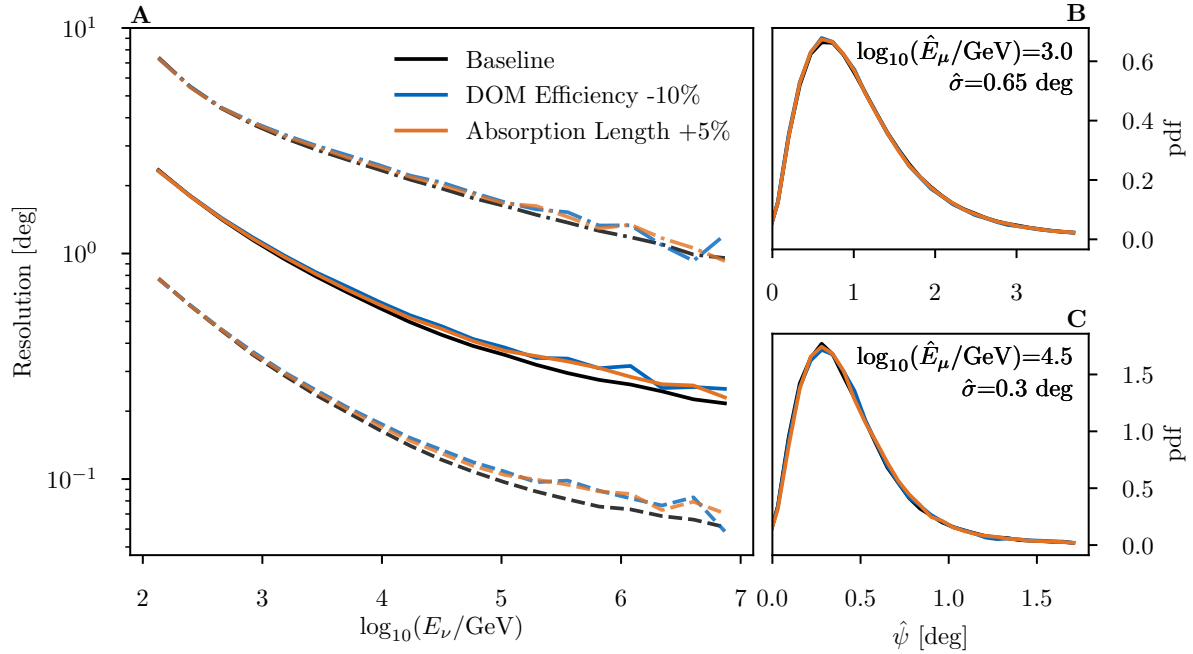


Figure S17: Impact of detector systematics on the pointing of track events. **(A)**: the 10%, 50% and 90% quantile of the opening angle between neutrino and reconstructed direction are shown as a function of the neutrino energy in dashed, solid and dashed-dotted, respectively. **(B)** and **(C)** show two exemplary point spread functions with the observables as indicated.

by one parameter p0, which ranges from -1 to 1 and modulates the acceptance of the face of the PMT (head-on). The parameterization covers a wide variety of acceptance curves obtained from calibration data (LED and lasers), lab measurements, and direct simulation. In Figure S17A we show the impact of the systematics on the angular resolution, i.e. the opening angle between neutrino and reconstructed direction, as a function of energy and examples of the point spread functions that enter the likelihood function. Systematic uncertainties lead to a degradation of the angular resolution by less than $\sim 5\%$ below a neutrino energy of 10 TeV. The impact increases to $\sim 10\%$ above a few hundred TeV. Figure S18 shows the influence of these systematic uncertainties on the parameter estimation of the analysis at the position of NGC 1068 for different numbers of injected signal events. To estimate the systematic uncertainty for our measurement

of NGC 1068 we evaluate those plots for all pseudo experiments with 79 fitted events. Two variations have a non-negligible impact on the spectral index estimation: increasing the absorption length by 5% and reducing the DOM efficiency by 10%. Roughly, both systematic uncertainties manifest in a reduction of the number of detected photons and hence impact directly the energy estimation, i.e., the track energies are under-estimated. Consequently, the measured spectrum shifts, with a median change $\Delta\gamma = +0.07$. Increasing the DOM efficiency on the other hand does not change the spectral index, but reduces the estimated signal strength $\Delta\mu_{\text{ns}} = -2$. Those effects are substantially smaller than the statistical uncertainties of the analysis. We conclude that systematic uncertainties have a small influence on the estimated source parameters, but the total uncertainty in this analysis remains dominated by the statistical one.

Table S1: Data sources. List of data in the electromagnetic spectrum used in Fig. 4 and related references.

Survey	Reference
NRAO VLA Sky Survey	(79)
XMM-Newton serendipitous survey IX	(80)
XMM-Newton slew survey catalog	(81)
Second ROSAT all-sky survey	(82)
2SXPS (Swift-XRT Point Source) catalog	(83)
Australia Telescope 20 GHz Survey	(84)
Very Large Array Low-frequency Sky Survey Redux (VLSSr)	(85)
Giant Metrewave Radio Telescope (GMRT) 150 MHz All-sky Survey	(86)
All-sky Murchison Widefield Array (GLEAM) survey—I	(87)
NRAOMPI 5 GHz Strong Source Surveys and the Parkes 2.7 GHz Surveys	(88)
Planck 2018	(89)
Two Micron All Sky Survey (2MASS)	(90)
AllWISE data release products	(91)
Second-Generation Guide Star Catalog	(92)
Pan-starrs1 surveys	(93)
Fourteenth data release of the Sloan Digital Sky Survey	(94)
GR2 and GR3 of the Galaxy Evolution Explorer (GALEX)	(95)
Serendipitous UV source catalogues	(96, 97)
Swift-BAT all-sky hard X-ray survey	(98)
HYPERLEDA	(61)

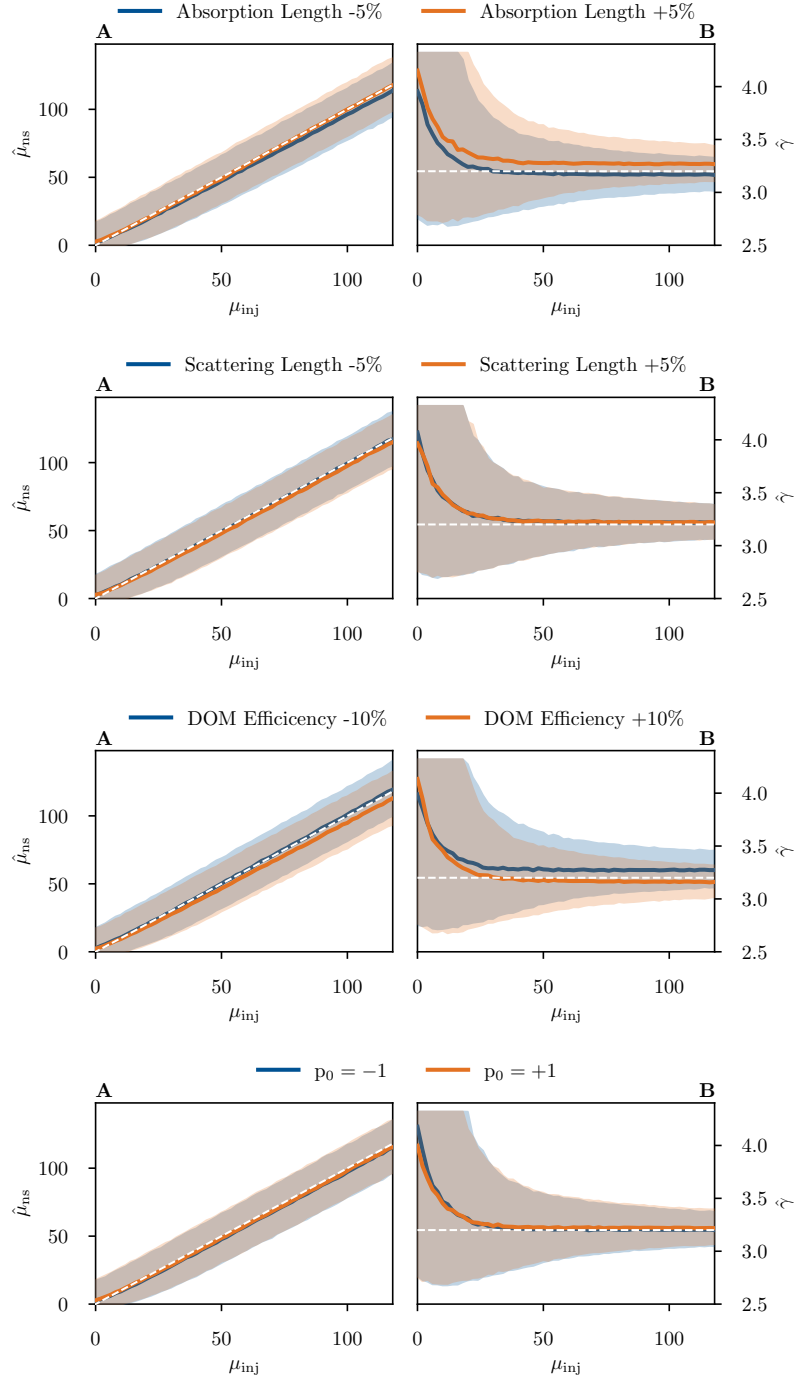


Figure S18: Impact of systematic variation on the parameter estimation at the position of NGC 1068. The estimation of the number of signal events (A) and the spectral index (B) are shown for varying systematics. The dashed white line gives the unbiased expectation, the solid line the median estimation and the shaded band the 68% quantile. See text for detailed explanation of the systematics.

Supplementary Text

Additional Searches for Point Sources of Neutrino Emission

Searching the Northern Hemisphere

We have searched the entire sky testing three different spectral index hypotheses. Searching the entire sky reduces the most significant location from a local significance of 5.3σ , found for the free spectral index scan, to 2.3σ . Correcting further for having tested multiple spectral indexes, the final significance is 2.0σ (see Fig. S13 and Fig. S14). Fig. 2A shows a zoom in on the most significant location in the Northern Sky, and Fig. S19 shows a wider view of the same region. In Fig. S20 and Fig. S21 the two additional skymaps for the fixed spectral index hypotheses are shown. A summary of the five most significant locations from all three scans are shown in Tab. S2. Two of the sources that were selected by the catalog binomial test (see text below) are spatially consistent with spots in this table: NGC 1068 with the most significant location in the free γ and $\gamma = 2.5$ cases, and TXS 0506+056 with the third best location in the $\gamma = 2.0$ case. Moreover, we note a posteriori that the nearby Seyfert I galaxy NGC 4151 is located at a distance of 0.18° from the fourth best location in the skymap for $\gamma = 2.5$.

Pre-defined List of Sources

Tab. S3 reports the list of candidate neutrino sources. Each source in the list was analyzed individually by calculating the TS at its location in the sky. For each source, Tab. S3 lists the estimated flux parameters and corresponding significances. It also provides 90% confidence level (C.L.) upper limits $\Phi_{90\%}$ on the flux normalization assuming emission with spectral index $\gamma = 2.0$

$$\Phi_{\nu_\mu + \bar{\nu}_\mu, 90\%} = \Phi_{90\%} (E_\nu/\text{TeV})^{-2} \times 10^{-13} \text{ TeV}^{-1} \text{ cm}^{-2} \text{ s}^{-1}. \quad (\text{S17})$$

The upper limit $\Phi_{90\%}$ is defined as the flux normalization for which one expects a *TS* larger or equal to the observed one with 90% probability (99). It is found by performing pseudo

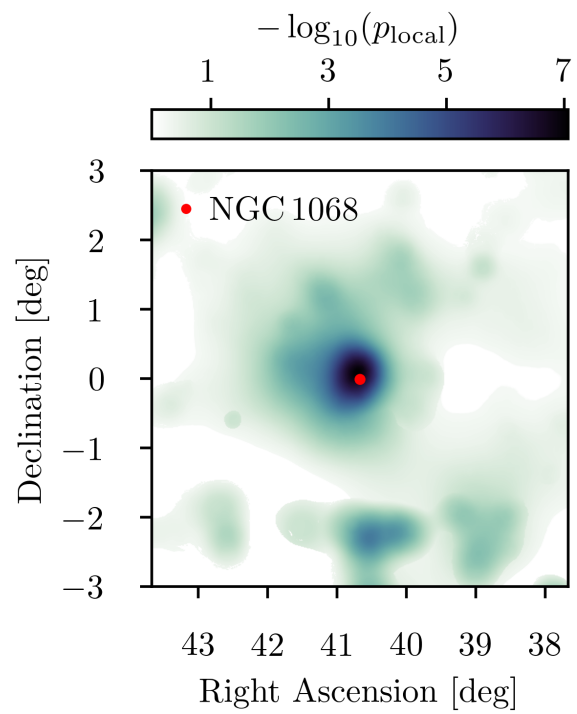


Figure S19: **Scan around the most significant location in the Northern Hemisphere (free spectral index).** The color represents the local p-value and the red dot the position of NGC 1068.

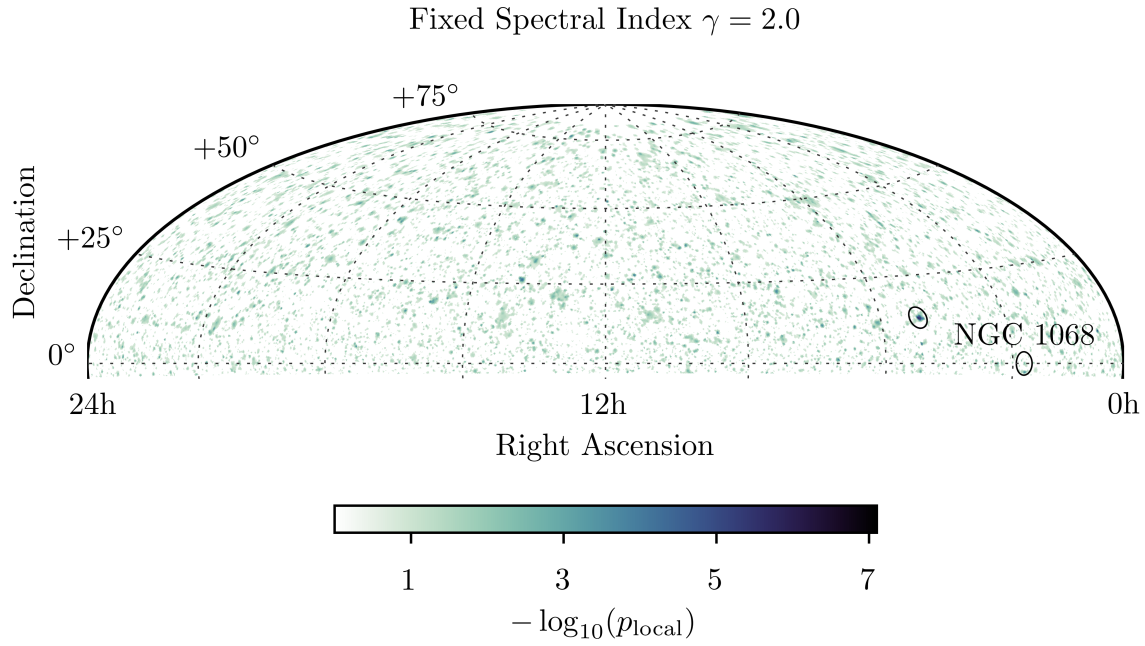


Figure S20: **Same as Fig. 1, but for a fixed spectral index of $\gamma = 2.0$.** The black circles indicate the position of NGC 1068, which is also labelled, and the most significant location.

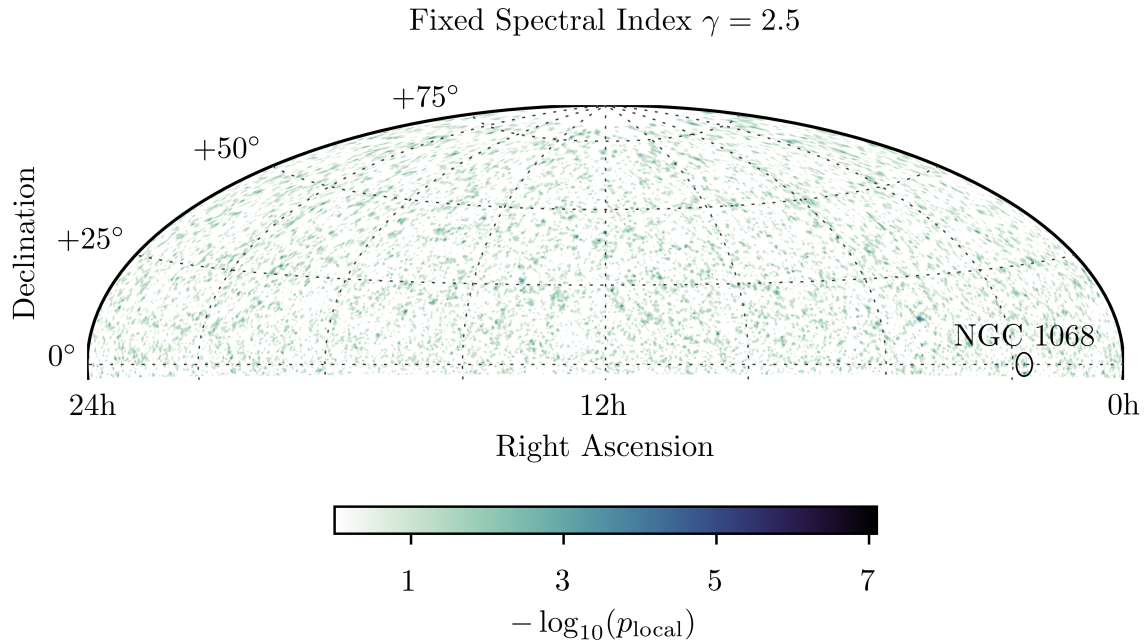


Figure S21: **Same as Fig. S20, but for a fixed spectral index of $\gamma = 2.5$.** Here the most significant location and the position of NGC 1068 are spatially consistent.

Table S2: **The five most significant locations in each of the three sky scans.** For each location in each of the three sky scans, we list the coordinates (right ascension α and declination δ) in degrees, the best-fitting number of signal events $\hat{\mu}_{\text{ns}}$ and spectral index $\hat{\gamma}$, and the negative common logarithm of the local p-value. The local p-values are not corrected for trials. The global p-value accounts for having evaluated a large number of positions in the sky using three spectral index assumptions (see text).

	α [°]	δ [°]	$\hat{\mu}_{\text{ns}}$	$\hat{\gamma}$	$-\log_{10}(p_{\text{local}})$
$\gamma = 2.0$					
#1	76.93	12.90	13.4	2.00	6.08
#2	9.76	7.50	4.9	2.00	5.04
#3	77.37	5.57	6.2	2.00	4.88
#4	179.25	52.44	5.5	2.00	4.87
#5	202.63	33.89	7.1	2.00	4.74
$\gamma = 2.5$					
#1	40.65	0.09	36.8	2.50	5.84
#2	177.91	23.24	21.4	2.50	5.45
#3	105.78	1.03	23.6	2.50	5.17
#4	182.46	39.52	22.2	2.50	4.91
#5	180.16	42.21	26.0	2.50	4.86
Free γ					
#1	40.69	0.09	80.7	3.20	7.30
#2	297.27	27.45	69.8	3.24	5.51
#3	76.93	12.90	11.2	1.81	5.37
#4	180.20	42.19	47.8	3.03	4.80
#5	208.15	23.16	55.5	3.19	4.60

experiments and injecting signal events with spectrum $\gamma = 2.0$ and varying flux normalizations. These limits are compared to the corresponding sensitivity and discovery potential fluxes in Fig. S22A. The 90% C.L. upper limits are also compared to the corresponding sensitivities and discovery potentials assuming neutrino emission with $\gamma = 2.5$ (Fig. S22B) and $\gamma = 3.2$ (Fig. S22C).

Binomial Test

After having applied the binomial test (23) to the three signal hypotheses ($\gamma = 2.0$, $\gamma = 2.5$, and γ free), the lowest binomial p-value is obtained when the spectral index is treated as unknown (Fig. S23), which yields $k = 3$ and identifies the candidate sources NGC 1068, PKS 1424+240, and TXS 0506+056. We find a significance of 3.7σ . After accounting for having tested three spectral index scenarios, the final binomial significance is 3.4σ . A previous search (23) reported a 3.3σ significance. There, only the free spectral index case hypothesis was tested.

Neutrinos From the Direction of NGC 1068

We compared the previously reported excess from the direction of the NGC 1068 (23) with our result. First, we have investigated the 79 neutrino-induced events contributing to the excess from the direction of NGC 1068. All events show a clear track-like signature. The 3D views of the 10 events that contribute most to the *TS* are shown in Fig. S24, together with the corresponding spatial term in the point source likelihood (Eq. (S10)). For all of these events, with properties summarized in Tab. S4, the spatial pdfs used in our analysis are consistent with the expectation from Monte Carlo simulations. For two events in particular (numbers 7 and 10) we find substantially different results to the previous search (23) due to their low reconstructed energies of ≈ 1 TeV and the soft spectral index of $\hat{\gamma} = 3.2$, which produce spatial pdfs wider than the Gaussian distribution.

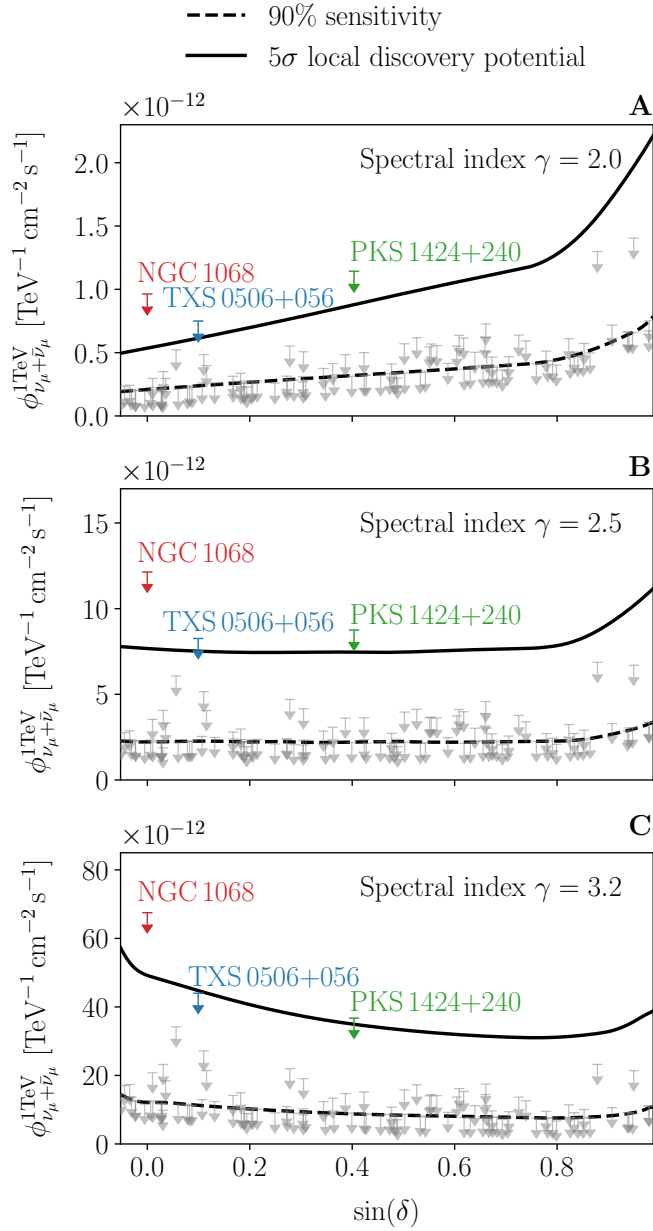


Figure S22: **Upper limit (90% C.L.) neutrino flux.** Each of the plots assumes a different spectral emission, with $\gamma = 2.0$ (**A**), $\gamma = 2.5$ (**B**) and $\gamma = 3.2$ (**C**). Each source in the searched catalog is represented by a downward-pointing arrow. The arrows of the three most significant objects in this analysis are annotated. The dashed and solid lines show the local sensitivity and 5σ discovery potential fluxes, respectively. In each case, the tested signal hypothesis assumes a free spectral index.

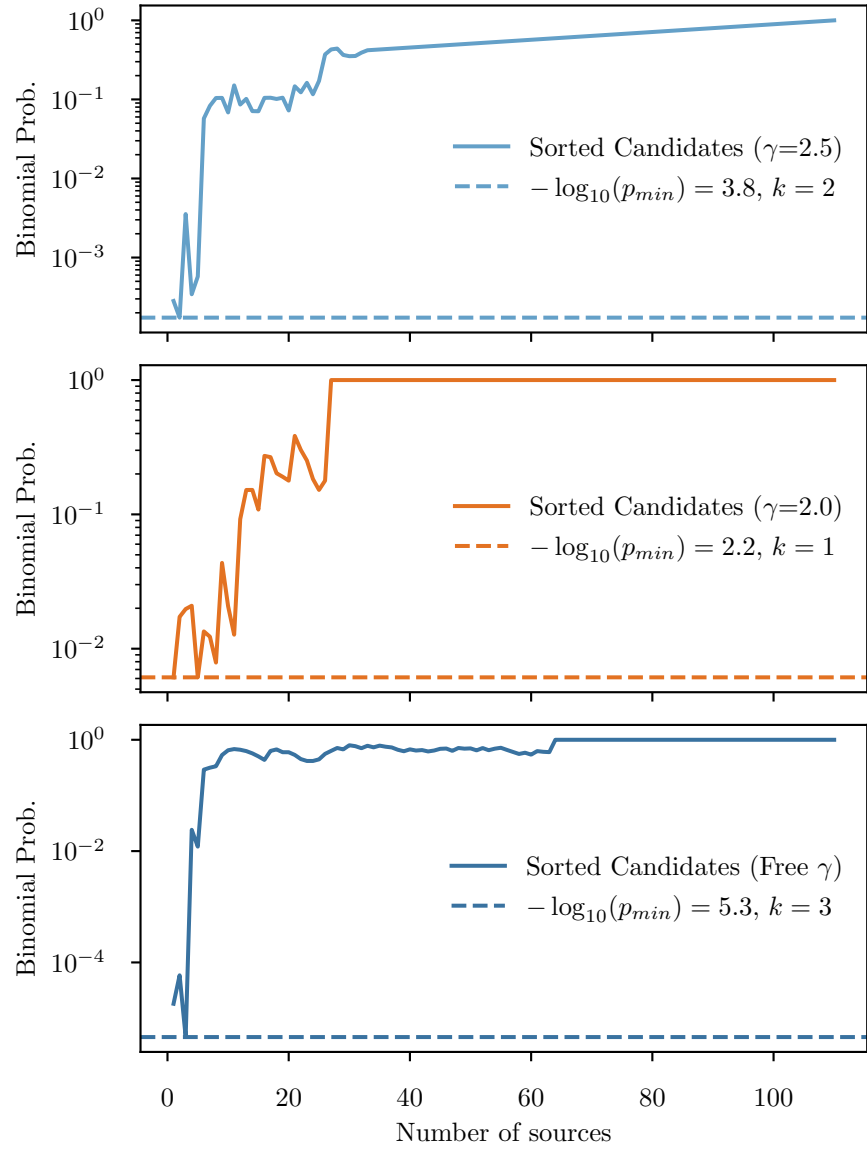


Figure S23: **Evolution of the binomial background probabilities for the three signal hypothesis.** In each plot the horizontal axis indicates the k most significant sources, while the vertical index gives the corresponding binomial probability. The minimum probability is indicated in each plot as a dashed line, numerical results are given in the legend. For $\gamma = 2.0$ the minimal p-value is found for $k = 1$ source (TXS 0506+056) and for $\gamma = 2.5$ for $k = 2$ sources (NGC 1068 and TXS 0506+056) contributing.

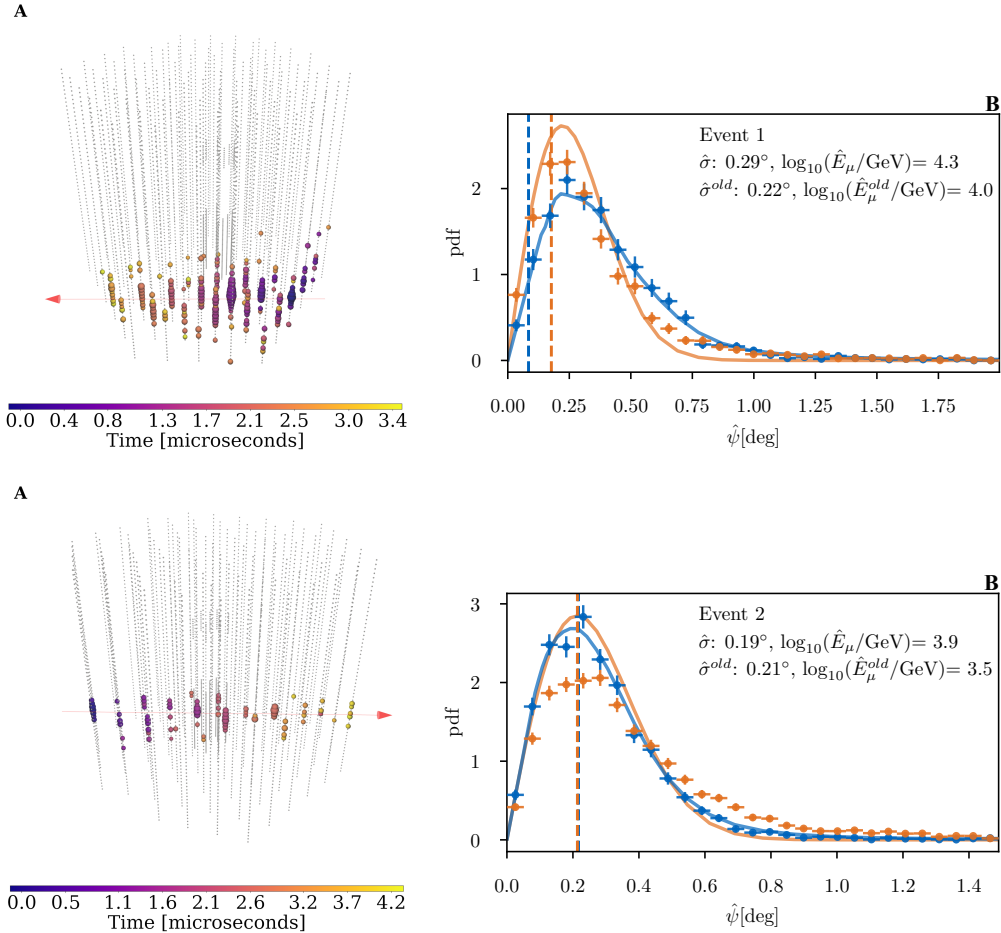


Figure S24: Event views of the top events (top 1 - top 2) contributing to the excess at the position of NGC 1068. In each row (A) shows a 3D view of the event, where the bubbles represent the DOMs with recorded photons, and the color represents the time of the first photon hit from purple (early) to yellow (late); the reconstructed event direction is shown as a red arrow. (B) shows the corresponding spatial term of the likelihood for our analysis (blue) and the previous search (23) (orange). Solid lines show the pdfs, markers with error bars show the Monte Carlo expectation, and the vertical dashed lines indicate the observed distance between the coordinates of NGC 1068 and the event. The Monte Carlo expectations differ because of the different energy and angular error estimators used in the respective analysis.

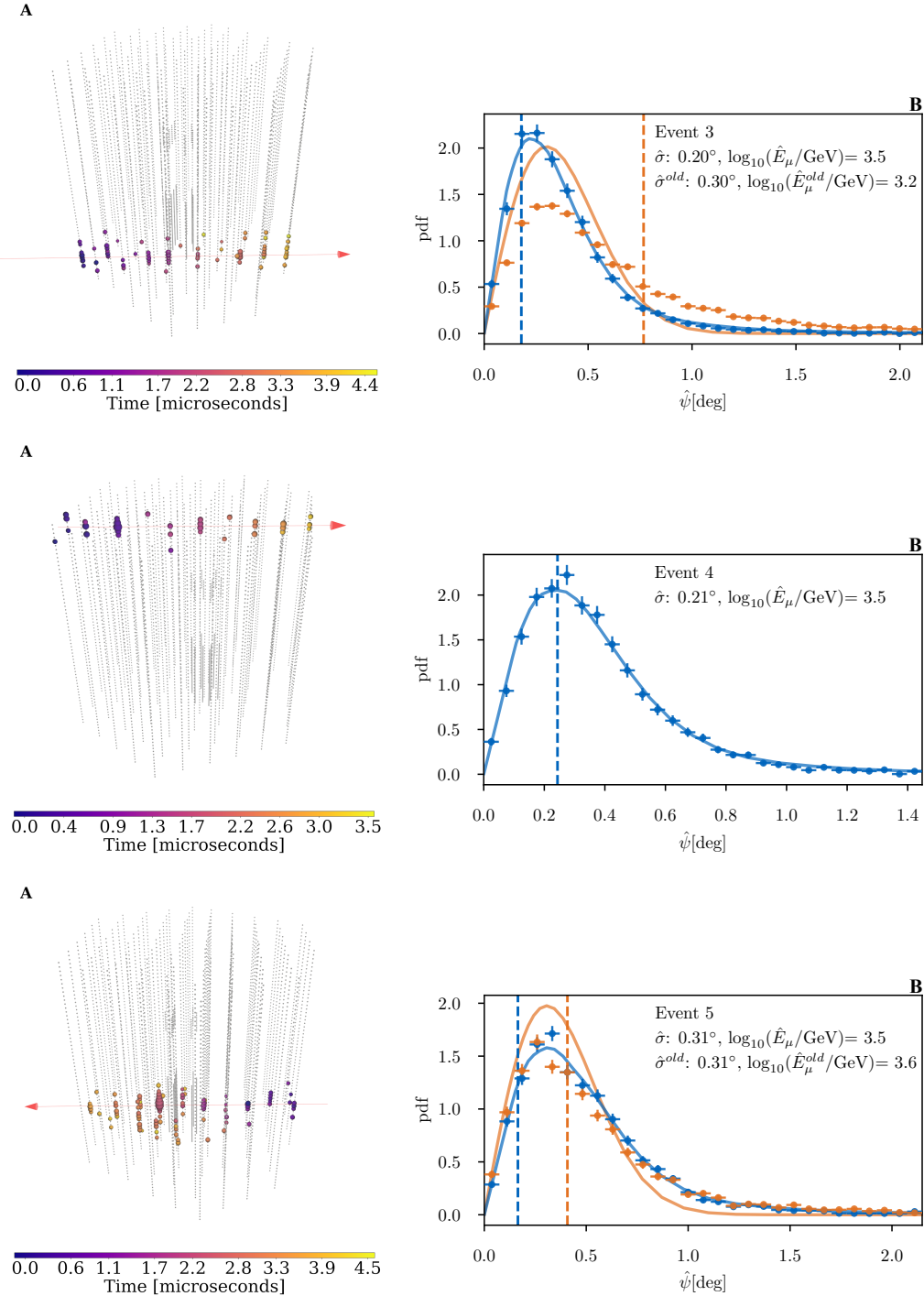


Figure S25: Same as Fig. S24, but for events 3-5

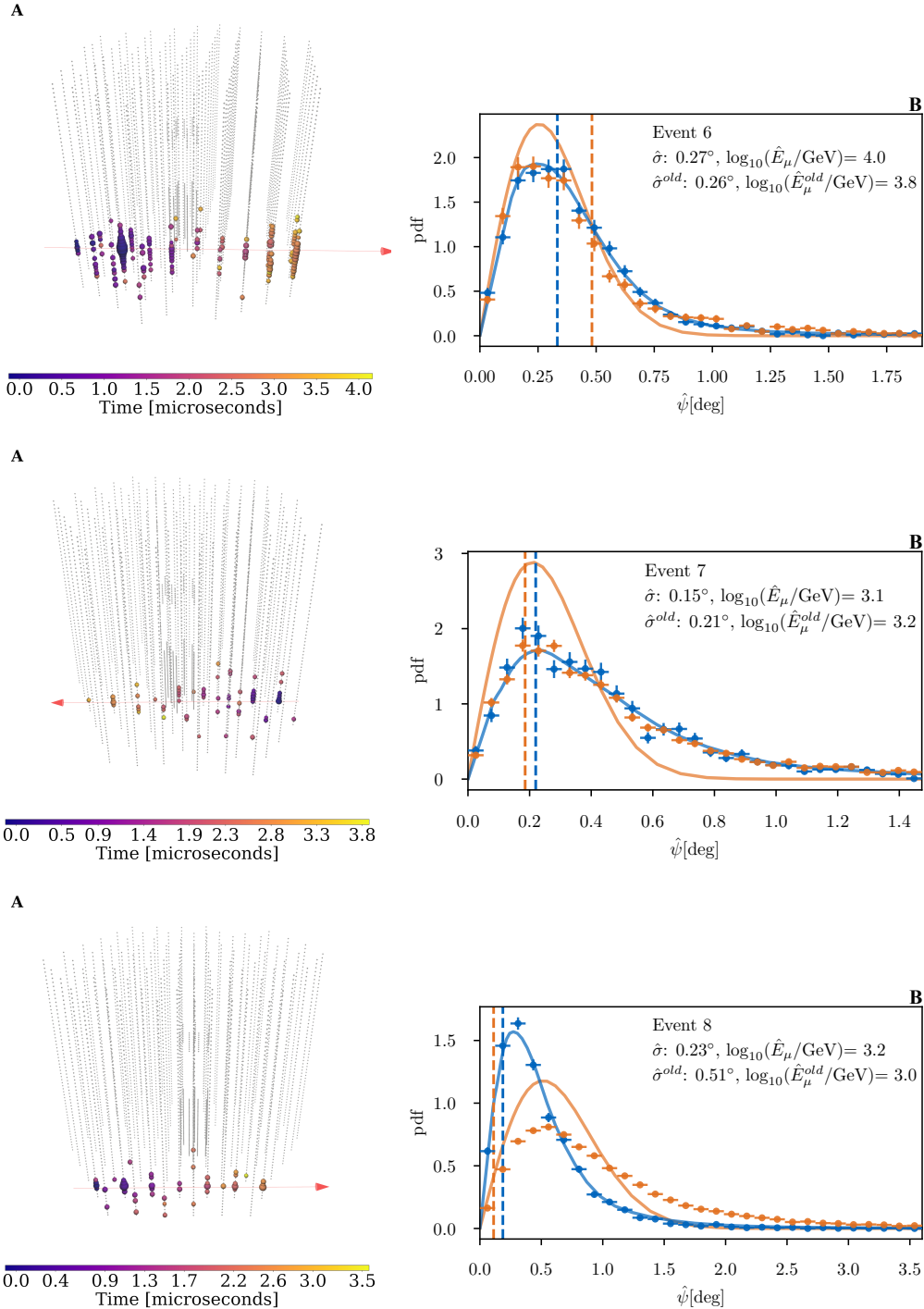


Figure S26: Same as Fig. S24, but for events 6-8

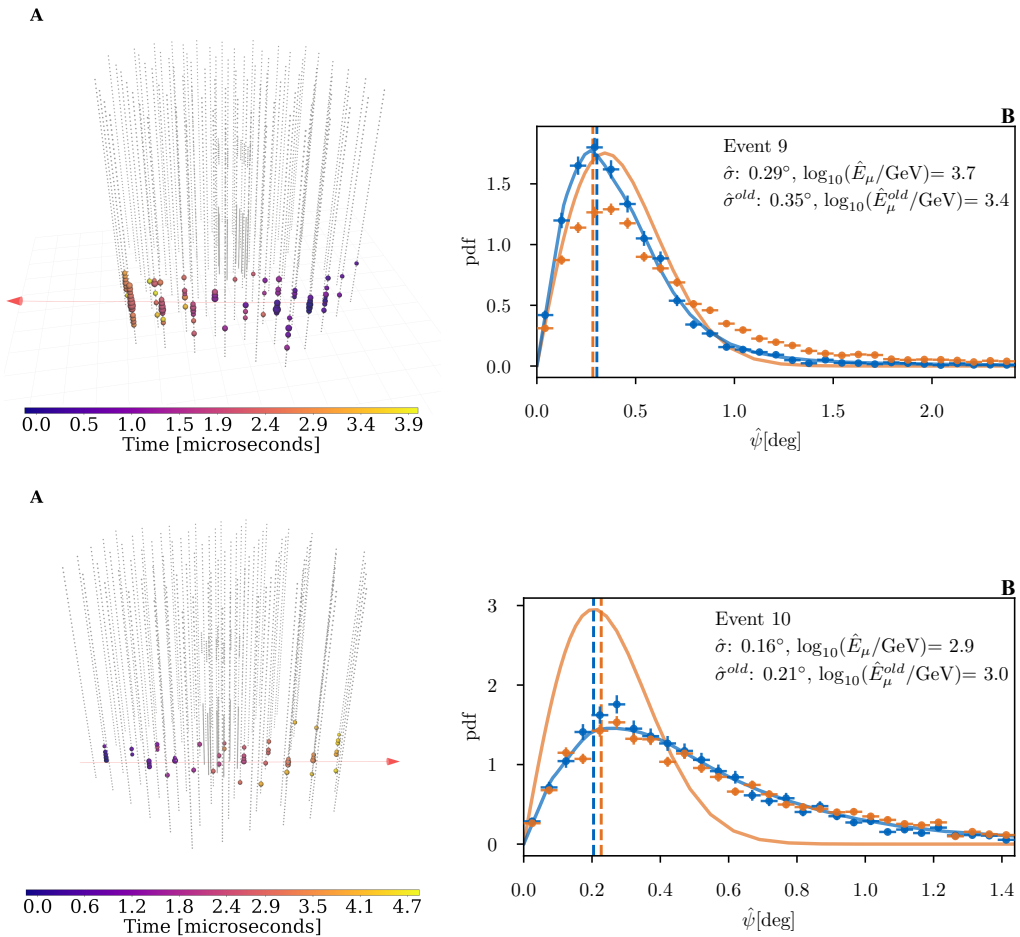


Figure S27: Same as Fig. S24, but for events 9-10

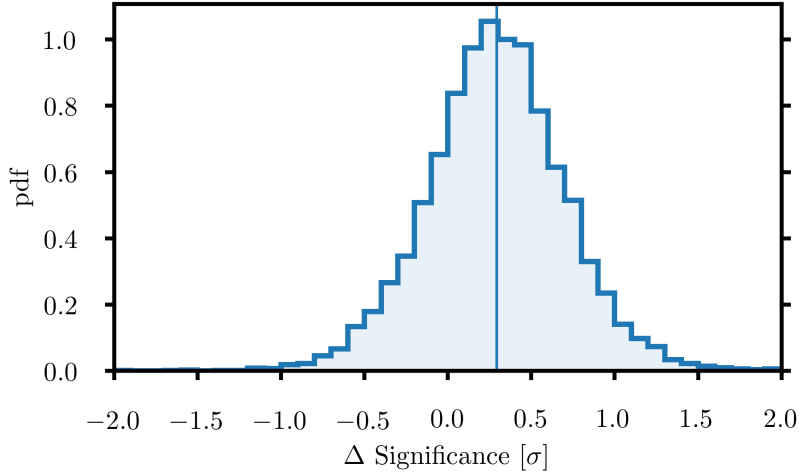


Figure S28: Significance difference between our result and a previous search (23). The distribution was determined from a set of pseudo experiments which is evaluated with both analysis approaches. The vertical solid line gives the median value of 0.3σ .

We have generated Monte Carlo pseudo experiments that model neutrino emission from NGC 1068 by generating background events and adding a signal at the source position using the best-fitting parameters we observed. These pseudo datasets were analyzed using both our method and that adopted in previous works, including (23).

As shown in Fig. S28, using identical events, we find a median significance higher by $\sim 0.3\sigma$ compared to previous methods. This is consistent with our a posteriori investigations of the experimental data: had we analyzed the identical experimental events using the same calibrations but with the previous analysis methods (likelihood function, energy reconstruction and angular error estimation), a lower significance of 3.8σ would have been obtained. The previous analysis (23), which used a slightly different event selection (different selection criteria, data taking period and older data calibration methods), reported a significance of 2.9σ at the location of NGC 1068. Fig. S29 compares our results (Fig. S29C) with the re-analysis using data sample, methods and calibrations from the previous analysis (Fig. S29A). In Fig. S29B, we have reverted the reconstructed directions of overlapping events to the ones reported in (23), thus, for

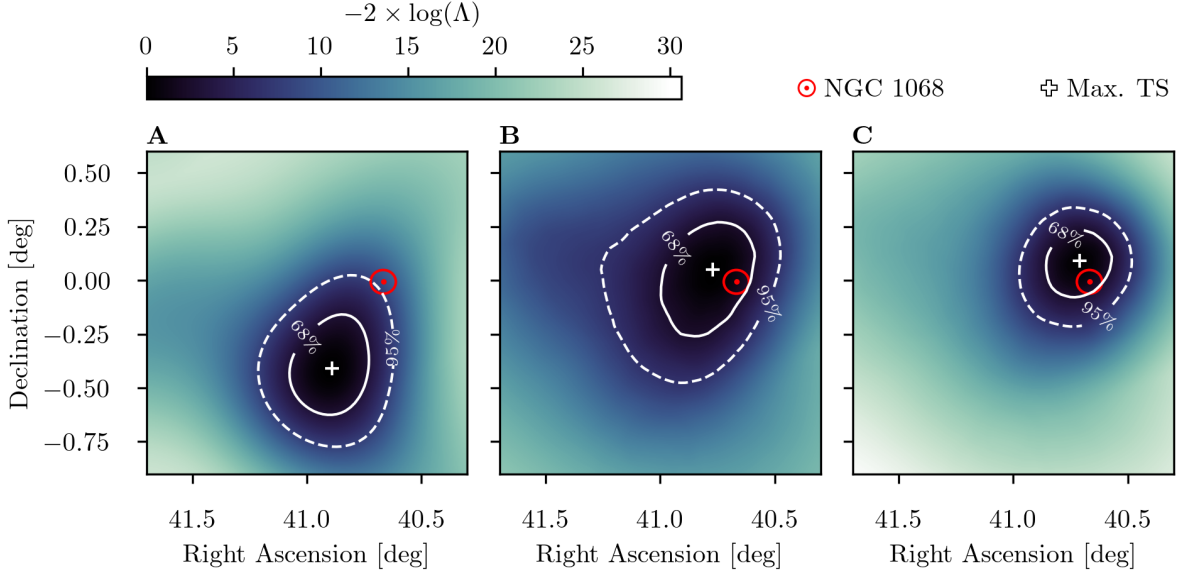


Figure S29: Regions around the best-fitting locations using different analysis methods. (A): the best-fitting position and the corresponding test-statistic value from the previous search (23). (C): our result from Fig. 2A but shown over a wider area. (B): our result when using the reconstructed directions from (23). The significance at the position of NGC 1068 (red dot with red circle indicating the dimension of the galaxy in the optical wavelength) changes from 2.9σ (A), 3.3σ (B) to 4.2σ (C). The 68% (solid) and 95% (dashed) confidence contours are derived from pseudo experiments assuming the best-fitting flux measured in this work.

the most part, removing the impact of our adopted calibrations and reprocessing (e.g. charge calibration and waveform unfolding). In this case the most significant location has a significance of 3.3σ . We find that, of the increase in significance of NGC 1068 compared to previous work, 0.4 sigma (2.9σ in Fig. S29A to 3.3σ in Fig. S29B) can be attributed to the differences in analysis methods, and 0.9 sigma (3.3σ in Fig. S29B to 4.2σ in Fig. S29C) to the differences in calibration and reprocessing. Another difference between this work and the previous one (23) concerns the derivation of the background test-statistics distributions that enter the significance calculation: this work uses a simulation based method, while the previous result was based on the data scrambling method. Using data scrambling in this work yields 4.4σ for NGC 1068.

Tab. S4 lists the ten events which contribute most to our observed *TS* (see Fig. S24-S27) and

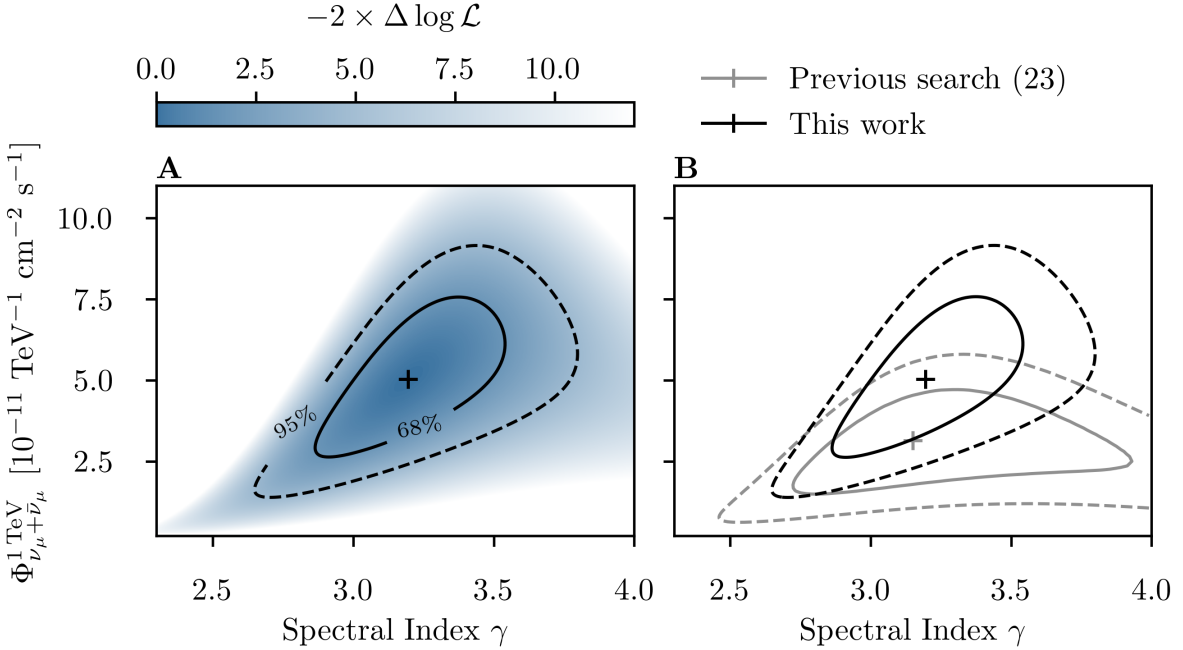


Figure S30: **Profile likelihood scan for the flux parameters of NGC 1068.** (A): same as Fig. 3. (B) compares the result of this analysis (black) to the previous search (23) (grey).

compares their signal-over-background ratio and ranking to those in the previous analysis (23).

The distance between the best-fitting position to the location of NGC 1068 changes only marginally, from 0.11° to 0.13° when the four highest weighted events are removed. We conclude the derived location is robust. The previous search (23) found an offset of 0.35deg , which we find only when the ten highest weighted events are removed.

The estimation of the NGC 1068 neutrino spectrum has changed slightly compared to the previous search (23) (Fig. S30B). The uncertainties have narrowed and the flux normalization has increased.

Table S3: Catalog of pre-defined candidate sources in the northern hemisphere. Sources are ordered by ascending right ascension coordinate α , except for the three most significant sources with pre-trial p-values less than 0.01 which are at the top of the table and are separated from the rest of the list by a horizontal line. For each source we list the name, source type, equatorial coordinates (J2000 equinox) from the gamma-ray catalog (32), and likelihood search results: number of signal events \hat{n}_s , spectral index $\hat{\gamma}$, negative common logarithm of the local p-value and corresponding significance in brackets, 90% CL astrophysical flux upper-limit ($\Phi_{90\%}$) with $\Phi_{\nu_\mu + \bar{\nu}_\mu, 90\%} = \Phi_{90\%} (E_\nu/\text{TeV})^{-2} \times 10^{-13} \text{ TeV}^{-1} \text{ cm}^{-2} \text{ s}^{-1}$. NGC 1068 is also an AGN and TXS 0506+056 has been classified as FSRQ (22). Sources followed by (*) were not included in the previous search (23). Abbreviations are: BLL = BL Lac, FSRQ = Flat Spectrum Radio Quasar, AGN = Active Galactic Nuclei, SBG = Starburst Galaxy, GAL = Galaxy, NLSY1 = Narrow-line Seyfert I Galaxy, RDG = Radio Galaxy, UID = Unidentified Gamma-Ray Source, BCU = Blazar Candidate of Uncertain Type.

Source Name	Source Type	α [°]	δ [°]	\hat{n}_s	$\hat{\gamma}$	$-\log_{10} p_{\text{local}}$	$\Phi_{90\%}$
NGC 1068	SBG/AGN	40.67	-0.01	79	3.2	7.0 (5.2 σ)	9.6
PKS 1424+240	BLL	216.76	23.80	77	3.5	4.0 (3.7 σ)	11.4
TXS 0506+056	BLL/FSRQ	77.36	5.70	5	2.0	3.6 (3.5 σ)	7.5
PKS 0019+058	BLL	5.64	6.13	1	2.4	0.4 (0.2 σ)	2.6
1ES 0033+595 (*)	BLL	8.98	59.83	0	4.3	0.0 (0.0 σ)	5.0
M 31	GAL	10.82	41.24	13	3.3	0.8 (1.0 σ)	6.2
4C +01.02	FSRQ	17.17	1.58	0	4.3	0.0 (0.0 σ)	2.1
S2 0109+22	BLL	18.03	22.75	10	2.8	0.7 (0.8 σ)	4.8
B3 0133+388	BLL	24.14	39.10	0	4.3	0.0 (0.0 σ)	3.8
TXS 0141+268	BLL	26.15	27.09	0	4.3	0.0 (0.0 σ)	3.2
MITG J021114+1051	BLL	32.81	10.86	0	4.3	0.0 (0.0 σ)	2.6
PKS 0215+015	FSRQ	34.46	1.73	2	3.9	0.2 (0.0 σ)	1.9
B2 0218+357	FSRQ	35.28	35.94	8	4.3	0.4 (0.2 σ)	4.1
3C 66A	BLL	35.67	43.04	0	4.3	0.0 (0.0 σ)	3.9
4C +28.07	FSRQ	39.47	28.80	3	2.9	0.3 (0.0 σ)	3.4
PKS 0235+164	BLL	39.67	16.62	5	3.9	0.3 (0.0 σ)	2.8
NGC 1275	RDG	49.96	41.51	8	3.0	0.5 (0.5 σ)	5.1
PKS 0336-01	FSRQ	54.88	-1.78	4	4.3	0.3 (0.1 σ)	2.1
PKS 0420-01	FSRQ	65.83	-1.33	0	4.3	0.0 (0.0 σ)	2.0
4C +41.11 (*)	BLL	65.98	41.83	0	4.3	0.0 (0.0 σ)	3.9
PKS 0422+00	BLL	66.19	0.60	0	4.3	0.0 (0.0 σ)	2.1
MG2 J043337+2905	BLL	68.41	29.10	0	4.3	0.0 (0.0 σ)	3.4
PKS 0440-00	FSRQ	70.66	-0.30	1	2.7	0.3 (0.0 σ)	2.0
S3 0458-02	FSRQ	75.30	-1.97	9	4.3	0.5 (0.4 σ)	2.4
PKS 0502+049	FSRQ	76.34	5.00	0	4.3	0.0 (0.0 σ)	2.3

Source Name	Source Type	α [°]	δ [°]	\hat{n}_s	$\hat{\gamma}$	$-\log_{10} p_{\text{local}}$	$\Phi_{90\%}$
PKS 0507+17 (*)	FSRQ	77.52	18.01	0	4.3	0.0 (0.0 σ)	2.9
TXS 0518+211	BLL	80.44	21.21	8	2.8	0.6 (0.6 σ)	4.1
OG 050	FSRQ	83.17	7.55	10	3.8	0.4 (0.2 σ)	2.6
TXS 0603+476 (*)	BLL	91.86	47.66	19	4.3	0.6 (0.7 σ)	5.9
B3 0609+413	BLL	93.22	41.37	5	2.1	1.1 (1.4 σ)	7.3
NGC 2146 (*)	SBG	94.53	78.33	0	3.0	0.0 (0.0 σ)	6.7
B2 0619+33 (*)	BCU	95.73	33.43	22	3.8	0.7 (0.9 σ)	5.5
1ES 0647+250	BLL	102.70	25.05	0	4.3	0.0 (0.0 σ)	3.2
PMN J0709-0255 (*)	FSRQ	107.45	-2.93	0	2.5	0.0 (0.0 σ)	2.0
S5 0716+71	BLL	110.49	71.34	0	4.3	0.0 (0.0 σ)	6.6
4C +14.23	FSRQ	111.32	14.42	6	4.3	0.3 (0.0 σ)	2.6
PKS 0735+17	BLL	114.54	17.71	9	4.3	0.3 (0.1 σ)	3.1
PKS 0736+01	FSRQ	114.82	1.62	8	4.3	0.3 (0.1 σ)	2.1
1ES 0806+524	BLL	122.46	52.31	0	4.3	0.0 (0.0 σ)	4.3
OJ 014	BLL	122.86	1.78	30	4.0	0.9 (1.1 σ)	3.5
S4 0814+42	BLL	124.56	42.38	0	2.9	0.0 (0.0 σ)	3.9
PKS 0829+046	BLL	127.97	4.49	0	3.0	0.0 (0.0 σ)	2.2
SBS 0846+513 (*)	NLSY1	132.51	51.14	6	3.3	0.4 (0.3 σ)	5.1
OJ 287	BLL	133.71	20.12	16	4.3	0.5 (0.4 σ)	3.7
S4 0917+44 (*)	FSRQ	140.23	44.70	0	4.3	0.0 (0.0 σ)	4.1
PMN J0948+0022	NLSY1	147.24	0.37	6	4.3	0.3 (0.1 σ)	2.3
M 82	SBG	148.95	69.67	0	4.3	0.0 (0.0 σ)	6.6
4C +55.17	FSRQ	149.42	55.38	9	3.1	0.6 (0.6 σ)	6.1
1H 1013+498	BLL	153.77	49.43	0	4.3	0.0 (0.0 σ)	4.1
GB6 J1037+5711 (*)	BLL	159.43	57.19	0	4.3	0.0 (0.0 σ)	4.8
S5 1044+71 (*)	FSRQ	162.11	71.73	45	4.3	1.3 (1.6 σ)	14.0
NGC 3424 (*)	SBG	162.91	32.89	0	4.3	0.0 (0.0 σ)	3.5
4C +01.28	BLL	164.62	1.56	0	4.3	0.0 (0.0 σ)	2.1
TXS 1055+567 (*)	BLL	164.67	56.46	8	4.3	0.4 (0.3 σ)	5.0
Mkn 421	BLL	166.12	38.21	4	4.3	0.3 (0.0 σ)	3.7
IC 678 (*)	GAL	168.56	6.63	22	3.1	0.9 (1.2 σ)	4.0
Arp 299	SBG	172.07	58.52	10	4.3	0.4 (0.4 σ)	5.7
PKS B1130+008	BLL	173.20	0.57	20	3.9	0.7 (0.8 σ)	3.0
Ton 599	FSRQ	179.88	29.24	2	4.3	0.2 (0.0 σ)	3.0
B2 1215+30	BLL	184.48	30.12	15	3.1	0.9 (1.1 σ)	5.7
PKS 1216-010	BLL	184.64	-1.33	0	3.7	0.0 (0.0 σ)	2.0

Source Name	Source Type	α [°]	δ [°]	\hat{n}_s	$\hat{\gamma}$	$-\log_{10} p_{\text{local}}$	$\Phi_{90\%}$
PG 1218+304	BLL	185.34	30.17	0	3.1	0.0 (0.0 σ)	3.4
W Comae	BLL	185.38	28.24	0	4.3	0.0 (0.0 σ)	3.3
4C +21.35	FSRQ	186.23	21.38	0	4.3	0.0 (0.0 σ)	3.2
3C 273	FSRQ	187.27	2.05	21	4.3	0.6 (0.7 σ)	3.0
ON 246	BLL	187.56	25.30	0	4.3	0.0 (0.0 σ)	3.2
M 87	RDG	187.71	12.39	0	0.6	0.0 (0.0 σ)	2.8
MITG J123931+0443	FSRQ	189.89	4.73	0	4.3	0.0 (0.0 σ)	2.4
PG 1246+586	BLL	192.08	58.34	0	4.3	0.0 (0.0 σ)	4.8
S4 1250+53	BLL	193.31	53.02	0	4.3	0.0 (0.0 σ)	4.0
B3 1343+451	FSRQ	206.39	44.88	5	2.9	0.4 (0.3 σ)	4.7
NGC 5380 (*)	GAL	209.33	37.50	4	2.4	0.9 (1.2 σ)	6.4
NVSS J141826-023336	BLL	214.61	-2.56	6	3.9	0.4 (0.4 σ)	2.3
PKS 1441+25	FSRQ	220.99	25.03	3	2.1	0.7 (0.9 σ)	5.0
TXS 1452+516 (*)	BLL	223.62	51.41	0	2.3	0.0 (0.0 σ)	4.4
PKS 1502+106	FSRQ	226.10	10.50	1	1.8	0.5 (0.5 σ)	3.4
PKS 1502+036	NLSY1	226.27	3.45	0	4.3	0.0 (0.0 σ)	2.1
B2 1520+31	FSRQ	230.55	31.74	35	4.3	1.0 (1.3 σ)	6.2
Arp 220 (*)	SBG	233.70	23.53	0	4.3	0.0 (0.0 σ)	3.1
GB6 J1542+6129	BLL	235.76	61.50	16	3.0	1.9 (2.2 σ)	13.0
PG 1553+113	BLL	238.93	11.19	2	4.3	0.2 (0.0 σ)	2.3
4C +15.54 (*)	BLL	241.77	15.84	0	4.3	0.0 (0.0 σ)	2.9
4C +38.41	FSRQ	248.82	38.14	4	2.3	0.9 (1.1 σ)	6.2
Mkn 501	BLL	253.47	39.76	15	4.3	0.5 (0.5 σ)	5.0
PKS 1717+177	BLL	259.81	17.75	34	4.3	1.0 (1.2 σ)	5.1
1H 1720+117	BLL	261.27	11.87	0	4.3	0.0 (0.0 σ)	2.7
S4 1749+70	BLL	267.16	70.10	0	4.3	0.0 (0.0 σ)	6.6
OT 081	BLL	267.88	9.65	0	2.9	0.0 (0.0 σ)	2.7
RX J1754.1+3212 (*)	BLL	268.55	32.20	0	4.3	0.0 (0.0 σ)	3.4
S5 1803+784 (*)	BLL	270.17	78.47	0	2.7	0.0 (0.0 σ)	7.5
NVSS J184425+154646 (*)	BLL	281.12	15.79	11	4.3	0.4 (0.2 σ)	3.1
LQAC 284+003 (*)	BCU	284.48	3.22	12	2.5	2.0 (2.3 σ)	5.2
TXS 1902+556	BLL	285.81	55.68	3	4.3	0.3 (0.0 σ)	4.6
MGRO J1908+06	UID	286.91	6.32	2	1.8	1.4 (1.7 σ)	4.8
RX J1931.1+0937	BLL	292.78	9.63	15	4.3	0.5 (0.4 σ)	3.1
87GB 194024.3+102612 (*)	BLL	295.70	10.56	0	4.3	0.0 (0.0 σ)	2.6
1ES 1959+650	BLL	300.01	65.15	8	3.4	0.5 (0.4 σ)	7.2

Source Name	Source Type	α [°]	δ [°]	\hat{n}_s	$\hat{\gamma}$	$-\log_{10} p_{\text{local}}$	$\Phi_{90\%}$
MITG J200112+4352	BLL	300.30	43.89	3	4.3	0.3 (0.0 σ)	3.6
7C 2010+4619 (*)	BLL	303.02	46.49	4	2.5	0.7 (0.9 σ)	6.4
MITG J201534+3710	FSRQ	303.89	37.18	19	3.6	0.7 (0.9 σ)	5.5
PKS 2032+107	FSRQ	308.85	10.94	0	4.3	0.0 (0.0 σ)	2.8
B2 2114+33	BLL	319.06	33.66	12	2.9	0.8 (0.9 σ)	5.7
OX 169	FSRQ	325.89	17.73	4	4.3	0.3 (0.0 σ)	2.7
BL Lac	BLL	330.69	42.28	11	4.3	0.4 (0.3 σ)	4.7
CTA 102	FSRQ	338.15	11.73	0	4.3	0.0 (0.0 σ)	2.6
B2 2234+28A (*)	FSRQ	339.10	28.48	8	3.2	0.4 (0.3 σ)	4.1
RGB J2243+203	BLL	340.99	20.36	5	3.6	0.3 (0.0 σ)	2.8
TXS 2241+406	FSRQ	341.06	40.96	0	4.3	0.0 (0.0 σ)	3.9
3C 454.3	FSRQ	343.50	16.15	1	1.5	1.2 (1.6 σ)	5.5
B2 2308+34 (*)	FSRQ	347.77	34.42	19	3.6	0.7 (0.9 σ)	5.6

Table S4: The ten events which contribute most to the test statistic at the position of NGC 1068. Ranking and characteristic of the top 10 events contributing to the neutrino excess from the direction of NGC 1068. For each event we provide the ranking in our analysis and the in previous search (23), together with the DNN energy ($\log_{10}(\hat{E}_{\mu}/\text{GeV})$), the distance between reconstructed direction and NGC 1068 coordinates ($\hat{\psi}$), and the BDT angular uncertainty ($\hat{\sigma}$). The signal-over-background ratio (SoB/100) is defined as the ratio between signal and background likelihood in Eq. S9 and Eq. S10, and is divided by 100 for readability.

Rank	Previous Rank (23)	$\log_{10}(\frac{\hat{E}_{\mu}}{\text{GeV}})$	$\hat{\psi}$ [°]	$\hat{\sigma}$ [°]	SoB/100	Previous SoB/100 (23)
1	1	4.33	0.08	0.29	465	714
2	4	3.92	0.22	0.19	377	451
3	226	3.49	0.18	0.20	282	13
4	–	3.51	0.24	0.21	212	–
5	14	3.55	0.16	0.31	188	191
6	21	3.97	0.33	0.27	175	132
7	2	3.09	0.22	0.15	174	459
8	24	3.19	0.19	0.23	172	126
9	9	3.74	0.30	0.29	159	234
10	3	2.92	0.20	0.16	156	453

References and Notes

1. Auger Collaboration, J. Abraham, M. Aglietta, I. C. Aguirre, M. Albrow, D. Allard, I. Allekotte, P. Allison, J. Alvarez Muñiz, M. G. do Amaral, M. Ambrosio, L. Anchordoqui, R. Andrews, M. Anguiano, J. C. dos Anjos, C. Aramo, S. Argiro, K. Arisaka, J. C. Arteaga, S. Atulugama, M. Ave, G. Avila, R. Baggio, X. Bai, A. F. Barbosa, H. M. J. Barbosa, D. Barnhill, S. L. C. Barroso, P. Bauleo, J. Beatty, T. Beau, K.-H. Becker, J. A. Bellido, P. Bello, T. Bergmann, E. Berman, X. Bertou, P. Biermann, P. Billoir, R. Biral, H. Bluemer, M. Bohacova, E. Bollmann, C. Bonifazi, M. Boratav, A. Boselli, J. Brack, J.-M. Brunet, H. Bui-Duc, V. Cabrera, D. V. Camin, J.-N. Capdevielle, A. Carreño, N. Cartiglia, R. Caruso, L. A. de Carvalho, S. Casanova, E. Casimiro, A. Castellina, J. Castro, P. W. Cattaneo, L. Cazon, R. Cester, N. Chávez, D. Cheam, A. Chiavassa, J. A. Chinellato, M. Chiosso, A. Chou, J. Chye, A. Cillis, B. Civit, D. Claeis, P. D. J. Clark, R. W. Clay, F. Cohen, A. Cordero, A. Cordier, E. Cormier, J. Cotzomi, U. Cotti, S. Coutu, C. E. Covault, A. Creusot, J. W. Cronin, M. Cuautle, S. Dagoret-Campagne, T. Dang-Quang, P. Da Silva, J. Darling, P. Darriulat, K. Daumiller, B. R. Dawson, L. de Bruijn, A. De Capoa, M. A. L. de Oliveira, V. de Souza, A. Della Selva, O. Deligny, J. C. Diaz, C. Dobrigkeit, J. C. D'Olivo, A. Dorofeev, M. T. Dova, A. Dye, M. A. DuVernois, R. Engel, L. N. Epele, P. Eschstruth, C. O. Escobar, A. Etchegoyen, P. Facal San Luis, A. C. Fauth, N. Fazzini, A. Fernández, A. M. J. Ferrero, B. Fick, A. Filevich, A. Filipčič, R. Fonte, W. Fulgione, E. Gámez, B. Garcia, C. A. Garcia, H. Geenen, H. Gemmeke, C. Germain-Renaud, P. L. Ghia, K. Gibbs, M. Giller, J. Gitto, H. Glass, M. Gómez Berisso, P. F. Gomez Vitale, J. González, J. González, D. Gora, A. Goodwin, P. Gouffon, V. Grassi, A. F. Grillo, C. Grunfeld, J. Grygar, F. Guarino, G. Guedes, C. Guerard, R. Gumbsheimer, J. L. Harton, F. Hasenbalg, D. Heck, J. M. Hernández, D. Hoffer, C. Hojvat, P. Homola, M. Horvat, M. Hrabovsky, A. Insolia, S. Jaminion, Y. Jerónimo, L. Jiang, M. Kaducak, K.-H. Kampert, B. Keilhauer, E. Kemp, H. Klages, M. Kleifges, J. Kleinfeller, J. Knapp, A. Kopmann, N. Kunka, M. Kutschera, C. Lachaud, M. Lapolla, A. Letessier-Selvon, I. Lhenry-Yvon, J. Lloyd-Evans, R. López, A. Lopez Aguera, M. Lucano, R. Luna, Y. Ma, M. E. Manceñido, P. F. Manfredi, L. Manhaes, P. Mantsch, A. G. Mariazzi, M. J. Markus, G. Martin, O. Martineau, J. Martinez, N. Martinez, O. Martínez, H.-J. Mathes, J. A. J. Matthews, J. Matthews, G. Matthiae, E. Marques, P. Matussek, G. Maurin, D. Maurizio, P. Mazur, T. McCauley, M. McEwen, R. R. McNeil, C. Medina, M. C. Medina, G. Medina-Tanco, D. Melo, M. Melocchi, E. Menichetti, A. Menshikov, F. Meyer, R. Meyhandan, J. C. Meza, G. Miele, W. Miller, M. Mohammed, D. Monnier-Ragaigne, C. Morello, E. Moreno, M. Mostafa, R. Mussa, H. Nassini, G. Navarra, L. Nellen, F. Nerling, C. Newman-Holmes, D. Nicotra, S. Nigro, D. Nitz, H. Nogima, D. Nosek, M. Nuñez, T. Ohnuki, A. Olinto, S. Ostaptchenko, M. Palatka, G. Parente, E. Parizot, E. H. Pasaye, N. Pastrone, M. Patel, T. Paul, I. Pedraza, J. Pekala, R. Pelayo, I. M. Pepe, A. Pérez-Lorenzana, L. Perrone, N. Peshman, S. Petrera, P. Petrinca, D. Pham-Ngoc, P. Pham-Trung, T. Pierog, O. Pisanti, N. Playez, E. Ponce, T. A. Porter, L. Prado Junior, P. Privitera, M. Prouza, C. L. Pryke, J. B. Rafert, G. Raia, S. Ranchon, L. Ratti, D. Ravignani, V. Re, H. C. Reis, S. Reucroft, B. Revenue, M. Richter, J. Ridky, A. Risi, M. Risse, V. Rizi, M. D. Roberts, C. Robledo, G. Rodriguez, J. Rodriquez, J. Rodriguez Martino, S. Román, L. Rosa, M. Roth, A. C. Rovero, H. Salazar, G. Salina, F. Sanchez, M. Santander, L. G. dos Santos, R. Sato, P.

Schovanek, V. Scherini, S. J. Sciutto, G. Sequeiros-Haddad, R. C. Shellard, E. Shibuya, F. V. Siguas, W. Slater, N. Smetniansky-De Grande, K. Smith, G. R. Snow, P. Sommers, C. Song, H. Spinka, F. Suarez, T. Suomijärvi, D. Supanitsky, J. Swain, Z. Szadkowski, A. Tamashiro, G. J. Thornton, T. Thouw, R. Ticona, W. Tkaczyk, C. J. Todero Peixoto, A. Tripathi, G. Tristram, M. Trombley, D. Tscherriakhovski, P. Tuckey, V. Tunnicliffe, M. Urban, C. Uribe Estrada, J. F. Valdés, A. Vargas, C. Vargas, R. Vazquez, D. Veberič, A. Veiga, A. Velarde, F. Vernotte, V. Verzi, M. Videla, C. Vigorito, L. M. Villaseñor, M. Vlcek, L. Voyvodic, T. Vo-Van, T. Waldenmaier, P. Walker, D. Warner, A. A. Watson, C. Wiebusch, G. Wieczorek, B. Wilczynska, H. Wilczynski, N. R. Wild, T. Yamamoto, E. Zas, D. Zavrtanik, M. Zavrtanik, A. Zepeda, C. Zhang, Q. Zhu, Properties and performance of the prototype instrument for the Pierre Auger Observatory. *Nucl. Instrum. Methods Phys. Res. A* **523**, 50–95 (2004). [doi:10.1016/j.nima.2003.12.012](https://doi.org/10.1016/j.nima.2003.12.012)

2. The Pierre Auger Collaboration, The Pierre Auger Cosmic Ray Observatory. *Nucl. Instrum. Methods Phys. Res. A* **798**, 172–213 (2015). [doi:10.1016/j.nima.2015.06.058](https://doi.org/10.1016/j.nima.2015.06.058)
3. T. Abu-Zayyad, R. Aida, M. Allen, R. Anderson, R. Azuma, E. Barcikowski, J. W. Belz, D. R. Bergman, S. A. Blake, R. Cady, B. G. Cheon, J. Chiba, M. Chikawa, E. J. Cho, W. R. Cho, H. Fujii, T. Fujii, T. Fukuda, M. Fukushima, D. Gorbunov, W. Hanlon, K. Hayashi, Y. Hayashi, N. Hayashida, K. Hibino, K. Hiyama, K. Honda, T. Iguchi, D. Ikeda, K. Ikuta, N. Inoue, T. Ishii, R. Ishimori, D. Ivanov, S. Iwamoto, C. C. H. Jui, K. Kadota, F. Kakimoto, O. Kalashev, T. Kanbe, K. Kasahara, H. Kawai, S. Kawakami, S. Kawana, E. Kido, H. B. Kim, H. K. Kim, J. H. Kim, J. H. Kim, K. Kitamoto, K. Kobayashi, Y. Kobayashi, Y. Kondo, K. Kuramoto, V. Kuzmin, Y. J. Kwon, S. I. Lim, S. Machida, K. Martens, J. Martineau, T. Matsuda, T. Matsuura, T. Matsuyama, J. N. Matthews, I. Myers, M. Minamino, K. Miyata, H. Miyauchi, Y. Murano, T. Nakamura, S. W. Nam, T. Nonaka, S. Ogio, M. Ohnishi, H. Ohoka, K. Oki, D. Oku, T. Okuda, A. Oshima, S. Ozawa, I. H. Park, M. S. Pshirkov, D. Rodriguez, S. Y. Roh, G. Rubtsov, D. Ryu, H. Sagawa, N. Sakurai, A. L. Sampson, L. M. Scott, P. D. Shah, F. Shibata, T. Shibata, H. Shimodaira, B. K. Shin, J. I. Shin, T. Shirahama, J. D. Smith, P. Sokolsky, T. J. Sonley, R. W. Springer, B. T. Stokes, S. R. Stratton, T. A. Stroman, S. Suzuki, Y. Takahashi, M. Takeda, A. Taketa, M. Takita, Y. Tameda, H. Tanaka, K. Tanaka, M. Tanaka, S. B. Thomas, G. B. Thomson, P. Tinyakov, I. Tkachev, H. Tokuno, T. Tomida, S. Troitsky, Y. Tsunesada, K. Tsutsumi, Y. Tsuyuguchi, Y. Uchihori, S. Udo, H. Ukai, G. Vasiloff, Y. Wada, T. Wong, M. Wood, Y. Yamakawa, H. Yamaoka, K. Yamazaki, J. Yang, S. Yoshida, H. Yoshii, R. Zollinger, Z. Zundel, The surface detector array of the Telescope Array experiment. *Nucl. Instrum. Methods Phys. Res. A* **689**, 87–97 (2012). [doi:10.1016/j.nima.2012.05.079](https://doi.org/10.1016/j.nima.2012.05.079)
4. S. R. Kelner, F. A. Aharonian, V. V. Bugayov, Energy spectra of gamma rays, electrons, and neutrinos produced at proton-proton interactions in the very high energy regime. *Phys. Rev. D* **74**, 034018 (2006). [doi:10.1103/PhysRevD.74.034018](https://doi.org/10.1103/PhysRevD.74.034018)
5. S. R. Kelner, F. A. Aharonian, Energy spectra of gamma rays, electrons, and neutrinos produced at interactions of relativistic protons with low energy radiation. *Phys. Rev. D* **78**, 034013 (2008). [doi:10.1103/PhysRevD.78.034013](https://doi.org/10.1103/PhysRevD.78.034013)
6. A. De Angelis, G. Galanti, M. Roncadelli, Transparency of the Universe to gamma-rays. *Mon. Not. R. Astron. Soc.* **432**, 3245–3249 (2013). [doi:10.1093/mnras/stt684](https://doi.org/10.1093/mnras/stt684)

7. P. Padovani, D. M. Alexander, R. J. Assef, B. De Marco, P. Giommi, R. C. Hickox, G. T. Richards, V. Smolčić, E. Hatziminaoglou, V. Mainieri, M. Salvato, Active galactic nuclei: What's in a name? *Astron. Astrophys. Rev.* **25**, 2 (2017). [doi:10.1007/s00159-017-0102-9](https://doi.org/10.1007/s00159-017-0102-9)
8. C. K. Seyfert, Nuclear Emission in Spiral Nebulae. *Astrophys. J.* **97**, 28 (1943). [doi:10.1086/144488](https://doi.org/10.1086/144488)
9. R. Antonucci, Unified Models for Active Galactic Nuclei and Quasars. *Annu. Rev. Astron. Astrophys.* **31**, 473–521 (1993). [doi:10.1146/annurev.aa.31.090193.002353](https://doi.org/10.1146/annurev.aa.31.090193.002353)
10. C. M. Urry, P. Padovani, Unified Schemes for Radio-Loud Active Galactic Nuclei. *Publ. Astron. Soc. Pac.* **107**, 803 (1995). [doi:10.1086/133630](https://doi.org/10.1086/133630)
11. D. Eichler, High-energy neutrino astronomy: A probe of galactic nuclei? *Astrophys. J.* **232**, 106 (1979). [doi:10.1086/157269](https://doi.org/10.1086/157269)
12. V. S. Berezinsky, V. L. Ginzburg, On high-energy neutrino radiation of quasars and active galactic nuclei. *Mon. Not. R. Astron. Soc.* **194**, 3–14 (1981). [doi:10.1093/mnras/194.1.3](https://doi.org/10.1093/mnras/194.1.3)
13. K. Mannheim, P. L. Biermann, Photomeson production in active galactic nuclei. *Astron. Astrophys.* **221**, 211–220 (1989).
14. F. Halzen, E. Zas, Neutrino Fluxes from Active Galaxies: A Model-Independent Estimate. *Astrophys. J.* **488**, 669–674 (1997). [doi:10.1086/304741](https://doi.org/10.1086/304741)
15. M. G. Aartsen, M. Ackermann, J. Adams, J. A. Aguilar, M. Ahlers, M. Ahrens, D. Altmann, K. Andeen, T. Anderson, I. Ansseau, G. Anton, M. Archinger, C. Argüelles, R. Auer, J. Auffenberg, S. Axani, J. Baccus, X. Bai, S. Barnet, S. W. Barwick, V. Baum, R. Bay, K. Beattie, J. J. Beatty, J. B. Tjus, K.-H. Becker, T. Bendfelt, S. BenZvi, D. Berley, E. Bernardini, A. Bernhard, D. Z. Besson, G. Binder, D. Bindig, M. Bissok, E. Blaufuss, S. Blot, D. Boersma, C. Bohm, M. Börner, F. Bos, D. Bose, S. Böser, O. Botner, A. Bouchta, J. Braun, L. Brayeur, H.-P. Bretz, S. Bron, A. Burgman, C. Burreson, T. Carver, M. Casier, E. Cheung, D. Chirkin, A. Christov, K. Clark, L. Classen, S. Coenders, G. H. Collin, J. M. Conrad, D. F. Cowen, R. Cross, C. Day, M. Day, J. P. A. M. de André, C. D. Clercq, E. P. Rosendo, H. Dembinski, S. D. Ridder, F. Descamps, P. Desiati, K. D. de Vries, G. de Wasseige, M. de With, T. DeYoung, J. C. Díaz-Vélez, V. di Lorenzo, H. Dujmovic, J. P. Dumm, M. Dunkman, B. Eberhardt, W. R. Edwards, T. Ehrhardt, B. Eichmann, P. Eller, S. Euler, P. A. Evenson, S. Fahey, A. R. Fazely, J. Feintzeig, J. Felde, K. Filimonov, C. Finley, S. Flis, C.-C. Fösig, A. Franckowiak, M. Frère, E. Friedman, T. Fuchs, T. K. Gaisser, J. Gallagher, L. Gerhardt, K. Ghorbani, W. Giang, L. Gladstone, T. Glauch, D. Glowacki, T. Glüsenkamp, A. Goldschmidt, J. G. Gonzalez, D. Grant, Z. Griffith, L. Gustafsson, C. Haack, A. Hallgren, F. Halzen, E. Hansen, T. Hansmann, K. Hanson, J. Haugen, D. Hebecker, D. Heereman, K. Helbing, R. Hellauer, R. Heller, S. Hickford, J. Hignight, G. C. Hill, K. D. Hoffman, R. Hoffmann, K. Hoshina, F. Huang, M. Huber, P. O. Hulth, K. Hultqvist, S. In, M. Inaba, A. Ishihara, E. Jacobi, J. Jacobsen, G. S. Japaridze, M. Jeong, K. Jero, A. Jones, B. J. P. Jones, J. Joseph, W. Kang, A. Kappes, T. Karg, A. Karle, U. Katz, M. Kauer, A. Keivani, J. L. Kelley, J. Kemp, A. Kheirandish, J. Kim, M. Kim, T. Kintscher, J. Kiryluk, N. Kitamura, T. Kittler, S. R. Klein, S. Kleinfelder, M. Kleist, G. Kohnen, R. Koirlala, H. Kolanoski, R. Konietz, L. Köpke, C. Kopper, S. Kopper, D. J. Koskinen, M. Kowalski, M. Krasberg, K. Krings,

M. Kroll, G. Krückl, C. Krüger, J. Kunnen, S. Kunwar, N. Kurahashi, T. Kuwabara, M. Labare, K. Laihem, H. Landsman, J. L. Lanfranchi, M. J. Larson, F. Lauber, A. Laundrie, D. Lennarz, H. Leich, M. Lesiak-Bzdak, M. Leuermann, L. Lu, J. Ludwig, J. Lünemann, C. Mackenzie, J. Madsen, G. Maggi, K. B. M. Mahn, S. Mancina, M. Mandelartz, R. Maruyama, K. Mase, H. Matis, R. Maunu, F. McNally, C. P. McParland, P. Meade, K. Meagher, M. Medici, M. Meier, A. Meli, T. Menne, G. Merino, T. Meures, S. Miarecki, R. H. Minor, T. Montaruli, M. Moulai, T. Murray, R. Nahnhauer, U. Naumann, G. Neer, M. Newcomb, H. Niederhausen, S. C. Nowicki, D. R. Nygren, A. O. Pollmann, A. Olivas, A. O'Murchadha, T. Palczewski, H. Pandya, D. V. Pankova, S. Patton, P. Peiffer, Ö. Penek, J. A. Pepper, C. P. Heros, C. Pettersen, D. Pieloth, E. Pinat, P. B. Price, G. T. Przybylski, M. Quinnan, C. Raab, L. Rädel, M. Rameez, K. Rawlins, R. Reimann, B. Relethford, M. Relich, E. Resconi, W. Rhode, M. Richman, B. Riedel, S. Robertson, M. Rongen, C. Roucelle, C. Rott, T. Ruhe, D. Ryckbosch, D. Rysewyk, L. Sabbatini, S. E. S. Herrera, A. Sandrock, J. Sandroos, P. Sandstrom, S. Sarkar, K. Satalecka, P. Schlunder, T. Schmidt, S. Schoenen, S. Schöneberg, A. Schukraft, L. Schumacher, D. Seckel, S. Seunarine, M. Solarz, D. Soldin, M. Song, G. M. Spiczak, C. Spiering, T. Stanev, A. Stasik, J. Stettner, A. Steuer, T. Stezelberger, R. G. Stokstad, A. Stößl, R. Ström, N. L. Strotjohann, K.-H. Sulanke, G. W. Sullivan, M. Sutherland, H. Taavola, I. Taboada, J. Tatar, F. Tenholt, S. Ter-Antonyan, A. Terliuk, G. Tešić, L. Thollander, S. Tilav, P. A. Toale, M. N. Tobin, S. Toscano, D. Tosi, M. Tselengidou, A. Turcati, E. Unger, M. Usner, J. Vandenbroucke, N. Eijndhoven, S. Vanheule, M. Rossem, J. Santen, M. Vehring, M. Voge, E. Vogel, M. Vraeghe, D. Wahl, C. Walck, A. Wallace, M. Wallraff, N. Wandkowsky, C. Weaver, M. J. Weiss, C. Wendt, S. Westerhoff, D. Wharton, B. J. Whelan, S. Wickmann, K. Wiebe, C. H. Wiebusch, L. Wille, D. R. Williams, L. Wills, P. Wisniewski, M. Wolf, T. R. Wood, E. Woolsey, K. Woschnagg, D. L. Xu, X. W. Xu, Y. Xu, J. P. Yanez, G. Yodh, S. Yoshida, M. Zoll, The IceCube Neutrino Observatory: Instrumentation and online systems. *J. Instrum.* **12**, P03012 (2017). [doi:10.1088/1748-0221/12/03/P03012](https://doi.org/10.1088/1748-0221/12/03/P03012)

16. IceCube Collaboration, Evidence for high-energy extraterrestrial neutrinos at the IceCube detector. *Science* **342**, 1242856 (2013). [doi:10.1126/science.1242856](https://doi.org/10.1126/science.1242856) [Medline](#)
17. M. G. Aartsen, M. Ackermann, J. Adams, J. A. Aguilar, M. Ahlers, M. Ahrens, C. Alispach, K. Andeen, T. Anderson, I. Ansseau, G. Anton, C. Argüelles, J. Auffenberg, S. Axani, P. Backes, H. Bagherpour, X. Bai, A. Balagopal V, A. Barbano, S. W. Barwick, B. Bastian, V. Baum, S. Baur, R. Bay, J. J. Beatty, K.-H. Becker, J. Becker Tjus, S. BenZvi, D. Berley, E. Bernardini, D. Z. Besson, G. Binder, D. Bindig, E. Blaufuss, S. Blot, C. Bohm, S. Böser, O. Botner, J. Böttcher, E. Bourbeau, J. Bourbeau, F. Bradascio, J. Braun, S. Bron, J. Brostean-Kaiser, A. Burgman, J. Buscher, R. S. Busse, T. Carver, C. Chen, E. Cheung, D. Chirkin, S. Choi, K. Clark, L. Classen, A. Coleman, G. H. Collin, J. M. Conrad, P. Coppin, P. Correa, D. F. Cowen, R. Cross, P. Dave, C. De Clercq, J. J. DeLaunay, H. Dembinski, K. Deoskar, S. De Ridder, P. Desiati, K. D. de Vries, G. de Wasseige, M. de With, T. DeYoung, A. Diaz, J. C. Díaz-Vélez, H. Dujmovic, M. Dunkman, E. Dvorak, B. Eberhardt, T. Ehrhardt, P. Eller, R. Engel, P. A. Evenson, S. Fahey, A. R. Fazely, J. Felde, K. Filimonov, C. Finley, D. Fox, A. Franckowiak, E. Friedman, A. Fritz, T. K. Gaisser, J. Gallagher, E. Ganster, S. Garrappa, L. Gerhardt, K. Ghorbani, T. Glauch, T. Glüsenkamp, A. Goldschmidt, J. G. Gonzalez, D. Grant, T. Grégoire, Z. Griffith, S. Griswold, M. Günder, M. Gündüz, C. Haack, A. Hallgren, R.

Halliday, L. Halve, F. Halzen, K. Hanson, A. Haungs, D. Hebecker, D. Heereman, P. Heix, K. Helbing, R. Hellauer, F. Henningsen, S. Hickford, J. Hignight, G. C. Hill, K. D. Hoffman, R. Hoffmann, T. Hoinka, B. Hokanson-Fasig, K. Hoshina, F. Huang, M. Huber, T. Huber, K. Hultqvist, M. Hünnefeld, R. Hussain, S. In, N. Iovine, A. Ishihara, M. Jansson, G. S. Japaridze, M. Jeong, K. Jero, B. J. P. Jones, F. Jonske, R. Joppe, D. Kang, W. Kang, A. Kappes, D. Kappesser, T. Karg, M. Karl, A. Karle, U. Katz, M. Kauer, J. L. Kelley, A. Kheirandish, J. Kim, T. Kintscher, J. Kiryluk, T. Kittler, S. R. Klein, R. Koirala, H. Kolanoski, L. Köpke, C. Kopper, S. Kopper, D. J. Koskinen, M. Kowalski, K. Krings, G. Krückl, N. Kulacz, N. Kurahashi, A. Kyriacou, J. L. Lanfranchi, M. J. Larson, F. Lauber, J. P. Lazar, K. Leonard, M. Lesiak-Bzdak, A. Leszczyńska, M. Leuermann, Q. R. Liu, E. Lohfink, C. J. Lozano Mariscal, L. Lu, F. Lucarelli, J. Lünemann, W. Luszczak, Y. Lyu, W. Y. Ma, J. Madsen, G. Maggi, K. B. M. Mahn, Y. Makino, P. Mallik, K. Mallot, S. Mancina, I. C. Mariş, R. Maruyama, K. Mase, R. Maunu, F. McNally, K. Meagher, M. Medici, A. Medina, M. Meier, S. Meighen-Berger, G. Merino, T. Meures, J. Micallef, D. Mockler, G. Momenté, T. Montaruli, R. W. Moore, R. Morse, M. Moulai, P. Muth, R. Nagai, U. Naumann, G. Neer, H. Niederhausen, M. U. Nisa, S. C. Nowicki, D. R. Nygren, A. Obertacke Pollmann, M. Oehler, A. Olivas, A. O'Murchadha, E. O'Sullivan, T. Palczewski, H. Pandya, D. V. Pankova, N. Park, P. Peiffer, C. Pérez de Los Heros, S. Philippen, D. Pieloth, S. Pieper, E. Pinat, A. Pizzuto, M. Plum, A. Porcelli, P. B. Price, G. T. Przybylski, C. Raab, A. Raissi, M. Rameez, L. Rauch, K. Rawlins, I. C. Rea, A. Rehman, R. Reimann, B. Relethford, M. Renschler, G. Renzi, E. Resconi, W. Rhode, M. Richman, S. Robertson, M. Rongen, C. Rott, T. Ruhe, D. Ryckbosch, D. Rysewyk, I. Safa, S. E. Sanchez Herrera, A. Sandrock, J. Sandroos, M. Santander, S. Sarkar, S. Sarkar, K. Satalecka, M. Schaufel, H. Schieler, P. Schlunder, T. Schmidt, A. Schneider, J. Schneider, F. G. Schröder, L. Schumacher, S. Sclafani, D. Seckel, S. Seunarine, S. Shefali, M. Silva, R. Snihur, J. Soedingrekso, D. Soldin, M. Song, G. M. Spiczak, C. Spiering, J. Stachurska, M. Stamatikos, T. Stanev, R. Stein, J. Stettner, A. Steuer, T. Stezelberger, R. G. Stokstad, A. Stößl, N. L. Strotjohann, T. Stürwald, T. Stuttard, G. W. Sullivan, I. Taboada, F. Tenholt, S. Ter-Antonyan, A. Terliuk, S. Tilav, K. Tollefson, L. Tomankova, C. Tönnis, S. Toscano, D. Tosi, A. Trettin, M. Tselengidou, C. F. Tung, A. Turcati, R. Turcotte, C. F. Turley, B. Ty, E. Unger, M. A. Unland Elorrieta, M. Usner, J. Vandenbroucke, W. Van Driessche, D. van Eijk, N. van Eijndhoven, J. van Santen, S. Verpoest, M. Vraeghe, C. Walck, A. Wallace, M. Wallraff, N. Wandkowsky, T. B. Watson, C. Weaver, A. Weindl, M. J. Weiss, J. Weldert, C. Wendt, J. Werthebach, B. J. Whelan, N. Whitehorn, K. Wiebe, C. H. Wiebusch, L. Wille, D. R. Williams, L. Wills, M. Wolf, J. Wood, T. R. Wood, K. Woschnagg, G. Wrede, D. L. Xu, X. W. Xu, Y. Xu, J. P. Yanez, G. Yodh, S. Yoshida, T. Yuan, M. Zöcklein, IceCube Collaboration, Characteristics of the Diffuse Astrophysical Electron and Tau Neutrino Flux with Six Years of IceCube High Energy Cascade Data. *Phys. Rev. Lett.* **125**, 121104 (2020). [doi:10.1103/PhysRevLett.125.121104](https://doi.org/10.1103/PhysRevLett.125.121104) Medline

18. R. Abbasi, M. Ackermann, J. Adams, J. A. Aguilar, M. Ahlers, M. Ahrens, C. Alispach, A. A. Alves, N. M. Amin, K. Andeen, T. Anderson, I. Ansseau, G. Anton, C. Argüelles, S. Axani, X. Bai, A. Balagopal V, A. Barbano, S. W. Barwick, B. Bastian, V. Basu, V. Baum, S. Baur, R. Bay, J. J. Beatty, K.-H. Becker, J. Becker Tjus, C. Bellenghi, S. BenZvi, D. Berley, E. Bernardini, D. Z. Besson, G. Binder, D. Bindig, E. Blaufuss, S. Blot, S. Böser, O. Botner, J. Böttcher, E. Bourbeau, J. Bourbeau, F. Bradascio, J. Braun,

S. Bron, J. Brostean-Kaiser, A. Burgman, R. S. Busse, M. A. Campana, C. Chen, D. Chirkin, S. Choi, B. A. Clark, K. Clark, L. Classen, A. Coleman, G. H. Collin, J. M. Conrad, P. Coppin, P. Correa, D. F. Cowen, R. Cross, P. Dave, C. De Clercq, J. J. DeLaunay, H. Dembinski, K. Deoskar, S. De Ridder, A. Desai, P. Desiati, K. D. de Vries, G. de Wasseige, M. de With, T. DeYoung, S. Dharani, A. Diaz, J. C. Díaz-Vélez, H. Dujmovic, M. Dunkman, M. A. DuVernois, E. Dvorak, T. Ehrhardt, P. Eller, R. Engel, J. Evans, P. A. Evenson, S. Fahey, A. R. Fazely, S. Fiedlschuster, A. T. Fienberg, K. Filimonov, C. Finley, L. Fischer, D. Fox, A. Franckowiak, E. Friedman, A. Fritz, P. Fürst, T. K. Gaisser, J. Gallagher, E. Ganster, S. Garrappa, L. Gerhardt, A. Ghadimi, T. Glauch, T. Glüsenkamp, A. Goldschmidt, J. G. Gonzalez, S. Goswami, D. Grant, T. Grégoire, Z. Griffith, S. Griswold, M. Gündüz, C. Haack, A. Hallgren, R. Halliday, L. Halve, F. Halzen, M. Ha Minh, K. Hanson, J. Hardin, A. Haungs, S. Hauser, D. Hebecker, K. Helbing, F. Henningsen, S. Hickford, J. Hignight, C. Hill, G. C. Hill, K. D. Hoffman, R. Hoffmann, T. Hoinka, B. Hokanson-Fasig, K. Hoshina, F. Huang, M. Huber, T. Huber, K. Hultqvist, M. Hünnefeld, R. Hussain, S. In, N. Iovine, A. Ishihara, M. Jansson, G. S. Japaridze, M. Jeong, B. J. P. Jones, R. Joppe, D. Kang, W. Kang, X. Kang, A. Kappes, D. Kappesser, T. Karg, M. Karl, A. Karle, T. Katori, U. Katz, M. Kauer, M. Kellermann, J. L. Kelley, A. Kheirandish, J. Kim, K. Kin, T. Kintscher, J. Kiryluk, S. R. Klein, R. Koirala, H. Kolanoski, L. Köpke, C. Kopper, S. Kopper, D. J. Koskinen, P. Koundal, M. Kovacevich, M. Kowalski, K. Krings, G. Krückl, N. Kulacz, N. Kurahashi, A. Kyriacou, C. Lagunas Gualda, J. L. Lanfranchi, M. J. Larson, F. Lauber, J. P. Lazar, K. Leonard, A. Leszczyńska, Y. Li, Q. R. Liu, E. Lohfink, C. J. Lozano Mariscal, L. Lu, F. Lucarelli, A. Ludwig, W. Luszczak, Y. Lyu, W. Y. Ma, J. Madsen, K. B. M. Mahn, Y. Makino, P. Mallik, S. Mancina, S. Mandalia, I. C. Mariş, R. Maruyama, K. Mase, F. McNally, K. Meagher, A. Medina, M. Meier, S. Meighen-Berger, J. Merz, J. Micallef, D. Mockler, G. Momenté, T. Montaruli, R. W. Moore, R. Morse, M. Moulai, R. Naab, R. Nagai, U. Naumann, J. Necker, G. Neer, L. V. Nguyẽn, H. Niederhausen, M. U. Nisa, S. C. Nowicki, D. R. Nygren, A. Obertacke Pollmann, M. Oehler, A. Olivas, E. O'Sullivan, H. Pandya, D. V. Pankova, N. Park, G. K. Parker, E. N. Paudel, P. Peiffer, C. Pérez de los Heros, S. Philippen, D. Pieloth, S. Pieper, A. Pizzuto, M. Plum, Y. Popovych, A. Porcelli, M. Prado Rodriguez, P. B. Price, G. T. Przybylski, C. Raab, A. Raissi, M. Rameez, K. Rawlins, I. C. Rea, A. Rehman, R. Reimann, M. Renschler, G. Renzi, E. Resconi, S. Reusch, W. Rhode, M. Richman, B. Riedel, S. Robertson, G. Roellinghoff, M. Rongen, C. Rott, T. Ruhe, D. Ryckbosch, D. Rysewyk Cantu, I. Safa, S. E. Sanchez Herrera, A. Sandrock, J. Sandroos, M. Santander, S. Sarkar, S. Sarkar, K. Satalecka, M. Scharf, M. Schaufel, H. Schieler, P. Schlunder, T. Schmidt, A. Schneider, J. Schneider, F. G. Schröder, L. Schumacher, S. Sclafani, D. Seckel, S. Seunarine, S. Shefali, M. Silva, B. Smithers, R. Snihur, J. Soedingrekso, D. Soldin, G. M. Spiczak, C. Spiering, J. Stachurska, M. Stamatikos, T. Stanev, R. Stein, J. Stettner, A. Steuer, T. Stezelberger, R. G. Stokstad, N. L. Strotjohann, T. Stuttard, G. W. Sullivan, I. Taboada, F. Tenholt, S. Ter-Antonyan, S. Tilav, F. Tischbein, K. Tollefson, L. Tomankova, C. Tönnis, S. Toscano, D. Tosi, A. Trettin, M. Tselengidou, C. F. Tung, A. Turcati, R. Turcotte, C. F. Turley, J. P. Twagirayezu, B. Ty, E. Unger, M. A. Unland Elorrieta, J. Vandebroucke, D. van Eijk, N. van Eijndhoven, D. Vannerom, J. van Santen, S. Verpoest, M. Vraeghe, C. Walck, A. Wallace, N. Wandkowsky, T. B. Watson, C. Weaver, A. Weindl, M. J. Weiss, J. Weldert, C. Wendt, J. Werthebach, M. Weyrauch,

B. J. Whelan, N. Whitehorn, K. Wiebe, C. H. Wiebusch, D. R. Williams, M. Wolf, T. R. Wood, K. Woschnagg, G. Wrede, J. Wulff, X. W. Xu, Y. Xu, J. P. Yanez, S. Yoshida, T. Yuan, Z. Zhang, IceCube high-energy starting event sample: Description and flux characterization with 7.5 years of data. *Phys. Rev. D* **104**, 022002 (2021).
[doi:10.1103/PhysRevD.104.022002](https://doi.org/10.1103/PhysRevD.104.022002)

19. M. G. Aartsen, M. Ackermann, J. Adams, J. A. Aguilar, M. Ahlers, M. Ahrens, D. Altmann, K. Andeen, T. Anderson, I. Ansseau, G. Anton, M. Archinger, C. Argüelles, J. Auffenberg, S. Axani, X. Bai, S. W. Barwick, V. Baum, R. Bay, J. J. Beatty, J. Becker Tjus, K.-H. Becker, S. BenZvi, D. Berley, E. Bernardini, A. Bernhard, D. Z. Besson, G. Binder, D. Bindig, M. Bissok, E. Blaufuss, S. Blot, C. Bohm, M. Börner, F. Bos, D. Bose, S. Böser, O. Botner, J. Braun, L. Brayeur, H.-P. Bretz, S. Bron, A. Burgman, T. Carver, M. Casier, E. Cheung, D. Chirkin, A. Christov, K. Clark, L. Classen, S. Coenders, G. H. Collin, J. M. Conrad, D. F. Cowen, R. Cross, M. Day, J. P. A. M. de André, C. De Clercq, E. del Pino Rosendo, H. Dembinski, S. De Ridder, P. Desiati, K. D. de Vries, G. de Wasseige, M. de With, T. DeYoung, J. C. Díaz-Vélez, V. di Lorenzo, H. Dujmovic, J. P. Dumm, M. Dunkman, B. Eberhardt, T. Ehrhardt, B. Eichmann, P. Eller, S. Euler, P. A. Evenson, S. Fahey, A. R. Fazely, J. Feintzeig, J. Felde, K. Filimonov, C. Finley, S. Flis, C.-C. Fösig, A. Franckowiak, E. Friedman, T. Fuchs, T. K. Gaisser, J. Gallagher, L. Gerhardt, K. Ghorbani, W. Giang, L. Gladstone, T. Glauch, T. Glüsenkamp, A. Goldschmidt, J. G. Gonzalez, D. Grant, Z. Griffith, C. Haack, A. Hallgren, F. Halzen, E. Hansen, T. Hansmann, K. Hanson, D. Hebecker, D. Heereman, K. Helbing, R. Hellauer, S. Hickford, J. Hignight, G. C. Hill, K. D. Hoffman, R. Hoffmann, K. Hoshina, F. Huang, M. Huber, K. Hultqvist, S. In, A. Ishihara, E. Jacobi, G. S. Japaridze, M. Jeong, K. Jero, B. J. P. Jones, W. Kang, A. Kappes, T. Karg, A. Karle, U. Katz, M. Kauer, A. Keivani, J. L. Kelley, A. Kheirandish, J. Kim, M. Kim, T. Kintscher, J. Kiryluk, T. Kittler, S. R. Klein, G. Kohnen, R. Koirlala, H. Kolanoski, R. Konietz, L. Köpke, C. Kopper, S. Kopper, D. J. Koskinen, M. Kowalski, K. Krings, M. Kroll, G. Krückl, C. Krüger, J. Kunnen, S. Kunwar, N. Kurahashi, T. Kuwabara, M. Labare, J. L. Lanfranchi, M. J. Larson, F. Lauber, D. Lennarz, M. Lesiak-Bzdak, M. Leuermann, L. Lu, J. Lünemann, J. Madsen, G. Maggi, K. B. M. Mahn, S. Mancina, M. Mandelartz, R. Maruyama, K. Mase, R. Maunu, F. McNally, K. Meagher, M. Medici, M. Meier, A. Meli, T. Menne, G. Merino, T. Meures, S. Miarecki, T. Montaruli, M. Moulai, R. Nahnhauer, U. Naumann, G. Neer, H. Niederhausen, S. C. Nowicki, D. R. Nygren, A. Obertacke Pollmann, A. Olivas, A. O'Murchadha, T. Palczewski, H. Pandya, D. V. Pankova, P. Peiffer, Ö. Penek, J. A. Pepper, C. Pérez de los Heros, D. Pieloth, E. Pinat, P. B. Price, G. T. Przybylski, M. Quinnan, C. Raab, L. Rädel, M. Rameez, K. Rawlins, R. Reimann, B. Relethford, M. Relich, E. Resconi, W. Rhode, M. Richman, B. Riedel, S. Robertson, M. Rongen, C. Rott, T. Ruhe, D. Ryckbosch, D. Rysewyk, L. Sabbatini, S. E. Sanchez Herrera, A. Sandrock, J. Sandroos, S. Sarkar, K. Satalecka, P. Schlunder, T. Schmidt, S. Schoenen, S. Schöneberg, L. Schumacher, D. Seckel, S. Seunarine, D. Soldin, M. Song, G. M. Spiczak, C. Spiering, T. Stanev, A. Stasik, J. Stettner, A. Steuer, T. Stezelberger, R. G. Stokstad, A. Stößl, R. Ström, N. L. Strotjohann, G. W. Sullivan, M. Sutherland, H. Taavola, I. Taboada, J. Tatar, F. Tenholt, S. Ter-Antonyan, A. Terliuk, G. Tešić, S. Tilav, P. A. Toale, M. N. Tobin, S. Toscano, D. Tosi, M. Tselengidou, A. Turcati, E. Unger, M. Usner, J. Vandembroucke, N. van Eijndhoven, S. Vanheule, M. van Rossem, J. van Santen, M. Vehring, M. Voge, E. Vogel, M. Vraeghe, C. Walck, A.

- Wallace, M. Wallraff, N. Wandkowsky, C. Weaver, M. J. Weiss, C. Wendt, S. Westerhoff, B. J. Whelan, S. Wickmann, K. Wiebe, C. H. Wiebusch, L. Wille, D. R. Williams, L. Wills, M. Wolf, T. R. Wood, E. Woolsey, K. Woschnagg, D. L. Xu, X. W. Xu, Y. Xu, J. P. Yanez, G. Yodh, S. Yoshida, M. Zoll, The IceCube realtime alert system. *Astropart. Phys.* **92**, 30–41 (2017). [doi:10.1016/j.astropartphys.2017.05.002](https://doi.org/10.1016/j.astropartphys.2017.05.002)
20. IceCube Collaboration *et al.*, *Fermi*-LAT, MAGIC, AGILE, ASAS-SN, HAWC, H.E.S.S., INTEGRAL, Kanata, Kiso, Kapteyn, Liverpool Telescope, Subaru, *Swift/NuSTAR*, VERITAS, VLA/17B-403 teams, Multimessenger observations of a flaring blazar coincident with high-energy neutrino IceCube-170922A. *Science* **361**, eaat1378 (2018). [doi:10.1126/science.aat1378](https://doi.org/10.1126/science.aat1378) Medline
21. IceCube Collaboration, Neutrino emission from the direction of the blazar TXS 0506+056 prior to the IceCube-170922A alert. *Science* **361**, 147–151 (2018). [doi:10.1126/science.aat2890](https://doi.org/10.1126/science.aat2890) Medline
22. P. Padovani, F. Oikonomou, M. Petropoulou, P. Giommi, E. Resconi, TXS 0506+056, the first cosmic neutrino source, is not a BL Lac. *Mon. Not. R. Astron. Soc.* **484**, L104–L108 (2019). [doi:10.1093/mnrasl/slz011](https://doi.org/10.1093/mnrasl/slz011)
23. M. G. Aartsen, M. Ackermann, J. Adams, J. A. Aguilar, M. Ahlers, M. Ahrens, C. Alispach, K. Andeen, T. Anderson, I. Ansseau, G. Anton, C. Argüelles, J. Auffenberg, S. Axani, P. Backes, H. Bagherpour, X. Bai, A. Balagopal, A. Barbano, S. W. Barwick, B. Bastian, V. Baum, S. Baur, R. Bay, J. J. Beatty, K.-H. Becker, J. Becker Tjus, S. BenZvi, D. Berley, E. Bernardini, D. Z. Besson, G. Binder, D. Bindig, E. Blaufuss, S. Blot, C. Bohm, M. Börner, S. Böser, O. Botner, J. Böttcher, E. Bourbeau, J. Bourbeau, F. Bradascio, J. Braun, S. Bron, J. Brostean-Kaiser, A. Burgman, J. Buscher, R. S. Busse, T. Carver, C. Chen, E. Cheung, D. Chirkin, S. Choi, K. Clark, L. Classen, A. Coleman, G. H. Collin, J. M. Conrad, P. Coppin, P. Correa, D. F. Cowen, R. Cross, P. Dave, C. De Clercq, J. J. DeLaunay, H. Dembinski, K. Deoskar, S. De Ridder, P. Desiati, K. D. de Vries, G. de Wasseige, M. de With, T. DeYoung, A. Diaz, J. C. Díaz-Vélez, H. Dujmovic, M. Dunkman, E. Dvorak, B. Eberhardt, T. Ehrhardt, P. Eller, R. Engel, P. A. Evenson, S. Fahey, A. R. Fazely, J. Felde, K. Filimonov, C. Finley, D. Fox, A. Franckowiak, E. Friedman, A. Fritz, T. K. Gaisser, J. Gallagher, E. Ganster, S. Garrappa, L. Gerhardt, K. Ghorbani, T. Glauch, T. Glüsenkamp, A. Goldschmidt, J. G. Gonzalez, D. Grant, Z. Griffith, S. Griswold, M. Günder, M. Gündüz, C. Haack, A. Hallgren, R. Halliday, L. Halve, F. Halzen, K. Hanson, A. Haungs, D. Hebecker, D. Heereman, P. Heix, K. Helbing, R. Hellauer, F. Henningsen, S. Hickford, J. Hignight, G. C. Hill, K. D. Hoffman, R. Hoffmann, T. Hoinka, B. Hokanson-Fasig, K. Hoshina, F. Huang, M. Huber, T. Huber, K. Hultqvist, M. Hünnefeld, R. Hussain, S. In, N. Iovine, A. Ishihara, G. S. Japaridze, M. Jeong, K. Jero, B. J. P. Jones, F. Jonske, R. Joppe, D. Kang, W. Kang, A. Kappes, D. Kappesser, T. Karg, M. Karl, A. Karle, U. Katz, M. Kauer, J. L. Kelley, A. Kheirandish, J. Kim, T. Kintscher, J. Kiryluk, T. Kittler, S. R. Klein, R. Koirala, H. Kolanoski, L. Köpke, C. Kopper, S. Kopper, D. J. Koskinen, M. Kowalski, K. Krings, G. Krückl, N. Kulacz, N. Kurahashi, A. Kyriacou, M. Labare, J. L. Lanfranchi, M. J. Larson, F. Lauber, J. P. Lazar, K. Leonard, A. Leszczyńska, M. Leuermann, Q. R. Liu, E. Lohfink, C. J. Lozano Mariscal, L. Lu, F. Lucarelli, J. Lünemann, W. Luszczak, Y. Lyu, W. Y. Ma, J. Madsen, G. Maggi, K. B. M. Mahn, Y. Makino, P. Mallik, K. Mallot, S. Mancina, I. C. Mariş, R. Maruyama, K. Mase, H. S. Matis, R. Maunu, F.

McNally, K. Meagher, M. Medici, A. Medina, M. Meier, S. Meighen-Berger, T. Menne, G. Merino, T. Meures, J. Micallef, D. Mockler, G. Momenté, T. Montaruli, R. W. Moore, R. Morse, M. Moulai, P. Muth, R. Nagai, U. Naumann, G. Neer, H. Niederhausen, M. U. Nisa, S. C. Nowicki, D. R. Nygren, A. Obertacke Pollmann, M. Oehler, A. Olivas, A. O'Murchadha, E. O'Sullivan, T. Palczewski, H. Pandya, D. V. Pankova, N. Park, P. Peiffer, C. Pérez de Los Heros, S. Philippen, D. Pieloth, E. Pinat, A. Pizzuto, M. Plum, A. Porcelli, P. B. Price, G. T. Przybylski, C. Raab, A. Raissi, M. Rameez, L. Rauch, K. Rawlins, I. C. Rea, R. Reimann, B. Relethford, M. Renschler, G. Renzi, E. Resconi, W. Rhode, M. Richman, S. Robertson, M. Rongen, C. Rott, T. Ruhe, D. Ryckbosch, D. Rysewyk, I. Safa, S. E. Sanchez Herrera, A. Sandrock, J. Sandroos, M. Santander, S. Sarkar, S. Sarkar, K. Satalecka, M. Schaufel, H. Schieler, P. Schlunder, T. Schmidt, A. Schneider, J. Schneider, F. G. Schröder, L. Schumacher, S. Sclafani, D. Seckel, S. Seunarine, S. Shefali, M. Silva, R. Snihur, J. Soedingrekso, D. Soldin, M. Song, G. M. Spiczak, C. Spiering, J. Stachurska, M. Stamatikos, T. Stanev, R. Stein, P. Steinmüller, J. Stettner, A. Steuer, T. Stezelberger, R. G. Stokstad, A. Stößl, N. L. Strotjohann, T. Stürwald, T. Stuttard, G. W. Sullivan, I. Taboada, F. Tenholt, S. Ter-Antonyan, A. Terliuk, S. Tilav, K. Tollefson, L. Tomankova, C. Tönnis, S. Toscano, D. Tosi, A. Trettin, M. Tselengidou, C. F. Tung, A. Turcati, R. Turcotte, C. F. Turley, B. Ty, E. Unger, M. A. Unland Elorrieta, M. Usner, J. Vandenbroucke, W. Van Driessche, D. van Eijk, N. van Eijndhoven, S. Vanheule, J. van Santen, M. Vraeghe, C. Walck, A. Wallace, M. Wallraff, N. Wandkowsky, T. B. Watson, C. Weaver, A. Weindl, M. J. Weiss, J. Weldert, C. Wendt, J. Werthebach, B. J. Whelan, N. Whitehorn, K. Wiebe, C. H. Wiebusch, L. Wille, D. R. Williams, L. Wills, M. Wolf, J. Wood, T. R. Wood, K. Woschnagg, G. Wrede, D. L. Xu, X. W. Xu, Y. Xu, J. P. Yanez, G. Yodh, S. Yoshida, T. Yuan, M. Zöcklein, Time-Integrated Neutrino Source Searches with 10 Years of IceCube Data. *Phys. Rev. Lett.* **124**, 051103 (2020). [doi:10.1103/PhysRevLett.124.051103](https://doi.org/10.1103/PhysRevLett.124.051103)
[Medline](#)

24. IceCube Collaboration, M. G. Aartsen, M. Ackermann, J. Adams, J. A. Aguilar, M. Ahlers, M. Ahrens, D. Altmann, K. Andeen, T. Anderson, I. Ansseau, G. Anton, C. Argüelles, J. Auffenberg, S. Axani, P. Backes, H. Bagherpour, X. Bai, A. Barbano, J. P. Barron, S. W. Barwick, V. Baum, R. Bay, J. J. Beatty, J. Becker Tjus, K.-H. Becker, S. BenZvi, D. Berley, E. Bernardini, D. Z. Besson, G. Binder, D. Bindig, E. Blaufuss, S. Blot, C. Bohm, M. Börner, F. Bos, S. Böser, O. Botner, E. Bourbeau, J. Bourbeau, F. Bradascio, J. Braun, H.-P. Bretz, S. Bron, J. Brostean-Kaiser, A. Burgman, R. S. Busse, T. Carver, C. Chen, E. Cheung, D. Chirkin, K. Clark, L. Classen, G. H. Collin, J. M. Conrad, P. Coppin, P. Correa, D. F. Cowen, R. Cross, P. Dave, M. Day, J. P. A. M. de André, C. De Clercq, J. J. DeLaunay, H. Dembinski, K. Deoskar, S. De Ridder, P. Desiati, K. D. de Vries, G. de Wasseige, M. de With, T. DeYoung, J. C. Díaz-Vélez, H. Dujmovic, M. Dunkman, E. Dvorak, B. Eberhardt, T. Ehrhardt, B. Eichmann, P. Eller, P. A. Evenson, S. Fahey, A. R. Fazely, J. Felde, K. Filimonov, C. Finley, A. Franckowiak, E. Friedman, A. Fritz, T. K. Gaisser, J. Gallagher, E. Ganster, S. Garrappa, L. Gerhardt, K. Ghorbani, W. Giang, T. Glauch, T. Glüsenkamp, A. Goldschmidt, J. G. Gonzalez, D. Grant, Z. Griffith, C. Haack, A. Hallgren, L. Halve, F. Halzen, K. Hanson, D. Hebecker, D. Heereman, K. Helbing, R. Hellauer, S. Hickford, J. Hignight, G. C. Hill, K. D. Hoffman, R. Hoffmann, T. Hoinka, B. Hokanson-Fasig, K. Hoshina, F. Huang, M. Huber, K. Hultqvist, M. Hünnefeld, R. Hussain, S. In, N. Iovine, A. Ishihara, E. Jacobi, G. S.

Japaridze, M. Jeong, K. Jero, B. J. P. Jones, P. Kalaczynski, W. Kang, A. Kappes, D. Kappesser, T. Karg, A. Karle, U. Katz, M. Kauer, A. Keivani, J. L. Kelley, A. Kheirandish, J. Kim, T. Kintscher, J. Kiryluk, T. Kittler, S. R. Klein, R. Koirala, H. Kolanoski, L. Köpke, C. Kopper, S. Kopper, D. J. Koskinen, M. Kowalski, K. Krings, M. Kroll, G. Krückl, S. Kunwar, N. Kurahashi, A. Kyriacou, M. Labare, J. L. Lanfranchi, M. J. Larson, F. Lauber, K. Leonard, M. Leuermann, Q. R. Liu, E. Lohfink, C. J. L. Mariscal, L. Lu, J. Lünemann, W. Luszczak, J. Madsen, G. Maggi, K. B. M. Mahn, Y. Makino, S. Mancina, I. C. Mariş, R. Maruyama, K. Mase, R. Maunu, K. Meagher, M. Medici, M. Meier, T. Menne, G. Merino, T. Meures, S. Miarecki, J. Micallef, G. Momenté, T. Montaruli, R. W. Moore, M. Moulai, R. Nagai, R. Nahnhauer, P. Nakarmi, U. Naumann, G. Neer, H. Niederhausen, S. C. Nowicki, D. R. Nygren, A. Obertacke Pollmann, A. Olivas, A. O'Murchadha, E. O'Sullivan, T. Palczewski, H. Pandya, D. V. Pankova, P. Peiffer, C. Pérez de los Heros, D. Pieloth, E. Pinat, A. Pizzuto, M. Plum, P. B. Price, G. T. Przybylski, C. Raab, M. Rameez, L. Rauch, K. Rawlins, I. C. Rea, R. Reimann, B. Relethford, G. Renzi, E. Resconi, W. Rhode, M. Richman, S. Robertson, M. Rongen, C. Rott, T. Ruhe, D. Ryckbosch, D. Rysewyk, I. Safa, S. E. Sanchez Herrera, A. Sandrock, J. Sandroos, M. Santander, S. Sarkar, S. Sarkar, K. Satalecka, M. Schaufel, P. Schlunder, T. Schmidt, A. Schneider, J. Schneider, S. Schöneberg, L. Schumacher, S. Sclafani, D. Seckel, S. Seunarine, J. Soedingrekso, D. Soldin, M. Song, G. M. Spiczak, C. Spiering, J. Stachurska, M. Stamatikos, T. Stanev, A. Stasik, R. Stein, J. Stettner, A. Steuer, T. Stezelberger, R. G. Stokstad, A. Stößl, N. L. Strotjohann, T. Stuttard, G. W. Sullivan, M. Sutherland, I. Taboada, F. Tenholt, S. Ter-Antonyan, A. Terliuk, S. Tilav, M. N. Tobin, C. Tönnis, S. Toscano, D. Tosi, M. Tselengidou, C. F. Tung, A. Turcati, R. Turcotte, C. F. Turley, B. Ty, E. Unger, M. A. Unland Elorrieta, M. Usner, J. Vandenbroucke, W. Van Driessche, D. van Eijk, N. van Eijndhoven, S. Vanheule, J. van Santen, M. Vraeghe, C. Walck, A. Wallace, M. Wallraff, F. D. Wandler, N. Wandkowsky, T. B. Watson, C. Weaver, M. J. Weiss, C. Wendt, J. Werthebach, S. Westerhoff, B. J. Whelan, N. Whitehorn, K. Wiebe, C. H. Wiebusch, L. Wille, D. R. Williams, L. Wills, M. Wolf, J. Wood, T. R. Wood, E. Woolsey, K. Woschnagg, G. Wrede, D. L. Xu, X. W. Xu, Y. Xu, J. P. Yanez, G. Yodh, S. Yoshida, T. Yuan, Search for steady point-like sources in the astrophysical muon neutrino flux with 8 years of IceCube data. *Eur. Phys. J. C* **79**, 234 (2019). [doi:10.1140/epjc/s10052-019-6680-0](https://doi.org/10.1140/epjc/s10052-019-6680-0)

25. M. G. Aartsen, K. Abraham, M. Ackermann, J. Adams, J. A. Aguilar, M. Ahlers, M. Ahrens, D. Altmann, K. Andeen, T. Anderson, I. Ansseau, G. Anton, M. Archinger, C. Argüelles, J. Auffenberg, S. Axani, X. Bai, S. W. Barwick, V. Baum, R. Bay, J. J. Beatty, J. B. Tjus, K.-H. Becker, S. BenZvi, P. Berghaus, D. Berley, E. Bernardini, A. Bernhard, D. Z. Besson, G. Binder, D. Bindig, M. Bissok, E. Blaufuss, S. Blot, C. Bohm, M. Börner, F. Bos, D. Bose, S. Böser, O. Botner, J. Braun, L. Brayeur, H.-P. Bretz, A. Burgman, T. Carver, M. Casier, E. Cheung, D. Chirkin, A. Christov, K. Clark, L. Classen, S. Coenders, G. H. Collin, J. M. Conrad, D. F. Cowen, R. Cross, M. Day, J. P. A. M. André, C. D. Clercq, E. P. Rosendo, H. Dembinski, S. D. Ridder, P. Desiati, K. D. Vries, G. Wasseige, M. With, T. DeYoung, J. C. Díaz-Vélez, V. Lorenzo, H. Dujmovic, J. P. Dumm, M. Dunkman, B. Eberhardt, T. Ehrhardt, B. Eichmann, P. Eller, S. Euler, P. A. Evenson, S. Fahey, A. R. Fazely, J. Feintzeig, J. Felde, K. Filimonov, C. Finley, S. Flis, C.-C. Fösig, A. Franckowiak, E. Friedman, T. Fuchs, T. K. Gaisser, J. Gallagher, L. Gerhardt, K. Ghorbani, W. Giang, L. Gladstone, M. Glagla, T. Glüsenkamp, A.

Goldschmidt, G. Golup, J. G. Gonzalez, D. Grant, Z. Griffith, C. Haack, A. H. Ismail, A. Hallgren, F. Halzen, E. Hansen, B. Hansmann, T. Hansmann, K. Hanson, D. Hebecker, D. Heereman, K. Helbing, R. Hellauer, S. Hickford, J. Hignight, G. C. Hill, K. D. Hoffman, R. Hoffmann, K. Holzapfel, K. Hoshina, F. Huang, M. Huber, K. Hultqvist, S. In, A. Ishihara, E. Jacobi, G. S. Japaridze, M. Jeong, K. Jero, B. J. P. Jones, M. Jurkovic, A. Kappes, T. Karg, A. Karle, U. Katz, M. Kauer, A. Keivani, J. L. Kelley, J. Kemp, A. Kheirandish, M. Kim, T. Kintscher, J. Kiryluk, T. Kittler, S. R. Klein, G. Kohnen, R. Koirala, H. Kolanoski, R. Konietz, L. Köpke, C. Kopper, S. Kopper, D. J. Koskinen, M. Kowalski, K. Krings, M. Kroll, G. Krückl, C. Krüger, J. Kunnen, S. Kunwar, N. Kurahashi, T. Kuwabara, M. Labare, J. L. Lanfranchi, M. J. Larson, F. Lauber, D. Lennarz, M. Lesiak-Bzdak, M. Leuermann, J. Leuner, L. Lu, J. Lünemann, J. Madsen, G. Maggi, K. B. M. Mahn, S. Mancina, M. Mandelartz, R. Maruyama, K. Mase, R. Maunu, F. McNally, K. Meagher, M. Medici, M. Meier, A. Meli, T. Menne, G. Merino, T. Meures, S. Miarecki, L. Mohrmann, T. Montaruli, M. Moulai, R. Nahnhauer, U. Naumann, G. Neer, H. Niederhausen, S. C. Nowicki, D. R. Nygren, A. O. O. Pollmann, A. Olivas, A. O'Murchadha, T. Palczewski, H. Pandya, D. V. Pankova, P. Peiffer, Ö. Penek, J. A. Pepper, C. P. Heros, D. Pieloth, E. Pinat, P. B. Price, G. T. Przybylski, M. Quinnan, C. Raab, L. Rädel, M. Rameez, K. Rawlins, R. Reimann, B. Relethford, M. Relich, E. Resconi, W. Rhode, M. Richman, B. Riedel, S. Robertson, M. Rongen, C. Rott, T. Ruhe, D. Ryckbosch, D. Rysewyk, L. Sabbatini, S. E. S. Herrera, A. Sandrock, J. Sandroos, S. Sarkar, K. Satalecka, M. Schimp, P. Schlunder, T. Schmidt, S. Schoenen, S. Schöneberg, L. Schumacher, D. Seckel, S. Seunarine, D. Soldin, M. Song, G. M. Spiczak, C. Spiering, M. Stahlberg, T. Stanev, A. Stasik, A. Steuer, T. Stezelberger, R. G. Stokstad, A. Stößl, R. Ström, N. L. Strotjohann, G. W. Sullivan, M. Sutherland, H. Taavola, I. Taboada, J. Tatar, F. Tenholt, S. Ter-Antonyan, A. Terliuk, G. Tešić, S. Tilav, P. A. Toale, M. N. Tobin, S. Toscano, D. Tosi, M. Tselengidou, A. Turcati, E. Unger, M. Usner, J. Vandenbroucke, N. Eijndhoven, S. Vanheule, M. Rossem, J. Santen, J. Veenkamp, M. Vehring, M. Voge, M. Vraeghe, C. Walck, A. Wallace, M. Wallraff, N. Wandkowsky, C. Weaver, M. J. Weiss, C. Wendt, S. Westerhoff, B. J. Whelan, S. Wickmann, K. Wiebe, C. H. Wiebusch, L. Wille, D. R. Williams, L. Wills, M. Wolf, T. R. Wood, E. Woolsey, K. Woschnagg, D. L. Xu, X. W. Xu, Y. Xu, J. P. Yanez, G. Yodh, S. Yoshida, M. Zoll, IceCube Collaboration, Observation and characterization of a cosmic muon neutrino flux from the Northern Hemisphere using six years of IceCube data. *Astrophys. J.* **833**, 3 (2016). [doi:10.3847/0004-637X/833/1/3](https://doi.org/10.3847/0004-637X/833/1/3)

26. Materials and methods are available as supplementary materials.
27. J. Ahrens, X. Bai, R. Bay, S. W. Barwick, T. Becka, J. K. Becker, K.-H. Becker, E. Bernardini, D. Bertrand, A. Biron, D. J. Boersma, S. Böser, O. Botner, A. Bouchta, O. Bouhali, T. Burgess, S. Carius, T. Castermans, D. Chirkin, B. Collin, J. Conrad, J. Cooley, D. F. Cowen, A. Davour, C. De Clercq, T. DeYoung, P. Desiati, J.-P. Dewulf, P. Ekström, T. Feser, M. Gaug, T. K. Gaisser, R. Ganugapati, H. Geenen, L. Gerhardt, A. Groß, A. Goldschmidt, A. Hallgren, F. Halzen, K. Hanson, R. Hardtke, T. Harenberg, T. Hauschildt, K. Helbing, M. Hellwig, P. Herquet, G. C. Hill, D. Hubert, B. Hughey, P. O. Hulth, K. Hultqvist, S. Hundertmark, J. Jacobsen, A. Karle, M. Kestel, L. Köpke, M. Kowalski, K. Kuehn, J. I. Lamoureux, H. Leich, M. Leuthold, P. Lindahl, I. Liubarsky, J. Madsen, P. Marciniewski, H. S. Matis, C. P. McParland, T. Messarius, Y. Minaeva, P. Miočinović, P. C. Mock, R. Morse, K. S. Münnich, J. Nam, R. Nahnhauer, T. Neunhöffer,

P. Niessen, D. R. Nygren, H. Ögelman, P. Olbrechts, C. Pérez de los Heros, A. C. Pohl, R. Porrata, P. B. Price, G. T. Przybylski, K. Rawlins, E. Resconi, W. Rhode, M. Ribordy, S. Richter, J. Rodríguez Martino, D. Ross, H.-G. Sander, K. Schinarakis, S. Schlenstedt, T. Schmidt, D. Schneider, R. Schwarz, A. Silvestri, M. Solarz, G. M. Spiczak, C. Spiering, M. Stamatikos, D. Steele, P. Steffen, R. G. Stokstad, K.-H. Sulanke, O. Streicher, I. Taboada, L. Thollander, S. Tilav, W. Wagner, C. Walck, Y.-R. Wang, C. H. Wiebusch, C. Wiedemann, R. Wischnewski, H. Wissing, K. Woschnagg, G. Yodh, Muon track reconstruction and data selection techniques in AMANDA. *Nucl. Instrum. Methods Phys. Res. A* **524**, 169–194 (2004). [doi:10.1016/j.nima.2004.01.065](https://doi.org/10.1016/j.nima.2004.01.065)

28. R. Abbasi, M. Ackermann, J. Adams, J. A. Aguilar, M. Ahlers, M. Ahrens, C. Alispach, A. A. Alves Jr., N. M. Amin, R. An, K. Andeen, T. Anderson, I. Ansseau, G. Anton, C. Argüelles, S. Axani, X. Bai, A. Balagopal V, A. Barbano, S. W. Barwick, B. Bastian, V. Basu, S. Baur, R. Bay, J. J. Beatty, K. -H. Becker, J. Becker Tjus, C. Bellenghi, S. BenZvi, D. Berley, E. Bernardini, D. Z. Besson, G. Binder, D. Bindig, E. Blaufuss, S. Blot, J. Borowka, S. Böser, O. Botner, J. Böttcher, E. Bourbeau, J. Bourbeau, F. Bradascio, J. Braun, S. Bron, J. Brostean-Kaiser, S. Browne, A. Burgman, R. S. Busse, M. A. Campana, C. Chen, D. Chirkin, K. Choi, B. A. Clark, K. Clark, L. Classen, A. Coleman, G. H. Collin, J. M. Conrad, P. Coppin, P. Correa, D. F. Cowen, R. Cross, P. Dave, C. De Clercq, J. J. DeLaunay, H. Dembinski, K. Deoskar, S. De Ridder, A. Desai, P. Desiati, K. D. de Vries, G. de Wasseige, M. de With, T. DeYoung, S. Dharani, A. Diaz, J. C. Díaz-Vélez, H. Dujmovic, M. Dunkman, M. A. DuVernois, E. Dvorak, T. Ehrhardt, P. Eller, R. Engel, H. Erpenbeck, J. Evans, P. A. Evenson, S. Fahey, A. R. Fazely, S. Fiedlschuster, A. T. Fienberg, K. Filimonov, C. Finley, L. Fischer, D. Fox, A. Franckowiak, E. Friedman, A. Fritz, P. Fürst, T. K. Gaisser, J. Gallagher, E. Ganster, S. Garrappa, L. Gerhardt, A. Ghadimi, C. Glaser, T. Glauch, T. Glüsenkamp, A. Goldschmidt, J. G. Gonzalez, S. Goswami, D. Grant, T. Grégoire, Z. Griffith, S. Griswold, M. Gündüz, C. Günther, C. Haack, A. Hallgren, R. Halliday, L. Halve, F. Halzen, M. Ha Minh, K. Hanson, J. Hardin, A. A. Harnisch, A. Haungs, S. Hauser, D. Hebecker, K. Helbing, F. Henningsen, E. C. Hettinger, S. Hickford, J. Hignight, C. Hill, G. C. Hill, K. D. Hoffman, R. Hoffmann, T. Hoinka, B. Hokanson-Fasig, K. Hoshina, F. Huang, M. Huber, T. Huber, K. Hultqvist, M. Hünnefeld, R. Hussain, S. In, N. Iovine, A. Ishihara, M. Jansson, G. S. Japaridze, M. Jeong, B. J. P. Jones, R. Joppe, D. Kang, W. Kang, X. Kang, A. Kappes, D. Kappesser, T. Karg, M. Karl, A. Karle, U. Katz, M. Kauer, M. Kellermann, J. L. Kelley, A. Kheirandish, K. Kin, T. Kintscher, J. Kiryluk, S. R. Klein, R. Koirala, H. Kolanoski, L. Köpke, C. Kopper, S. Kopper, D. J. Koskinen, P. Koundal, M. Kovacevich, M. Kowalski, K. Krings, N. Kurahashi, A. Kyriacou, C. Lagunas Gualda, J. L. Lanfranchi, M. J. Larson, F. Lauber, J. P. Lazar, J. W. Lee, K. Leonard, A. Leszczyńska, Y. Li, Q. R. Liu, E. Lohfink, C. J. Lozano Mariscal, L. Lu, F. Lucarelli, A. Ludwig, W. Luszczak, Y. Lyu, W. Y. Ma, J. Madsen, K. B. M. Mahn, Y. Makino, S. Mancina, I. C. Mariş, R. Maruyama, K. Mase, F. McNally, K. Meagher, A. Medina, M. Meier, S. Meighen-Berger, J. Merz, J. Micallef, D. Mockler, T. Montaruli, R. W. Moore, R. Morse, M. Moulai, R. Naab, R. Nagai, U. Naumann, J. Necker, L. V. Nguyẽn, H. Niederhausen, M. U. Nisa, S. C. Nowicki, D. R. Nygren, A. Obertacke Pollmann, M. Oehler, A. Olivas, E. O’Sullivan, H. Pandya, D. V. Pankova, N. Park, G. K. Parker, E. N. Paudel, L. Paul, C. Pérez de los Heros, S. Philippen, D. Pieloth, S. Pieper, A. Pizzuto, M. Plum, Y. Popovych, A. Porcelli, M. Prado Rodriguez, P. B. Price,

- B. Pries, G. T. Przybylski, C. Raab, A. Raissi, M. Rameez, K. Rawlins, I. C. Rea, A. Rehman, R. Reimann, G. Renzi, E. Resconi, S. Reusch, W. Rhode, M. Richman, B. Riedel, S. Robertson, G. Roellinghoff, M. Rongen, C. Rott, T. Ruhe, D. Ryckbosch, D. Rysewyk Cantu, I. Safa, J. Saffer, S. E. Sanchez Herrera, A. Sandrock, J. Sandroos, M. Santander, S. Sarkar, S. Sarkar, K. Satalecka, M. Scharf, M. Schaafel, H. Schieler, P. Schlunder, T. Schmidt, A. Schneider, J. Schneider, F. G. Schröder, L. Schumacher, S. Sclafani, D. Seckel, S. Seunarine, A. Sharma, S. Shefali, M. Silva, B. Skrzypek, B. Smithers, R. Snihur, J. Soedingrekso, D. Soldin, G. M. Spiczak, C. Spiering, J. Stachurska, M. Stamatikos, T. Stanev, R. Stein, J. Stettner, A. Steuer, T. Stezelberger, T. Stürwald, T. Stuttard, G. W. Sullivan, I. Taboada, F. Tenholt, S. Ter-Antonyan, S. Tilav, F. Tischbein, K. Tollefson, L. Tomankova, C. Tönnis, S. Toscano, D. Tosi, A. Trettin, M. Tselengidou, C. F. Tung, A. Turcati, R. Turcotte, C. F. Turley, J. P. Twagirayezu, B. Ty, M. A. Unland Elorrieta, N. Valtonen-Mattila, J. Vandebroucke, D. van Eijk, N. van Eijndhoven, D. Vannerom, J. van Santen, S. Verpoest, M. Vraeghe, C. Walck, A. Wallace, T. B. Watson, C. Weaver, P. Weigel, A. Weindl, M. J. Weiss, J. Weldert, C. Wendt, J. Werthebach, M. Weyrauch, B. J. Whelan, N. Whitehorn, C. H. Wiebusch, D. R. Williams, M. Wolf, K. Woschnagg, G. Wrede, J. Wulff, X. W. Xu, Y. Xu, J. P. Yanez, S. Yoshida, T. Yuan, Z. Zhang, A muon-track reconstruction exploiting stochastic losses for large-scale Cherenkov detectors. *J. Instrum.* **16**, P08034 (2021). [doi:10.1088/1748-0221/16/08/P08034](https://doi.org/10.1088/1748-0221/16/08/P08034)
29. R. Abbasi, Y. Abdou, T. Abu-Zayyad, J. Adams, J. A. Aguilar, M. Ahlers, K. Andeen, J. Auffenberg, X. Bai, M. Baker, S. W. Barwick, R. Bay, J. L. Bazo Alba, K. Beattie, J. J. Beatty, S. Bechet, J. K. Becker, K.-H. Becker, M. L. Benabderahmane, J. Berdermann, P. Berghaus, D. Berley, E. Bernardini, D. Bertrand, D. Z. Besson, M. Bissok, E. Blaufuss, D. J. Boersma, C. Bohm, S. Böser, O. Botner, L. Bradley, J. Braun, S. Buitink, M. Carson, D. Chirkin, B. Christy, J. Clem, F. Clevermann, S. Cohen, C. Colnard, D. F. Cowen, M. V. D'Agostino, M. Danninger, C. De Clercq, L. Demirörs, O. Depaepe, F. Descamps, P. Desiati, G. de Vries-Uiterweerd, T. DeYoung, J. C. Díaz-Vélez, J. Dreyer, J. P. Dumm, M. R. Duvoort, R. Ehrlich, J. Eisch, R. W. Ellsworth, O. Engdegård, S. Euler, P. A. Evenson, O. Fadiran, A. R. Fazely, A. Fedynitch, T. Feusels, K. Filimonov, C. Finley, M. M. Foerster, B. D. Fox, A. Franckowiak, R. Franke, T. K. Gaisser, J. Gallagher, R. Ganugapati, M. Geisler, L. Gerhardt, L. Gladstone, T. Glüsenkamp, A. Goldschmidt, J. A. Goodman, D. Grant, T. Griesel, A. Groß, S. Grullon, R. M. Gunasingha, M. Gurtner, C. Ha, A. Hallgren, F. Halzen, K. Han, K. Hanson, K. Helbing, P. Herquet, S. Hickford, G. C. Hill, K. D. Hoffman, A. Homeier, K. Hoshina, D. Hubert, W. Huelsnitz, J.-P. Hülf, P. O. Hulth, K. Hultqvist, S. Hussain, R. L. Imlay, A. Ishihara, J. Jacobsen, G. S. Japaridze, H. Johansson, J. M. Joseph, K.-H. Kampert, A. Kappes, T. Karg, A. Karle, J. L. Kelley, N. Kemming, P. Kenny, J. Kiryluk, F. Kislat, S. R. Klein, S. Knops, J.-H. Köhne, G. Kohnen, H. Kolanoski, L. Köpke, D. J. Koskinen, M. Kowalski, T. Kowarik, M. Krasberg, T. Krings, G. Kroll, K. Kuehn, T. Kuwabara, M. Labare, S. Lafrebre, K. Laihem, H. Landsman, R. Lauer, R. Lehmann, D. Lennarz, J. Lünemann, J. Madsen, P. Majumdar, R. Maruyama, K. Mase, H. S. Matis, M. Matusik, K. Meagher, M. Merck, P. Mészáros, T. Meures, E. Middell, N. Milke, T. Montaruli, R. Morse, S. M. Movit, K. Münich, R. Nahnhauer, J. W. Nam, U. Naumann, P. Nießen, D. R. Nygren, S. Odrowski, A. Olivas, M. Olivo, M. Ono, S. Panknin, L. Paul, C. Pérez de los Heros, J. Petrovic, A. Piesga, D. Pieloth, R. Porrata, J. Posselt, P. B. Price, M. Prikockis, G. T.

- Przybylski, K. Rawlins, P. Redl, E. Resconi, W. Rhode, M. Ribordy, A. Rizzo, J. P. Rodrigues, P. Roth, F. Rothmaier, C. Rott, C. Roucelle, T. Ruhe, D. Rutledge, B. Ruzybayev, D. Ryckbosch, H.-G. Sander, S. Sarkar, K. Schatto, S. Schlenstedt, T. Schmidt, D. Schneider, A. Schukraft, A. Schultes, O. Schulz, M. Schunck, D. Seckel, B. Semburg, S. H. Seo, Y. Sestayo, S. Seunarine, A. Silvestri, A. Slipak, G. M. Spiczak, C. Spiering, M. Stamatikos, T. Stanev, G. Stephens, T. Stezelberger, R. G. Stokstad, S. Stoyanov, E. A. Strahler, T. Straszheim, G. W. Sullivan, Q. Swillens, I. Taboada, A. Tamburro, O. Tarasova, A. Tepe, S. Ter-Antonyan, S. Tilav, P. A. Toale, D. Tosi, D. Turčan, N. van Eijndhoven, J. Vandebroucke, A. Van Overloop, J. van Santen, B. Voigt, C. Walck, T. Waldenmaier, M. Wallraff, M. Walter, C. Wendt, S. Westerhoff, N. Whitehorn, K. Wiebe, C. H. Wiebusch, G. Wikström, D. R. Williams, R. Wischnewski, H. Wissing, K. Woschnagg, C. Xu, X. W. Xu, G. Yodh, S. Yoshida, P. Zarzhitsky, The energy spectrum of atmospheric neutrinos between 2 and 200 TeV with the AMANDA-II detector. *Astropart. Phys.* **34**, 48–58 (2010). [doi:10.1016/j.astropartphys.2010.05.001](https://doi.org/10.1016/j.astropartphys.2010.05.001)
30. T. K. Gaisser, R. Engel, E. Resconi, *Cosmic Rays and Particle Physics: Second Edition* (Cambridge Univ. Press, 2016).
31. M. Aartsen, K. Abraham, M. Ackermann, J. Adams, J. A. Aguilar, M. Ahlers, M. Ahrens, D. Altmann, K. Andeen, T. Anderson, I. Ansseau, G. Anton, M. Archinger, C. Argüelles, J. Auffenberg, S. Axani, X. Bai, S. W. Barwick, V. Baum, R. Bay, J. J. Beatty, J. B. Tjus, K.-H. Becker, S. BenZvi, D. Berley, E. Bernardini, A. Bernhard, D. Z. Besson, G. Binder, D. Bindig, M. Bissok, E. Blaufuss, S. Blot, C. Bohm, M. Börner, F. Bos, D. Bose, S. Böser, O. Botner, J. Braun, L. Brayeur, H.-P. Bretz, S. Bron, A. Burgman, T. Carver, M. Casier, E. Cheung, D. Chirkin, A. Christov, K. Clark, L. Classen, S. Coenders, G. H. Collin, J. M. Conrad, D. F. Cowen, R. Cross, M. Day, J. P. A. M. André, C. D. Clercq, E. P. Rosendo, H. Dembinski, S. D. Ridder, P. Desiati, K. D. de Vries, G. de Wasseige, M. de With, T. DeYoung, J. C. Díaz-Vélez, V. Lorenzo, H. Dujmovic, J. P. Dumm, M. Dunkman, B. Eberhardt, T. Ehrhardt, B. Eichmann, P. Eller, S. Euler, P. A. Evenson, S. Fahey, A. R. Fazely, J. Feintzeig, J. Felde, K. Filimonov, C. Finley, S. Flis, C.-C. Fösig, A. Franckowiak, E. Friedman, T. Fuchs, T. K. Gaisser, J. Gallagher, L. Gerhardt, K. Ghorbani, W. Giang, L. Gladstone, T. Glauch, T. Glüsenkamp, A. Goldschmidt, G. Golup, J. G. Gonzalez, D. Grant, Z. Griffith, C. Haack, A. H. Ismail, A. Hallgren, F. Halzen, E. Hansen, T. Hansmann, K. Hanson, D. Hebecker, D. Heereman, K. Helbing, R. Hellauer, S. Hickford, J. Hignight, G. C. Hill, K. D. Hoffman, R. Hoffmann, K. Holzapfel, K. Hoshina, F. Huang, M. Huber, K. Hultqvist, S. In, A. Ishihara, E. Jacobi, G. S. Japaridze, M. Jeong, K. Jero, B. J. P. Jones, M. Jurkovic, A. Kappes, T. Karg, A. Karle, U. Katz, M. Kauer, A. Keivani, J. L. Kelley, A. Kheirandish, M. Kim, T. Kintscher, J. Kiryluk, T. Kittler, S. R. Klein, G. Kohnen, R. Koirala, H. Kolanoski, R. Konietz, L. Köpke, C. Kopper, S. Kopper, D. J. Koskinen, M. Kowalski, K. Krings, M. Kroll, G. Krückl, C. Krüger, J. Kunnen, S. Kunwar, N. Kurahashi, T. Kuwabara, M. Labare, J. L. Lanfranchi, M. J. Larson, F. Lauber, D. Lennarz, M. Lesiak-Bzdak, M. Leuermann, L. Lu, J. Lünemann, J. Madsen, G. Maggi, K. B. M. Mahn, S. Mancina, M. Mandelartz, R. Maruyama, K. Mase, R. Maunu, F. McNally, K. Meagher, M. Medici, M. Meier, A. Meli, T. Menne, G. Merino, T. Meures, S. Miarecki, L. Mohrmann, T. Montaruli, M. Moulai, R. Nahnhauer, U. Naumann, G. Neer, H. Niederhausen, S. C. Nowicki, D. R. Nygren, A. O. Pollmann, A. Olivas, A. O'Murchadha, T. Palczewski, H. Pandya, D. V. Pankova, P. Peiffer, Ö. Penek, J. A.

Pepper, C. P. Heros, D. Pieloth, E. Pinat, P. B. Price, G. T. Przybylski, M. Quinnan, C. Raab, L. Rädel, M. Rameez, K. Rawlins, R. Reimann, B. Relethford, M. Relich, E. Resconi, W. Rhode, M. Richman, B. Riedel, S. Robertson, M. Rongen, C. Rott, T. Ruhe, D. Ryckbosch, D. Rysewyk, L. Sabbatini, S. E. S. Herrera, A. Sandrock, J. Sandroos, S. Sarkar, K. Satalecka, P. Schlunder, T. Schmidt, S. Schoenen, S. Schöneberg, L. Schumacher, D. Seckel, S. Seunarine, D. Soldin, M. Song, G. M. Spiczak, C. Spiering, T. Staney, A. Stasik, J. Stettner, A. Steuer, T. Stezelberger, R. G. Stokstad, A. Stössl, R. Ström, N. L. Strotjohann, G. W. Sullivan, M. Sutherland, H. Taavola, I. Taboada, J. Tatar, F. Tenholt, S. Ter-Antonyan, A. Terliuk, G. Tešić, S. Tilav, P. A. Toale, M. N. Tobin, S. Toscano, D. Tosi, M. Tselengidou, A. Turcati, E. Unger, M. Usner, J. Vandenbroucke, N. Eijndhoven, S. Vanheule, M. Rossem, J. Santen, J. Veenkamp, M. Vehring, M. Voge, E. Vogel, M. Vraeghe, C. Walck, A. Wallace, M. Wallraff, N. Wandkowsky, C. Weaver, M. J. Weiss, C. Wendt, S. Westerhoff, B. J. Whelan, S. Wickmann, K. Wiebe, C. H. Wiebusch, L. Wille, D. R. Williams, L. Wills, M. Wolf, T. R. Wood, E. Woolsey, K. Woschnagg, D. L. Xu, X. W. Xu, Y. Xu, J. P. Yanez, G. Yodh, S. Yoshida, M. Zoll, IceCube Collaboration, All-sky Search for Time-integrated Neutrino Emission from Astrophysical Sources with 7 yr of IceCube Data. *Astrophys. J.* **835**, 151 (2017). [doi:10.3847/1538-4357/835/2/151](https://doi.org/10.3847/1538-4357/835/2/151)

32. S. Abdollahi, F. Acero, M. Ackermann, M. Ajello, W. B. Atwood, M. Axelsson, L. Baldini, J. Ballet, G. Barbiellini, D. Bastieri, J. Becerra Gonzalez, R. Bellazzini, A. Berretta, E. Bissaldi, R. D. Blandford, E. D. Bloom, R. Bonino, E. Bottacini, T. J. Brandt, J. Bregeon, P. Bruel, R. Buehler, T. H. Burnett, S. Buson, R. A. Cameron, R. Caputo, P. A. Caraveo, J. M. Casandjian, D. Castro, E. Cavazzuti, E. Charles, S. Chaty, S. Chen, C. C. Cheung, G. Chiaro, S. Ciprini, J. Cohen-Tanugi, L. R. Cominsky, J. Coronado-Blázquez, D. Costantin, A. Cuoco, S. Cutini, F. D'Ammando, M. DeKlotz, P. Torre Luque, F. de Palma, A. Desai, S. W. Digel, N. D. Lalla, M. D. Mauro, L. D. Venere, A. Domínguez, D. Dumora, F. F. Dirirsa, S. J. Fegan, E. C. Ferrara, A. Franckowiak, Y. Fukazawa, S. Funk, P. Fusco, F. Gargano, D. Gasparini, N. Giglietto, P. Giommi, F. Giordano, M. Giroletti, T. Glanzman, D. Green, I. A. Grenier, S. Griffin, M.-H. Grondin, J. E. Grove, S. Guiriec, A. K. Harding, K. Hayashi, E. Hays, J. W. Hewitt, D. Horan, G. Jóhannesson, T. J. Johnson, T. Kamae, M. Kerr, D. Kocevski, M. Kovac'evic', M. Kuss, D. Landriu, S. Larsson, L. Latronico, M. Lemoine-Goumard, J. Li, I. Liodakis, F. Longo, F. Loparco, B. Lott, M. N. Lovellette, P. Lubrano, G. M. Madejski, S. Maldera, D. Malyshev, A. Manfreda, E. J. Marchesini, L. Marcotulli, G. Martí-Devesa, P. Martin, F. Massaro, M. N. Mazziotta, J. E. McEnery, I. Mereu, M. Meyer, P. F. Michelson, N. Mirabal, T. Mizuno, M. E. Monzani, A. Morselli, I. V. Moskalenko, M. Negro, E. Nuss, R. Ojha, N. Omodei, M. Orienti, E. Orlando, J. F. Ormes, M. Palatiello, V. S. Paliya, D. Paneque, Z. Pei, H. Peña-Herazo, J. S. Perkins, M. Persic, M. Pesce-Rollins, V. Petrosian, L. Petrov, F. Piron, H. Poon, T. A. Porter, G. Principe, S. Rainò, R. Rando, M. Razzano, S. Razzaque, A. Reimer, O. Reimer, Q. Remy, T. Reposeur, R. W. Romani, P. M. S. Parkinson, F. K. Schinzel, D. Serini, C. Sgrò, E. J. Siskind, D. A. Smith, G. Spandre, P. Spinelli, A. W. Strong, D. J. Suson, H. Tajima, M. N. Takahashi, D. Tak, J. B. Thayer, D. J. Thompson, L. Tibaldo, D. F. Torres, E. Torresi, J. Valverde, B. V. Klaveren, P. Zyl, K. Wood, M. Yassine, G. Zaharijas, *Fermi* Large Area Telescope Fourth Source Catalog. *Astrophys. J. Suppl. Ser.* **247**, 33 (2020). [doi:10.3847/1538-4365/ab6bcb](https://doi.org/10.3847/1538-4365/ab6bcb)

33. S. P. Wakely, D. Horan, *International Cosmic Ray Conference*, vol. 3 of *International Cosmic Ray Conference* (2008), pp. 1341–1344.
34. P. Padovani, P. Giommi, E. Resconi, T. Glauch, B. Arsioli, N. Sahakyan, M. Huber, Dissecting the region around IceCube-170922A: The blazar TXS 0506+056 as the first cosmic neutrino source. *Mon. Not. R. Astron. Soc.* **480**, 192–203 (2018). [doi:10.1093/mnras/sty1852](https://doi.org/10.1093/mnras/sty1852)
35. M. Bustamante, J. F. Beacom, W. Winter, Theoretically Palatable Flavor Combinations of Astrophysical Neutrinos. *Phys. Rev. Lett.* **115**, 161302 (2015). [doi:10.1103/PhysRevLett.115.161302](https://doi.org/10.1103/PhysRevLett.115.161302) Medline
36. C. A. Argüelles, T. Katori, J. Salvado, Effect of New Physics in Astrophysical Neutrino Flavor. *Phys. Rev. Lett.* **115**, 161303 (2015). [doi:10.1103/PhysRevLett.115.161303](https://doi.org/10.1103/PhysRevLett.115.161303) Medline
37. J. Bland-Hawthorn, J. F. Gallimore, L. J. Tacconi, E. Brinks, S. A. Baum, R. R. J. Antonucci, G. N. Cecil, *Astrophys. Space Sci.* **248**, 9–19 (1997). [doi:10.1023/A:1000567831370](https://doi.org/10.1023/A:1000567831370)
38. B. F. Madore, in *27th Rencontres de Moriond: Physics of Nearby Galaxies: Nature or Nurture?*, T. X. Thuan, J. Tran Thanh Van, C. Balkoski, Eds. (Ed. Frontieres, 1992), pp. 25–28.
39. Gravity Collaboration, O. Pfuhl, R. Davies, J. Dexter, H. Netzer, S. Höning, D. Lutz, M. Schartmann, E. Sturm, A. Amorim, W. Brandner, Y. Clénet, P. T. de Zeeuw, A. Eckart, F. Eisenhauer, N. M. Förster Schreiber, F. Gao, P. J. V. Garcia, R. Genzel, S. Gillessen, D. Gratadour, M. Kishimoto, S. Lacour, F. Millour, T. Ott, T. Paumard, K. Perraut, G. Perrin, B. M. Peterson, P. O. Petrucci, M. A. Prieto, D. Rouan, J. Shangguan, T. Shimizu, A. Sternberg, O. Straub, C. Straubmeier, L. J. Tacconi, K. R. W. Tristram, P. Vermot, I. Waisberg, F. Widmann, J. Woillez, An image of the dust sublimation region in the nucleus of NGC 1068. *Astron. Astrophys.* **634**, A1 (2020). [doi:10.1051/0004-6361/201936255](https://doi.org/10.1051/0004-6361/201936255)
40. M. Ajello, R. Angioni, M. Axelsson, J. Ballet, G. Barbiellini, D. Bastieri, J. Becerra Gonzalez, R. Bellazzini, E. Bissaldi, E. D. Bloom, R. Bonino, E. Bottacini, P. Bruel, S. Buson, F. Cafardo, R. A. Cameron, E. Cavazzuti, S. Chen, C. C. Cheung, S. Ciprini, D. Costantin, S. Cutini, F. D’Ammando, P. de la Torre Luque, R. de Menezes, F. de Palma, A. Desai, N. Di Lalla, L. Di Venere, A. Domínguez, F. F. Dirirsa, E. C. Ferrara, J. Finke, A. Franckowiak, Y. Fukazawa, S. Funk, P. Fusco, F. Gargano, S. Garrappa, D. Gasparrini, N. Giglietto, F. Giordano, M. Giroletti, D. Green, I. A. Grenier, S. Guiriec, S. Harita, E. Hays, D. Horan, R. Itoh, G. Jóhannesson, M. Kovac’evic’, F. Krauss, M. Kreter, M. Kuss, S. Larsson, C. Leto, J. Li, I. Liodakis, F. Longo, F. Loparco, B. Lott, M. N. Lovellette, P. Lubrano, G. M. Madejski, S. Maldera, A. Manfreda, G. Martí-Devesa, F. Massaro, M. N. Mazziotta, I. Mereu, M. Meyer, G. Migliori, N. Mirabal, T. Mizuno, M. E. Monzani, A. Morselli, I. V. Moskalenko, M. Negro, R. Nemmen, E. Nuss, L. S. Ojha, R. Ojha, N. Omodei, M. Orienti, E. Orlando, J. F. Ormes, V. S. Paliya, Z. Pei, H. Peña-Herazo, M. Persic, M. Pesce-Rollins, L. Petrov, F. Piron, H. Poon, G. Principe, S. Rainò, R. Rando, B. Rani, M. Razzano, S. Razzaque, A. Reimer, O. Reimer, F. K. Schinzel, D. Serini, C. Sgrò, E. J. Siskind, G. Spandre, P. Spinelli, D. J. Suson, Y. Tachibana, D. J. Thompson, D. F. Torres, E. Torresi, E. Troja, J. Valverde, P. van Zyl,

M. Yassine, The Fourth Catalog of Active Galactic Nuclei Detected by the *Fermi* Large Area Telescope. *Astrophys. J.* **892**, 105 (2020). [doi:10.3847/1538-4357/ab791e](https://doi.org/10.3847/1538-4357/ab791e)

41. S. Abdollahi, F. Acero, M. Ackermann, M. Ajello, W. B. Atwood, M. Axelsson, L. Baldini, J. Ballet, G. Barbiellini, D. Bastieri, J. Becerra Gonzalez, R. Bellazzini, A. Berretta, E. Bissaldi, R. D. Blandford, E. D. Bloom, R. Bonino, E. Bottacini, T. J. Brandt, J. Bregeon, P. Bruel, R. Buehler, T. H. Burnett, S. Buson, R. A. Cameron, R. Caputo, P. A. Caraveo, J. M. Casandjian, D. Castro, E. Cavazzuti, E. Charles, S. Chaty, S. Chen, C. C. Cheung, G. Chiaro, S. Ciprini, J. Cohen-Tanugi, L. R. Cominsky, J. Coronado-Blázquez, D. Costantin, A. Cuoco, S. Cutini, F. D'Ammando, M. DeKlotz, P. Torre Luque, F. de Palma, A. Desai, S. W. Digel, N. D. Lalla, M. D. Mauro, L. D. Venere, A. Domínguez, D. Dumora, F. F. Dirirsa, S. J. Fegan, E. C. Ferrara, A. Franckowiak, Y. Fukazawa, S. Funk, P. Fusco, F. Gargano, D. Gasparini, N. Giglietto, P. Giommi, F. Giordano, M. Giroletti, T. Glanzman, D. Green, I. A. Grenier, S. Griffin, M.-H. Grondin, J. E. Grove, S. Guiriec, A. K. Harding, K. Hayashi, E. Hays, J. W. Hewitt, D. Horan, G. Jóhannesson, T. J. Johnson, T. Kamae, M. Kerr, D. Kocevski, M. Kovac’evic’, M. Kuss, D. Landriu, S. Larsson, L. Latronico, M. Lemoine-Goumard, J. Li, I. Liodakis, F. Longo, F. Loparco, B. Lott, M. N. Lovellette, P. Lubrano, G. M. Madejski, S. Maldera, D. Malyshev, A. Manfreda, E. J. Marchesini, L. Marcotulli, G. Martí-Devesa, P. Martin, F. Massaro, M. N. Mazziotta, J. E. McEnery, I. Mereu, M. Meyer, P. F. Michelson, N. Mirabal, T. Mizuno, M. E. Monzani, A. Morselli, I. V. Moskalenko, M. Negro, E. Nuss, R. Ojha, N. Omodei, M. Orienti, E. Orlando, J. F. Ormes, M. Palatiello, V. S. Paliya, D. Paneque, Z. Pei, H. Peña-Herazo, J. S. Perkins, M. Persic, M. Pesce-Rollins, V. Petrosian, L. Petrov, F. Piron, H. Poon, T. A. Porter, G. Principe, S. Rainò, R. Rando, M. Razzano, S. Razzaque, A. Reimer, O. Reimer, Q. Remy, T. Reposeur, R. W. Romani, P. M. S. Parkinson, F. K. Schinzel, D. Serini, C. Sgrò, E. J. Siskind, D. A. Smith, G. Spandre, P. Spinelli, A. W. Strong, D. J. Suson, H. Tajima, M. N. Takahashi, D. Tak, J. B. Thayer, D. J. Thompson, L. Tibaldo, D. F. Torres, E. Torresi, J. Valverde, B. V. Klaveren, P. Zyl, K. Wood, M. Yassine, G. Zaharijas, *Fermi* Large Area Telescope Fourth Source Catalog. *Astrophys. J. Suppl. Ser.* **247**, 33 (2020). [doi:10.3847/1538-4365/ab6bcb](https://doi.org/10.3847/1538-4365/ab6bcb)
42. V. A. Acciari, S. Ansoldi, L. A. Antonelli, A. A. Engels, D. Baack, A. Babić, B. Banerjee, U. Barres de Almeida, J. A. Barrio, J. Becerra González, W. Bednarek, L. Bellizzi, E. Bernardini, A. Berti, J. Besenrieder, W. Bhattacharyya, C. Bigongiari, A. Biland, O. Blanch, G. Bonnoli, Ž. Bošnjak, G. Busetto, R. Carosi, G. Ceribella, Y. Chai, A. Chilingaryan, S. Cikota, S. M. Colak, U. Colin, E. Colombo, J. L. Contreras, J. Cortina, S. Covino, V. D’Elia, P. Da Vela, F. Dazzi, A. De Angelis, B. De Lotto, M. Delfino, J. Delgado, D. Depaoli, F. Di Pierro, L. Di Venere, E. D. Souto Espiñeira, D. Dominis Prester, A. Donini, D. Dorner, M. Doro, D. Elsaesser, V. Fallah Ramazani, A. Fattorini, G. Ferrara, D. Fidalgo, L. Foffano, M. V. Fonseca, L. Font, C. Fruck, S. Fukami, R. J. García López, M. Garczarczyk, S. Gasparyan, M. Gaug, N. Giglietto, F. Giordano, N. Godinović, D. Green, D. Guberman, D. Hadashch, A. Hahn, J. Herrera, J. Hoang, D. Hrupec, M. Hütten, T. Inada, S. Inoue, K. Ishio, Y. Iwamura, L. Jouvin, D. Kerszberg, H. Kubo, J. Kushida, A. Lamastra, D. Lelas, F. Leone, E. Lindfors, S. Lombardi, F. Longo, M. López, R. López-Coto, A. López-Oramas, S. Loporchio, B. Machado de Oliveira Fraga, C. Maggio, P. Majumdar, M. Makariev, M. Mallamaci, G. Maneva, M. Manganaro, K. Mannheim, L. Maraschi, M. Mariotti, M. Martínez, D. Mazin, S. Mićanović, D. Miceli, M. Minev, J. M. Miranda, R. Mirzoyan, E. Molina, A. Moralejo,

- D. Morcuende, V. Moreno, E. Moretti, P. Munar-Adrover, V. Neustroev, C. Nigro, K. Nilsson, D. Ninci, K. Nishijima, K. Noda, L. Nogués, S. Nozaki, S. Paiano, J. Palacio, M. Palatiello, D. Paneque, R. Paoletti, J. M. Paredes, P. Peñil, M. Peresano, M. Persic, P. G. Prada Moroni, E. Prandini, I. Puljak, W. Rhode, M. Ribó, J. Rico, C. Righi, A. Rugliancich, L. Saha, N. Sahakyan, T. Saito, S. Sakurai, K. Satalecka, K. Schmidt, T. Schweizer, J. Sitarek, I. Šnidarić, D. Sobczynska, A. Somero, A. Stamerra, D. Strom, M. Strzys, Y. Suda, T. Surić, M. Takahashi, F. Tavecchio, P. Temnikov, T. Terzić, M. Teshima, N. Torres-Albà, L. Tosti, V. Vagelli, J. van Scherpenberg, G. Vanzo, M. Vazquez Acosta, C. F. Vigorito, V. Vitale, I. Vovk, M. Will, D. Zarić, F. Fiore, C. Feruglio, Y. Rephaeli, Constraints on Gamma-Ray and Neutrino Emission from NGC 1068 with the MAGIC Telescopes. *Astrophys. J.* **883**, 135 (2019). [doi:10.3847/1538-4357/ab3a51](https://doi.org/10.3847/1538-4357/ab3a51)
43. C. Ricci, Y. Ueda, M. J. Koss, B. Trakhtenbrot, F. E. Bauer, P. Gandhi, Compton-thick accretion in the local universe. *Astrophys. J. Lett.* **815**, L13 (2015). [doi:10.1088/2041-8205/815/1/L13](https://doi.org/10.1088/2041-8205/815/1/L13)
44. A. Marinucci, S. Bianchi, G. Matt, D. M. Alexander, M. Baloković, F. E. Bauer, W. N. Brandt, P. Gandhi, M. Guainazzi, F. A. Harrison, K. Iwasawa, M. Koss, K. K. Madsen, F. Nicastro, S. Puccetti, C. Ricci, D. Stern, D. J. Walton, *NuSTAR* catches the unveiling nucleus of NGC 1068. *Mon. Not. R. Astron. Soc.* **456**, L94–L98 (2016). [doi:10.1093/mnrasl/slv178](https://doi.org/10.1093/mnrasl/slv178)
45. A. Zaino, S. Bianchi, A. Marinucci, G. Matt, F. E. Bauer, W. N. Brandt, P. Gandhi, M. Guainazzi, K. Iwasawa, S. Puccetti, C. Ricci, D. J. Walton, Probing the circumnuclear absorbing medium of the buried AGN in NGC 1068 through *NuSTAR* observations. *Mon. Not. R. Astron. Soc.* **492**, 3872–3884 (2020). [doi:10.1093/mnras/staa107](https://doi.org/10.1093/mnras/staa107)
46. A. B. Romeo, K. Fathi, What powers the starburst activity of NGC 1068? Star-driven gravitational instabilities caught in the act. *Mon. Not. R. Astron. Soc.* **460**, 2360–2367 (2016). [doi:10.1093/mnras/stw1147](https://doi.org/10.1093/mnras/stw1147)
47. B. Eichmann, J. B. Tjus, The radio–gamma correlation in starburst galaxies. *Astrophys. J.* **821**, 87 (2016). [doi:10.3847/0004-637X/821/2/87](https://doi.org/10.3847/0004-637X/821/2/87)
48. G. Cecil, J. Bland, R. B. Tully, Imaging spectrophotometry of ionized gas in NGC 1068. I. Kinematics of the narrow-line region. *Astrophys. J.* **355**, 70 (1990). [doi:10.1086/168742](https://doi.org/10.1086/168742)
49. R. Silberberg, M. M. Shapiro, *Neutrinos as a Probe for the Nature of and Processes in Active Galactic Nuclei*, vol. 10 of *16th International Cosmic Ray Conference*, S. Miyake, N. G. Kaigi, N. B. Gakkai, Eds. (Institute for Cosmic Ray Research, 1979), p. 357.
50. T. M. Yoast-Hull, J. S. Gallagher III, E. G. Zweibel, J. E. Everett, Active galactic nuclei, neutrinos, and interacting cosmic rays in NGC 253 and NGC 1068. *Astrophys. J.* **780**, 137 (2014). [doi:10.1088/0004-637X/780/2/137](https://doi.org/10.1088/0004-637X/780/2/137)
51. A. Lamastra, F. Fiore, D. Guetta, L. A. Antonelli, S. Colafrancesco, N. Menci, S. Puccetti, A. Stamerra, L. Zappacosta, Galactic outflow driven by the active nucleus and the origin of the gamma-ray emission in NGC 1068. *Astron. Astrophys.* **596**, A68 (2016). [doi:10.1051/0004-6361/201628667](https://doi.org/10.1051/0004-6361/201628667)

52. Y. Inoue, D. Khangulyan, A. Doi, On the Origin of High-energy Neutrinos from NGC 1068: The Role of Nonthermal Coronal Activity. *Astrophys. J. Lett.* **891**, L33 (2020). [doi:10.3847/2041-8213/ab7661](https://doi.org/10.3847/2041-8213/ab7661)
53. K. Murase, S. S. Kimura, P. Mészáros, Hidden Cores of Active Galactic Nuclei as the Origin of Medium-Energy Neutrinos: Critical Tests with the MeV Gamma-Ray Connection. *Phys. Rev. Lett.* **125**, 011101 (2020). [doi:10.1103/PhysRevLett.125.011101](https://doi.org/10.1103/PhysRevLett.125.011101) [Medline](#)
54. R. Silberberg, M. M. Shapiro, in *Composition and Origin of Cosmic Rays*, M. M. Shapiro, Ed., vol. 107 of *NATO Advanced Study Institute (ASI) Series C* (Springer, 1983), pp. 231–244.
55. Y. Inoue, D. Khangulyan, S. Inoue, A. Doi, On High-energy Particles in Accretion Disk Coronae of Supermassive Black Holes: Implications for MeV Gamma-rays and High-energy Neutrinos from AGN Cores. *Astrophys. J.* **880**, 40 (2019). [doi:10.3847/1538-4357/ab2715](https://doi.org/10.3847/1538-4357/ab2715)
56. F. W. Stecker, C. Done, M. H. Salamon, P. Sommers, High-energy neutrinos from active galactic nuclei. *Phys. Rev. Lett.* **66**, 2697–2700 (1991). [doi:10.1103/PhysRevLett.66.2697](https://doi.org/10.1103/PhysRevLett.66.2697) [Medline](#)
57. R. Silberberg, M. M. Shapiro, C. H. Starr, in *Particle Astrophysics and Cosmology*, M. M. Shapiro, R. Silberberg, J. P. Wefel, Eds., vol. 394 of *NATO Advanced Study Institute (ASI) Series C* (Springer, 1993), p. 53.
58. K. Murase, E. Waxman, Constraining high-energy cosmic neutrino sources: Implications and prospects. *Phys. Rev. D* **94**, 103006 (2016). [doi:10.1103/PhysRevD.94.103006](https://doi.org/10.1103/PhysRevD.94.103006)
59. F. Capel, D. J. Mortlock, C. Finley, Bayesian constraints on the astrophysical neutrino source population from IceCube data. *Phys. Rev. D* **101**, 123017 (2020). [doi:10.1103/PhysRevD.101.123017](https://doi.org/10.1103/PhysRevD.101.123017)
60. C. F. Tung, T. Glauch, M. Larson, A. Pizzuto, R. Reimann, I. Taboada, FIRESONG: A python package to simulate populations of extragalactic neutrino sources. *J. Open Source Softw.* **6**, 3194 (2021). [doi:10.21105/joss.03194](https://doi.org/10.21105/joss.03194)
61. G. Paturel, C. Petit, P. Prugniel, G. Theureau, J. Rousseau, M. Brouty, P. Dubois, L. Cambrésy, HYPERLEDA - I. Identification and designation of galaxies. *Astron. Astrophys.* **412**, 45–55 (2003). [doi:10.1051/0004-6361:20031411](https://doi.org/10.1051/0004-6361:20031411)
62. J. Stettner, Measurement of the diffuse astrophysical muon-neutrino spectrum with ten years of IceCube data. *PoS ICRC2019*, 1017 (2021). [doi:10.22323/1.358.1017](https://doi.org/10.22323/1.358.1017)
63. J. Braun, J. Dumm, F. De Palma, C. Finley, A. Karle, T. Montaruli, Methods for point source analysis in high energy neutrino telescopes. *Astropart. Phys.* **29**, 299–305 (2008). [doi:10.1016/j.astropartphys.2008.02.007](https://doi.org/10.1016/j.astropartphys.2008.02.007)
64. A. Fedynitch, R. Engel, T. K. Gaisser, F. Riehn, T. Stanev, Calculation of conventional and prompt lepton fluxes at very high energy. *EPJ Web Conf.* **99**, 08001 (2015). [doi:10.1051/epjconf/20159908001](https://doi.org/10.1051/epjconf/20159908001)
65. T. K. Gaisser, T. Stanev, S. Tilav, Cosmic ray energy spectrum from measurements of air showers. *Front. Phys.* **8**, 748–758 (2013). [doi:10.1007/s11467-013-0319-7](https://doi.org/10.1007/s11467-013-0319-7)

66. H. Dembinski, R. Engel, A. Fedynitch, T. Gaisser, F. Riehn, T. Stanev, Data-driven model of the cosmic-ray flux and mass composition from 10 GeV to 10^{11} GeV. *PoS ICRC2017*, 533 (2018). [doi:10.22323/1.301.0533](https://doi.org/10.22323/1.301.0533)
67. A. Fedynitch, F. Riehn, R. Engel, T. K. Gaisser, T. Stanev, Hadronic interaction model SIBYLL 2.3c and inclusive lepton fluxes. *Phys. Rev. D* **100**, 103018 (2019). [doi:10.1103/PhysRevD.100.103018](https://doi.org/10.1103/PhysRevD.100.103018)
68. P. Heix, S. Tilav, C. Wiebusch, M. Zöcklein, Seasonal Variation of Atmospheric Neutrinos in IceCube. *PoS ICRC2019*, 465 (2021). [doi:10.22323/1.358.0465](https://doi.org/10.22323/1.358.0465)
69. P. Virtanen, R. Gommers, T. E. Oliphant, M. Haberland, T. Reddy, D. Cournapeau, E. Burovski, P. Peterson, W. Weckesser, J. Bright, S. J. van der Walt, M. Brett, J. Wilson, K. J. Millman, N. Mayorov, A. R. J. Nelson, E. Jones, R. Kern, E. Larson, C. J. Carey, İ. Polat, Y. Feng, E. W. Moore, J. VanderPlas, D. Laxalde, J. Perktold, R. Cimrman, I. Henriksen, E. A. Quintero, C. R. Harris, A. M. Archibald, A. H. Ribeiro, F. Pedregosa, P. van Mulbregt, SciPy 1.0 Contributors, SciPy 1.0: Fundamental algorithms for scientific computing in Python. *Nat. Methods* **17**, 261–272 (2020). [doi:10.1038/s41592-019-0686-2](https://doi.org/10.1038/s41592-019-0686-2) [Medline](#)
70. A. Poluektov, Kernel density estimation of a multidimensional efficiency profile. *JINST* **10**, P02011 (2015). [doi:10.1088/1748-0221/10/02/P02011](https://doi.org/10.1088/1748-0221/10/02/P02011)
71. T. Neunhöffer, Estimating the angular resolution of tracks in neutrino telescopes based on a likelihood analysis. *Astropart. Phys.* **25**, 220–225 (2006). [doi:10.1016/j.astropartphys.2006.01.002](https://doi.org/10.1016/j.astropartphys.2006.01.002)
72. G. Ke, Q. Meng, T. Finley, T. Wang, W. Chen, W. Ma, Q. Ye, T.-Y. Liu, in *Advances in Neural Information Processing Systems*, I. Guyon, U. Von Luxburg, S. Bengio, H. Wallach, R. Fergus, S. Vishwanathan, R. Garnett, Eds. (Curran Associates, Inc., NIPS2017, 2017).
73. M. Kronmueller, T. Glauch, Application of Deep Neural Networks to Event Type Classification in IceCube. *PoS ICRC2019*, 937 (2021). [doi:10.22323/1.358.0937](https://doi.org/10.22323/1.358.0937)
74. C. Szegedy, S. Ioffe, V. Vanhoucke, A. Alemi, Inception-v4, Inception-ResNet and the Impact of Residual Connections on Learning. [arXiv:1602.07261](https://arxiv.org/abs/1602.07261) [cs.CV] (2016).
75. M. G. Aartsen, R. Abbasi, M. Ackermann, J. Adams, J. A. Aguilar, M. Ahlers, D. Altmann, C. Arguelles, J. Auffenberg, X. Bai, M. Baker, S. W. Barwick, V. Baum, R. Bay, J. J. Beatty, J. Becker Tjus, K.-H. Becker, S. BenZvi, P. Berghaus, D. Berley, E. Bernardini, A. Bernhard, D. Z. Besson, G. Binder, D. Bindig, M. Bissok, E. Blaufuss, J. Blumenthal, D. J. Boersma, C. Bohm, D. Bose, S. Böser, O. Botner, L. Brayeur, H.-P. Bretz, A. M. Brown, R. Bruijn, J. Casey, M. Casier, D. Chirkin, A. Christov, B. Christy, K. Clark, L. Classen, F. Clevermann, S. Coenders, S. Cohen, D. F. Cowen, A. H. Cruz Silva, M. Danninger, J. Daughhetee, J. C. Davis, M. Day, C. De Clercq, S. De Ridder, P. Desiati, K. D. de Vries, M. de With, T. DeYoung, J. C. Díaz-Vélez, M. Dunkman, R. Eagan, B. Eberhardt, B. Eichmann, J. Eisch, S. Euler, P. A. Evenson, O. Fadiran, A. R. Fazely, A. Fedynitch, J. Feintzeig, T. Feusels, K. Filimonov, C. Finley, T. Fischer-Wasels, S. Flis, A. Franckowiak, K. Frantzen, T. Fuchs, T. K. Gaisser, J. Gallagher, L. Gerhardt, L. Gladstone, T. Glüsenkamp, A. Goldschmidt, G. Golup, J. G. Gonzalez, J. A. Goodman, D. Góra, D. T. Grandmont, D. Grant, P. Gretskov, J. C.

Groh, A. Groß, C. Ha, A. Haj Ismail, P. Hallen, A. Hallgren, F. Halzen, K. Hanson, D. Hebecker, D. Heereman, D. Heinen, K. Helbing, R. Hellauer, S. Hickford, G. C. Hill, K. D. Hoffman, R. Hoffmann, A. Homeier, K. Hoshina, F. Huang, W. Huelsnitz, P. O. Hulth, K. Hultqvist, S. Hussain, A. Ishihara, S. Jackson, E. Jacobi, J. Jacobsen, K. Jagielski, G. S. Japaridze, K. Jero, O. Jlelati, B. Kaminsky, A. Kappes, T. Karg, A. Karle, M. Kauer, J. L. Kelley, J. Kiryluk, J. Kläs, S. R. Klein, J.-H. Köhne, G. Kohnen, H. Kolanoski, L. Köpke, C. Kopper, S. Kopper, D. J. Koskinen, M. Kowalski, M. Krasberg, A. Kriesten, K. Krings, G. Kroll, J. Kunnen, N. Kurahashi, T. Kuwabara, M. Labare, H. Landsman, M. J. Larson, M. Lesiak-Bzdak, M. Leuermann, J. Leute, J. Lünemann, O. Macías, J. Madsen, G. Maggi, R. Maruyama, K. Mase, H. S. Matis, F. McNally, K. Meagher, M. Merck, T. Meures, S. Miarecki, E. Middell, N. Milke, J. Miller, L. Mohrmann, T. Montaruli, R. Morse, R. Nahnhauer, U. Naumann, H. Niederhausen, S. C. Nowicki, D. R. Nygren, A. Obertacke, S. Odrowski, A. Olivas, A. Omairat, A. O'Murchadha, L. Paul, J. A. Pepper, C. Pérez de los Heros, C. Pfendner, D. Pieth, E. Pinat, J. Posselt, P. B. Price, G. T. Przybylski, M. Quinnan, L. Rädel, M. Rameez, K. Rawlins, P. Redl, R. Reimann, E. Resconi, W. Rhode, M. Ribordy, M. Richman, B. Riedel, S. Robertson, J. P. Rodrigues, C. Rott, T. Ruhe, B. Ruzybayev, D. Ryckbosch, S. M. Saba, H.-G. Sander, M. Santander, S. Sarkar, K. Schatto, F. Scheriau, T. Schmidt, M. Schmitz, S. Schoenen, S. Schöneberg, A. Schönwald, A. Schukraft, L. Schulte, O. Schulz, D. Seckel, Y. Sestayo, S. Seunarine, R. Shanidze, C. Sheremata, M. W. E. Smith, D. Soldin, G. M. Spiczak, C. Spiering, M. Stamatikos, T. Staney, N. A. Stanisha, A. Stasik, T. Stezelberger, R. G. Stokstad, A. Stößl, E. A. Strahler, R. Ström, N. L. Strotjohann, G. W. Sullivan, H. Taavola, I. Taboada, A. Tamburro, A. Tepe, S. Ter-Antonyan, G. Tešić, S. Tilav, P. A. Toale, M. N. Tobin, S. Toscano, M. Tselengidou, E. Unger, M. Usner, S. Vallecorsa, N. van Eijndhoven, A. Van Overloop, J. van Santen, M. Vehring, M. Voge, M. Vraeghe, C. Walck, T. Waldenmaier, M. Wallraff, C. Weaver, M. Wellons, C. Wendt, S. Westerhoff, B. Whelan, N. Whitehorn, K. Wiebe, C. H. Wiebusch, D. R. Williams, H. Wissing, M. Wolf, T. R. Wood, K. Woschnagg, D. L. Xu, X. W. Xu, J. P. Yanez, G. Yodh, S. Yoshida, P. Zarzhitsky, J. Ziemann, S. Zierke, M. Zoll, Energy reconstruction methods in the IceCube neutrino telescope. *JINST* **9**, P03009 (2014). [doi:10.1088/1748-0221/9/03/P03009](https://doi.org/10.1088/1748-0221/9/03/P03009)

76. K. M. Gorski, E. Hivon, A. J. Banday, B. D. Wandelt, F. K. Hansen, M. Reinecke, M. Bartelmann, HEALPix: A Framework for High-Resolution Discretization and Fast Analysis of Data Distributed on the Sphere. *Astrophys. J.* **622**, 759–771 (2005). [doi:10.1086/427976](https://doi.org/10.1086/427976)
77. A. Zonca, L. Singer, D. Lenz, M. Reinecke, C. Rosset, E. Hivon, K. Gorski, healpy: Equal area pixelization and spherical harmonics transforms for data on the sphere in Python. *J. Open Source Softw.* **4**, 1298 (2019). [doi:10.21105/joss.01298](https://doi.org/10.21105/joss.01298)
78. J. Neyman, H. Jeffreys, Outline of a Theory of Statistical Estimation Based on the Classical Theory of Probability. *Philos. Trans. R. Soc. Lond. A* **236**, 333–380 (1937). [doi:10.1098/rsta.1937.0005](https://doi.org/10.1098/rsta.1937.0005)
79. J. J. Condon, W. D. Cotton, E. W. Greisen, Q. F. Yin, R. A. Perley, G. B. Taylor, J. J. Broderick, The NRAO VLA Sky Survey. *Astron. J.* **115**, 1693–1716 (1998). [doi:10.1086/300337](https://doi.org/10.1086/300337)

80. N. A. Webb, M. Coriat, I. Traulsen, J. Ballet, C. Motch, F. J. Carrera, F. Koliopanos, J. Authier, I. de la Calle, M. T. Ceballos, E. Colomo, D. Chuard, M. Freyberg, T. Garcia, M. Kolehmainen, G. Lamer, D. Lin, P. Maggi, L. Michel, C. G. Page, M. J. Page, J. V. Perea-Calderon, F.-X. Pineau, P. Rodriguez, S. R. Rosen, M. Santos Lleo, R. D. Saxton, A. Schwope, L. Tomás, M. G. Watson, A. Zakardjian, The *XMM-Newton* serendipitous survey. *Astron. Astrophys.* **641**, A136 (2020). [doi:10.1051/0004-6361/201937353](https://doi.org/10.1051/0004-6361/201937353)
81. R. D. Saxton, A. M. Read, P. Esquej, M. J. Freyberg, B. Altieri, D. Bermejo, The first XMM-Newton slew survey catalogue: XMMSL1. *Astron. Astrophys.* **480**, 611–622 (2008). [doi:10.1051/0004-6361:20079193](https://doi.org/10.1051/0004-6361:20079193)
82. T. Boller, M. J. Freyberg, J. Trümper, F. Haberl, W. Voges, K. Nandra, Second ROSAT all-sky survey (2RXS) source catalogue. *Astron. Astrophys.* **588**, A103 (2016). [doi:10.1051/0004-6361/201525648](https://doi.org/10.1051/0004-6361/201525648)
83. P. A. Evans, K. L. Page, J. P. Osborne, A. P. Beardmore, R. Willingale, D. N. Burrows, J. A. Kennea, M. Perri, M. Capalbi, G. Tagliaferri, S. B. Cenko, 2SXPS: An Improved and Expanded Swift X-Ray Telescope Point-source Catalog. *Astrophys. J. Suppl. Ser.* **247**, 54 (2020). [doi:10.3847/1538-4365/ab7db9](https://doi.org/10.3847/1538-4365/ab7db9)
84. T. Murphy, E. M. Sadler, R. D. Ekers, M. Massardi, P. J. Hancock, E. Mahony, R. Ricci, S. Burke-Spolaor, M. Calabretta, R. Chhetri, G. De Zotti, P. G. Edwards, J. A. Ekers, C. A. Jackson, M. J. Kesteven, E. Lindley, K. Newton-McGee, C. Phillips, P. Roberts, R. J. Sault, L. Staveley-Smith, R. Subrahmanyan, M. A. Walker, W. E. Wilson, The Australia Telescope 20 GHz Survey: The source catalogue. *Mon. Not. R. Astron. Soc.* **402**, 2403–2423 (2010). [doi:10.1111/j.1365-2966.2009.15961.x](https://doi.org/10.1111/j.1365-2966.2009.15961.x)
85. W. M. Lane, W. D. Cotton, S. van Velzen, T. E. Clarke, N. E. Kassim, J. F. Helmboldt, T. J. W. Lazio, A. S. Cohen, The Very Large Array Low-frequency Sky Survey Redux (VLSSr). *Mon. Not. R. Astron. Soc.* **440**, 327–338 (2014). [doi:10.1093/mnras/stu256](https://doi.org/10.1093/mnras/stu256)
86. H. T. Intema, P. Jagannathan, K. P. Mooley, D. A. Frail, The GMRT 150 MHz all-sky radio survey. *Astron. Astrophys.* **598**, A78 (2017). [doi:10.1051/0004-6361/201628536](https://doi.org/10.1051/0004-6361/201628536)
87. N. Hurley-Walker, J. R. Callingham, P. J. Hancock, T. M. O. Franzen, L. Hindson, A. D. Kapińska, J. Morgan, A. R. Offringa, R. B. Wayth, C. Wu, Q. Zheng, T. Murphy, M. E. Bell, K. S. Dwarakanath, B. For, B. M. Gaensler, M. Johnston-Hollitt, E. Lenc, P. Procopio, L. Staveley-Smith, R. Ekers, J. D. Bowman, F. Briggs, R. J. Cappallo, A. A. Deshpande, L. Greenhill, B. J. Hazelton, D. L. Kaplan, C. J. Lonsdale, S. R. McWhirter, D. A. Mitchell, M. F. Morales, E. Morgan, D. Oberoi, S. M. Ord, T. Prabu, N. U. Shankar, K. S. Srivani, R. Subrahmanyan, S. J. Tingay, R. L. Webster, A. Williams, C. L. Williams, GaLactic and Extragalactic All-sky Murchison Widefield Array (GLEAM) survey – I. A low-frequency extragalactic catalogue. *Mon. Not. R. Astron. Soc.* **464**, 1146–1167 (2017). [doi:10.1093/mnras/stw2337](https://doi.org/10.1093/mnras/stw2337)
88. H. Kuehr, A. Witzel, I. I. K. Pauliny-Toth, U. Nauber, A Catalogue of Extragalactic Radio Sources Having Flux Densities Greater than 1-JY at 5-GHZ. *Astron. Astrophys.* **45**, 367 (1981).
89. Planck Collaboration, N. Aghanim, Y. Akrami, F. Arroja, M. Ashdown, J. Aumont, C. Baccigalupi, M. Ballardini, A. J. Banday, R. B. Barreiro, N. Bartolo, S. Basak, R. Battye, K. Benabed, J.-P. Bernard, M. Bersanelli, P. Bielewicz, J. J. Bock, J. R. Bond, J. Borrill,

- F. R. Bouchet, F. Boulanger, M. Bucher, C. Burigana, R. C. Butler, E. Calabrese, J.-F. Cardoso, J. Carron, B. Casaponsa, A. Challinor, H. C. Chiang, L. P. L. Colombo, C. Combet, D. Contreras, B. P. Crill, F. Cuttaia, P. de Bernardis, G. de Zotti, J. Delabrouille, J.-M. Delouis, F.-X. Désert, E. Di Valentino, C. Dickinson, J. M. Diego, S. Donzelli, O. Doré, M. Doussis, A. Ducout, X. Dupac, G. Efstathiou, F. Elsner, T. A. Enßlin, H. K. Eriksen, E. Falgarone, Y. Fantaye, J. Fergusson, R. Fernandez-Cobos, F. Finelli, F. Forastieri, M. Frailis, E. Franceschi, A. Frolov, S. Galeotta, S. Galli, K. Ganga, R. T. Génova-Santos, M. Gerbino, T. Ghosh, J. González-Nuevo, K. M. Górski, S. Gratton, A. Gruppuso, J. E. Gudmundsson, J. Hamann, W. Handley, F. K. Hansen, G. Helou, D. Herranz, S. R. Hildebrandt, E. Hivon, Z. Huang, A. H. Jaffe, W. C. Jones, A. Karakci, E. Keihänen, R. Keskitalo, K. Kiiveri, J. Kim, T. S. Kisner, L. Knox, N. Krachmalnicoff, M. Kunz, H. Kurki-Suonio, G. Lagache, J.-M. Lamarre, M. Langer, A. Lasenby, M. Lattanzi, C. R. Lawrence, M. Le Jeune, J. P. Leahy, J. Lesgourgues, F. Levrier, A. Lewis, M. Liguori, P. B. Lilje, M. Lilley, V. Lindholm, M. López-Caniego, P. M. Lubin, Y.-Z. Ma, J. F. Macías-Pérez, G. Maggio, D. Maino, N. Mandlesi, A. Mangilli, A. Marcos-Caballero, M. Maris, P. G. Martin, M. Martinelli, E. Martínez-González, S. Matarrese, N. Mauri, J. D. McEwen, P. D. Meerburg, P. R. Meinhold, A. Melchiorri, A. Mennella, M. Migliaccio, M. Millea, S. Mitra, M.-A. Miville-Deschénes, D. Molinari, A. Moneti, L. Montier, G. Morgante, A. Moss, S. Mottet, M. Münchmeyer, P. Natoli, H. U. Nørgaard-Nielsen, C. A. Oxborrow, L. Pagano, D. Paoletti, B. Partridge, G. Patanchon, T. J. Pearson, M. Peel, H. V. Peiris, F. Perrotta, V. Pettorino, F. Piacentini, L. Polastri, G. Polenta, J.-L. Puget, J. P. Rachen, M. Reinecke, M. Remazeilles, C. Renault, A. Renzi, G. Rocha, C. Rosset, G. Roudier, J. A. Rubiño-Martín, B. Ruiz-Granados, L. Salvati, M. Sandri, M. Savelainen, D. Scott, E. P. S. Shellard, M. Shiraishi, C. Sirignano, G. Sirri, L. D. Spencer, R. Sunyaev, A.-S. Suur-Uski, J. A. Tauber, D. Tavagnacco, M. Tenti, L. Terenzi, L. Toffolatti, M. Tomasi, T. Trombetti, J. Valiviita, B. Van Tent, L. Vibert, P. Vielva, F. Villa, N. Vittorio, B. D. Wandelt, I. K. Wehus, M. White, S. D. M. White, A. Zacchei, A. Zonca, *Planck* 2018 results: I. Overview and the cosmological legacy of *Planck*. *Astron. Astrophys.* **641**, A1 (2020). [doi:10.1051/0004-6361/201833880](https://doi.org/10.1051/0004-6361/201833880)
90. M. F. Skrutskie, R. M. Cutri, R. Stiening, M. D. Weinberg, S. Schneider, J. M. Carpenter, C. Beichman, R. Capps, T. Chester, J. Elias, J. Huchra, J. Liebert, C. Lonsdale, D. G. Monet, S. Price, P. Seitzer, T. Jarrett, J. D. Kirkpatrick, J. E. Gizis, E. Howard, T. Evans, J. Fowler, L. Fullmer, R. Hurt, R. Light, E. L. Kopan, K. A. Marsh, H. L. McCallon, R. Tam, S. Van Dyk, S. Wheelock, The Two Micron All Sky Survey (2MASS). *Astron. J.* **131**, 1163–1183 (2006). [doi:10.1086/498708](https://doi.org/10.1086/498708)
91. R. M. Cutri, E. L. Wright, T. Conrow, J. W. Fowler, P. R. M. Eisenhardt, C. Grillmair, J. D. Kirkpatrick, F. Masci, H. L. McCallon, S. L. Wheelock, S. Fajardo-Acosta, L. Yan, D. Benford, M. Harbut, T. Jarrett, S. Lake, D. Leisawitz, M. E. Ressler, S. A. Stanford, C.-W. Tsai, F. Liu, G. Helou, A. Mainzer, D. Gettings, A. Gonzalez, D. Hoffman, K. A. Marsh, D. Padgett, M. F. Skrutskie, R. Beck, M. Papin, M. Wittman, Explanatory Supplement to the AllWISE Data Release Products (Wise, 2013); <https://wise2.ipac.caltech.edu/docs/release/allwise/expsup/>.
92. B. M. Lasker, M. G. Lattanzi, B. J. McLean, B. Bucciarelli, R. Drimmel, J. Garcia, G. Greene, F. Guglielmetti, C. Hanley, G. Hawkins, V. G. Laidler, C. Loomis, M. Meakes, R. Mignani, R. Morbidelli, J. Morrison, R. Pannunzio, A. Rosenberg, M. Sarasso, R. L.

Smart, A. Spagna, C. R. Sturch, A. Volpicelli, R. L. White, D. Wolfe, A. Zacchei, The second-generation Guide Star Catalog: Description and properties. *Astron. J.* **136**, 735–766 (2008). [doi:10.1088/0004-6256/136/2/735](https://doi.org/10.1088/0004-6256/136/2/735)

93. K. C. Chambers, E. A. Magnier, N. Metcalfe, H. A. Flewelling, M. E. Huber, C. Z. Waters, L. Denneau, P. W. Draper, D. Farrow, D. P. Finkbeiner, C. Holmberg, J. Koppenhoefer, P. A. Price, A. Rest, R. P. Saglia, E. F. Schlafly, S. J. Smartt, W. Sweeney, R. J. Wainscoat, W. S. Burgett, S. Chastel, T. Grav, J. N. Heasley, K. W. Hodapp, R. Jedicke, N. Kaiser, R.-P. Kudritzki, G. A. Luppino, R. H. Lupton, D. G. Monet, J. S. Morgan, P. M. Onaka, B. Shiao, C. W. Stubbs, J. L. Tonry, R. White, E. Bañados, E. F. Bell, R. Bender, E. J. Bernard, M. Boegner, F. Boffi, M. T. Botticella, A. Calamida, S. Casertano, W.-P. Chen, X. Chen, S. Cole, N. Deacon, C. Frenk, A. Fitzsimmons, S. Gezari, V. Gibbs, C. Goessl, T. Goggia, R. Gourgue, B. Goldman, P. Grant, E. K. Grebel, N. C. Hambly, G. Hasinger, A. F. Heavens, T. M. Heckman, R. Henderson, T. Henning, M. Holman, U. Hopp, W.-H. Ip, S. Isani, M. Jackson, C. D. Keyes, A. M. Koekemoer, R. Kotak, D. Le, D. Liska, K. S. Long, J. R. Lucey, M. Liu, N. F. Martin, G. Masci, B. McLean, E. Mindel, P. Misra, E. Morganson, D. N. A. Murphy, A. Obaika, G. Narayan, M. A. Nieto-Santisteban, P. Norberg, J. A. Peacock, E. A. Pier, M. Postman, N. Primak, C. Rae, A. Rai, A. Riess, A. Riffeser, H. W. Rix, S. Röser, R. Russel , L. Rutz, E. Schilbach, A. S. B. Schultz, D. Scolnic, L. Strolger, A. Szalay, S. Seitz, E. Small, K. W. Smith, D. R. Soderblom, P. Taylor, R. Thomson, A. N. Taylor, A. R. Thakar, J. Thiel, D. Thilker, D. Unger, Y. Urata, J. Valenti, J. Wagner, T. Walder, F. Walter, S. P. Watters, S. Werner, W. M. Wood-Vasey, R. Wyse, The Pan-STARRS1 Surveys. [arXiv:1612.05560](https://arxiv.org/abs/1612.05560) [astro-ph.IM] (2016).
94. B. Abolfathi, D. S. Aguado, G. Aguilar, C. A. Prieto, A. Almeida, T. T. Ananna, F. Anders, S. F. Anderson, B. H. Andrews, B. Anguiano, A. Aragón-Salamanca, M. Argudo-Fernández, E. Armengaud, M. Ata, E. Aubourg, V. Avila-Reese, C. Badenes, S. Bailey, C. Balland, K. A. Barger, J. Barrera-Ballesteros, C. Bartosz, F. Bastien, D. Bates, F. Baumgarten, J. Bautista, R. Beaton, T. C. Beers, F. Belfiore, C. F. Bender, M. Bernardi, M. A. Bershadsky, F. Beutler, J. C. Bird, D. Bizyaev, G. A. Blanc, M. R. Blanton, M. Blomqvist, A. S. Bolton, M. Boquien, J. Borissova, J. Bovy, C. A. Bradna Diaz, W. Nielsen Brandt, J. Brinkmann, J. R. Brownstein, K. Bundy, A. J. Burgasser, E. Burtin, N. G. Busca, C. I. Cañas, M. Cano-Díaz, M. Cappellari, R. Carrera, A. R. Casey, B. C. Sodi, Y. Chen, B. Cherinka, C. Chiappini, P. D. Choi, D. Chojnowski, C.-H. Chuang, H. Chung, N. Clerc, R. E. Cohen, J. M. Comerford, J. Comparat, J. C. do Nascimento, L. da Costa, M.-C. Cousinou, K. Covey, J. D. Crane, I. Cruz-Gonzalez, K. Cunha, G. S. Ilha, G. J. Damke, J. Darling, J. W. Davidson Jr., K. Dawson, M. A. C. de Icaza Lizaola, A. Macorra, S. de la Torre, N. De Lee, V. Sainte Agathe, A. Deconto Machado, F. Dell'Agli, T. Delubac, A. M. Diamond-Stanic, J. Donor, J. J. Downes, N. Drory, H. Mas des Bourboux, C. J. Duckworth, T. Dwelly, J. Dyer, G. Ebelke, A. D. Eigenbrot, D. J. Eisenstein, Y. P. Elsworth, E. Emsellem, M. Eracleous, G. Erfanianfar, S. Escoffier, X. Fan, E. F. Alvar, J. G. Fernandez-Trincado, R. F. Cirolini, D. Feuillet, A. Finoguenov, S. W. Fleming, A. Font-Ribera, G. Freischlad, P. Frinchaboy, H. Fu, Y. G. M. Chew, L. Galbany, A. E. García Pérez, R. Garcia-Dias, D. A. García-Hernández, L. A. Garma Oehmichen, P. Gaulme, J. Gelfand, H. Gil-Marín, B. A. Gillespie, D. Goddard, J. I. González Hernández, V. Gonzalez-Perez, K. Grabowski, P. J. Green, C. J. Grier, A. Gueguen, H. Guo, J. Guy, A. Hagen, P. Hall, P. Harding, S. Hasselquist, S. Hawley, C.

R. Hayes, F. Hearty, S. Hekker, J. Hernandez, H. Hernandez Toledo, D. W. Hogg, K. Holley-Bockelmann, J. A. Holtzman, J. Hou, B.-C. Hsieh, J. A. S. Hunt, T. A. Hutchinson, H. S. Hwang, C. E. Jimenez Angel, J. A. Johnson, A. Jones, H. Jönsson, E. Jullo, F. Sakil Khan, K. Kinemuchi, D. Kirkby, C. C. Kirkpatrick IV, F.-S. Kitaura, G. R. Knapp, J.-P. Kneib, J. A. Kollmeier, I. Lacerna, R. R. Lane, D. Lang, D. R. Law, J.-M. Le Goff, Y.-B. Lee, H. Li, C. Li, J. Lian, Y. Liang, M. Lima, L. Lin, D. Long, S. Lucatello, B. Lundgren, J. T. Mackereth, C. L. MacLeod, S. Mahadevan, M. A. Geimba Maia, S. Majewski, A. Manchado, C. Maraston, V. Mariappan, R. Marques-Chaves, T. Masseron, K. L. Masters, R. M. McDermid, I. D. McGreer, M. Melendez, S. Meneses-Goytia, A. Merloni, M. R. Merrifield, S. Meszaros, A. Meza, I. Minchev, D. Minniti, E.-M. Mueller, F. Muller-Sanchez, D. Muna, R. R. Muñoz, A. D. Myers, P. Nair, K. Nandra, M. Ness, J. A. Newman, R. C. Nichol, D. L. Nidever, C. Nitschelm, P. Noterdaeme, J. O'Connell, R. J. Oelkers, A. Oravetz, D. Oravetz, E. A. Ortíz, Y. Osorio, Z. Pace, N. Padilla, N. Palanque-Delabrouille, P. A. Palicio, H.-A. Pan, K. Pan, T. Parikh, I. Pâris, C. Park, S. Peirani, M. Pellejero-Ibanez, S. Penny, W. J. Percival, I. Perez-Fournon, P. Petitjean, M. M. Pieri, M. Pinsonneault, A. Pisani, F. Prada, A. Prakash, A. B. de Andrade Queiroz, M. J. Raddick, A. Raichoor, S. B. Rembold, H. Richstein, R. A. Riffel, R. Riffel, H.-W. Rix, A. C. Robin, S. R. Torres, C. Román-Zúñiga, A. J. Ross, G. Rossi, J. Ruan, R. Ruggeri, J. Ruiz, M. Salvato, A. G. Sánchez, S. F. Sánchez, J. S. Almeida, J. R. Sánchez-Gallego, F. A. S. Rojas, B. X. Santiago, R. P. Schiavon, J. S. Schimoia, E. Schlafly, D. Schlegel, D. P. Schneider, W. J. Schuster, A. Schwope, H.-J. Seo, A. Serenelli, S. Shen, Y. Shen, M. Shetrone, M. Shull, V. S. Aguirre, J. D. Simon, M. Skrutskie, A. Slosar, R. Smethurst, V. Smith, J. Sobeck, G. Somers, B. J. Souter, D. Souto, A. Spindler, D. V. Stark, K. Stassun, M. Steinmetz, D. Stello, T. Storch-Bergmann, A. Streblyanska, G. S. Stringfellow, G. Suárez, J. Sun, L. Szigeti, M. Taghizadeh-Popp, M. S. Talbot, B. Tang, C. Tao, J. Tayar, M. Tembe, J. Teske, A. R. Thakar, D. Thomas, P. Tissera, R. Tojeiro, C. Tremonti, N. W. Troup, M. Urry, O. Valenzuela, R. Bosch, J. Vargas-González, M. Vargas-Magaña, J. A. Vazquez, S. Villanova, N. Vogt, D. Wake, Y. Wang, B. A. Weaver, A.-M. Weijmans, D. H. Weinberg, K. B. Westfall, D. G. Whelan, E. Wilcots, V. Wild, R. A. Williams, J. Wilson, W. M. Wood-Vasey, D. Wylezalek, T. Xiao, R. Yan, M. Yang, J. E. Ybarra, C. Yèche, N. Zakamska, O. Zamora, P. Zarrouk, G. Zasowski, K. Zhang, C. Zhao, G.-B. Zhao, Z. Zheng, Z. Zheng, Z.-M. Zhou, G. Zhu, J. C. Zinn, H. Zou, The Fourteenth Data Release of the Sloan Digital Sky Survey: First Spectroscopic Data from the Extended Baryon Oscillation Spectroscopic Survey and from the Second Phase of the Apache Point Observatory Galactic Evolution Experiment. *Astrophys. J. Suppl. Ser.* **235**, 42 (2018). [doi:10.3847/1538-4365/aa9e8a](https://doi.org/10.3847/1538-4365/aa9e8a)

95. P. Morrissey, T. Conrow, T. A. Barlow, T. Small, M. Seibert, T. K. Wyder, T. Budavari, S. Arnouts, P. G. Friedman, K. Forster, D. C. Martin, S. G. Neff, D. Schiminovich, L. Bianchi, J. Donas, T. M. Heckman, Y.-W. Lee, B. F. Madore, B. Milliard, R. M. Rich, A. S. Szalay, B. Y. Welsh, S. K. Yi, The Calibration and Data Products of GALEX. *Astrophys. J. Suppl. Ser.* **173**, 682–697 (2007). [doi:10.1086/520512](https://doi.org/10.1086/520512)
96. V. N. Yershov, Serendipitous UV source catalogues for 10 years of XMM and 5 years of Swift. *Astrophys. Space Sci.* **354**, 97–101 (2014). [doi:10.1007/s10509-014-1944-5](https://doi.org/10.1007/s10509-014-1944-5)

97. M. Page, C. Brindle, A. Talavera, M. Still, S. R. Rosen, V. N. Yershov, H. Ziaeepour, K. O. Mason, M. S. Cropper, A. A. Breeveld, N. Loiseau, R. Mignani, A. Smith, P. Murdin, The *XMM—Newton* serendipitous ultraviolet source survey catalogue. *Mon. Not. R. Astron. Soc.* **426**, 903–926 (2012). [doi:10.1111/j.1365-2966.2012.21706.x](https://doi.org/10.1111/j.1365-2966.2012.21706.x)
98. K. Oh, M. Koss, C. B. Markwardt, K. Schawinski, W. H. Baumgartner, S. D. Barthelmy, S. B. Cenko, N. Gehrels, R. Mushotzky, A. Petulante, C. Ricci, A. Lien, B. Trakhtenbrot, The 105-Month *Swift*-BAT All-sky Hard X-Ray Survey. *Astrophys. J. Suppl. Ser.* **235**, 4 (2018). [doi:10.3847/1538-4365/aaa7fd](https://doi.org/10.3847/1538-4365/aaa7fd)